FGF SIGNALING GOVERNS THE DIFFERENTIATION OF PARAPINEAL NEURONS IN ZEBRAFISH

By

Joshua Aaron Clanton

Dissertation

Submitted to the Faculty of the

Graduate School of Vanderbilt University

in partial fulfillment of the requirements

for the degree of

DOCTOR OF PHILOSOPHY

in

Biological Sciences

May, 2013

Nashville, Tennessee

Approved:

Associate Professor Joshua T. Gamse

Assistant Professor Jason R. Jessen

Assistant Professor Michael K. Cooper

Professor James G. Patton

Professor Douglas G. McMahon

For my wonderful and supportive family,
Roddy, Brenda, and Erica
And to the love of my life,
Sataree

ACKNOWLEDGEMENTS

Sometime in the 1980's, I sat back in a desk in 5th grade science class and realized that, as far as subjects go, Biology was the most interesting. Armed with an intellectual curiosity, I followed this thread of interest through my primary education and into my undergraduate years. This culminated with a Bachelor's degree in Biology, but not a concrete plan of what to do in life. At this important juncture, I cannot help wondering how a working class kid from rural Tennessee is on the cusp of obtaining a Ph.D. from a place with such a rich academic tradition as Vanderbilt University. The answer is that throughout my life and academic career I have been surrounded by many people that have offered advice, encouragement, and support that has proven integral to my success.

First and foremost, I extend immense gratitude to my mentor, Josh Gamse. He has demonstrated an unbelievable level of patience during my years in the lab when others would have grown weary of waiting for my data, figures, and manuscripts. In addition to the immeasurable contributions to my experiments, he has created an open and collegial atmosphere, which makes the lab a great place to work. For their past and present contributions to the lab, I thank Sataree Khuansuwan, Nancy Hernandez de Borsetti, Robert Taylor, Ben Dean, Caleb Doll, Stacey Lee, Corey Snelson, and Simon Wu. In addition, I recognize Erin Booton for all of her hard work, advice, and kindness. Also, our lab would not have a thriving fish facility without the efforts of Gena Guston and Qiang Guan. Also, Kyle

Hope, Eszter Szentirmentai, and Patirck Reppert are three former undergraduates who have all contributed to my project. This work was funded by the NIH/NICHD and the Vanderbilt University Medical Center Program for Developmental Biology Training Grant.

Among the first I would like to thank is Dr. Lila Solnica-Krezel for giving me my first job in science when she could have certainly found a better research technician elsewhere. In addition to Lila, I am grateful to the past members of Solnica-Krezel lab for showing me how science is done at a high level. Among these, I would like to highlight Jennifer Panizzi, Jason Jessen, and Terry Van Raay for creating a sense of comraderie and belonging for me in the lab, which encouraged me to choose research as a career. I wish them nothing but the best in their future endeavors.

I am extremely grateful to the members graduate committee, Doug McMahon, James Patton, Michael Cooper, and Jason Jessen for sheparding my project from the very beginning. For indulging my research interests and providing me with training grant and travel support, I thank the Program for Developmental Biology, especially Kim Kane and Chris Wright. Also, the work of all those in the Department of Biological Sciences, especially Roz Johnson and Leslie Maxwell, has provided me with a research “home” as a graduate student. Also, I extend gratitude to the department for the Mosig Travel Fund, which has proved instrumental in my growth as a scientist.

Finally, I am reminded how truly fortunate I am to have Sataree Khuansuwan in my life. Her kindness, wit, encouragement, and love are an inspiration for me. Words are inadequate to express my profound gratitude to my family, Roddy, Brenda, and Erica whose unconditional love and support have been without equal. I go forward from here hoping that I have been worthy to receive it.

TABLE OF CONTENTS

Page

DEDICATION……ii

ACKNOWLEDGEMENTS……...iii

LIST OF FIGURES……viii

LIST OF ABBREVIATIONS.....ix

Chapter

I. INTRODUCTION……1

The Human Brain is Highly Lateralized ……..1
Brain Asymmetry in Vertebrate Model Systems: Form and Function…….....……3
The Zebrafish Epithalamus as A Model for Brain Asymmetries…….5
Formation of the Zebrafish Pineal Complex……...8

II. FGF SIGNALING GOVERNS THE DIFFERENTIATION OF PARAPINEAL CELLS IN ZEBRAFISH.....15

Preface……15
Abstract……15
Methods……16
Zebrafish.....16
in situ hybridization...……..16
Cloning...……...……...17
Cryosectioning...……...……18
Whole mount antibody labeling. ……18
Heat shock conditions 19
Caged fluorescein injection, uncaging, and detection.....19
Morpholino injection…….....21
Inhibitor treatments.....21

Results....21
Fgf Ligands, Receptor, and a Target Gene are Expressed in the Pineal Complex Anlage....22
Attenuating Fgf Signaling Disrupts Parapineal Formation....26

Parapineal Differentiation Does Not Depend on Parapineal Cell Migration....33
Conditional Expression of Fgf8a is Not Sufficient to Induce Parapineal Cells or Rescue Parapineal Defects in *fgf8a*^{x15} Mutants....35
Reduced Fgf Activity Leads to a Selective Increase in Cone Cell Number....39
Parapineal Precursors Give Rise to Cone Cells in *fgf8a*^{x15} Mutants....45
Fgf8a and Tbx2b Act During Different Steps of Parapineal Development....51
Discussion....58

III. Fgf Signaling Does Not Regulate Bmp Activity During Parapineal Formation....61

Introduction....61
Methods....62
Zebrafish....62
in situ hybridization....63
Whole mount antibody labeling....63
Heat shock conditions....64
Results....64
Fgf Signaling Does Not Regulate Bmp Activity Via Chordin....62
Inhibition of Fgf Signaling Does Not Expand Bmp Activity....67
Inhibition of Bmp Activity Cannot Suppress Parapineal Defects in *fgf8a* Mutants....71
Discussion....74

IV. FGF SIGNALING MIGHT GOVERN PARAPINEAL DIFFERENTIATION THROUGH REGULATION OF LHX2B AND LHX9....76

Introduction....74
Methods....77
Zebrafish....78
in situ hybridization....78
Inhibitor treatments....78
Cloning....78
mRNA injection....80
Results....80

lhx2b and *lhx9* are Expressed in the Pineal Complex During Parapineal Formation....83
The Expression of *lhx2b* and *lhx9* is Regulated by Fgf Signaling....83
Lhx2b and Lhx9 Might Play a Role in Parapineal Formation....83
Discussion....87

V. CONCLUSIONS AND FUTURE DIRECTIONS....89

Fgf Signaling Might Mave Multiple Roles During Parapineal Development....90
Fgf8a is Required for Parapineal and Habenular Development....91
Fgf Signaling Governs a Binary Fate Decision in Pineal Complex Precursors....93
Fgf Signaling and Parapineal Cells: An Evolutionary Perspective....97

VI. REFERENCES....100

LIST OF FIGURES

Figure Page

CHAPTER I

1. The zebrafish epithalamus exhibits robust Left-Right (L-R) asymmetries....7
2. Pineal complex development....10

CHAPTER II

3. Fgf components are expressed in the epithalamus during parapineal formation....23
4. *fgfr4* is expressed in the pineal complex during parapineal formation....25
5. *sox1a* is expressed in parapineal cells near their time of differentiation....27
6. *fgf8a*^{x15} mutants have fewer newly differentiated parapineal cells....28
7. *fgf8a*^{x15} mutants have fewer mature parapineal cells....29
8. Conditional loss of Fgf signaling results in fewer parapineal cells....32
9. Parapineal differentiation is not dependent on migration....34
10. Fgf8a overexpression is not sufficient to induce supernumerary parapineal cells....36
11. Fgf8a over-expression cannot rescue parapineal cell number defects in *fgf8a*^{x15} mutants....37
12. *fgf8a* mutants show no change in the number of rod cells or projection neurons....41
13. *fgf8a*^{x15} mutants have a selective increase in pineal cone cells....42
14. Ectopic increase in cone cells persist in SU5402 treated larvae....44
15. Ectopic cone photoreceptors persist in *flh* depleted *fgf8a*^{x15} mutants....46
16. Cell fate analysis of the pineal complex....48
17. Cell fate analysis of anterior pineal complex indicates that parapineal precursors adopt a cone photoreceptor fate in *fgf8a*^{x15} mutants....50
18. Tbx2b and Fgf8a have no cross-regulatory relationship....52
19. Fgf8a and Tbx2b act additively in the formation of parapineal cells....54
20. Tbx2b is required to produce the extra cone cells in *fgf8a*^{x15} mutants....55
21. Model: Fgf8a acts on bi-potential parapineal/cone cells to promote

parapineal fate and/or inhibit cone photoreceptor fate.....57

CHAPTER III

22. *chordin* is expressed in or near the epithalamus during parapineal organ development and exhibits reduced *chordin* expression in *fgf8a* mutants.....65
23. *chordin*^{tt250} mutants display a reduced number of differentiated parapineal cells.....68
24. *chordin*^{tt250} (*chd*^{tt250})mutants show deficits in pineal complex cells.....69
25. Inhibition of Fgf signaling does not increase Bmp activity in the pineal complex.....68
26. Bmp inhibition cannot rescue parapineal deficits in *fgf8a*^{x15} mutants....72
27. Inhibition of Bmp signaling cannot suppress ectopic cone cells in *fgf8a*^{x15} mutants.....73

CHAPTER IV

28. *lhx2b* and *lhx9* are expressed in the anterior pineal complex during parapineal formation.....81
29. *lhx2b* and *lhx9* expression is reduced in *fgf8a*^{x15} mutants.....82
30. *lhx2b* and *lhx9* expression is responsive to Fgf signaling.....84
31. *lhx2b* mutants might have fewer parapineal cells.....85
32. *lhx9* overexpression can partially rescue parapineal deficits in *fgf8a*^{x15} mutants.....86

LIST OF ABBREVIATIONS

L-R	Left-Right
GluR1	Glutamate receptor subunit R1
NR2B	NDMA receptor type 2B
LTP	long term potentiation
SLF	superior longitudinal fasciculus
IPN	interpeduncular nucleus
hpf	hours post fertilization
Flh	Floating head
D-V	dorsal-ventral
Bmp	Bone morphogenic protein
Tbx2b	T-box containing transcription factor 2b
Fgf	Fibroblast growth factor
erm	*ETS-related molecule*
fgfr	*fibroblast growth factor receptor*
sox1a	*sex determining y-box transcription factor*
gfi-1.2	*growth factor inhibited 1.2*
WT	wild-type
NI	non-injected
NIC	non-injected controls
Arr3a	Arrestin 3a
chd	*chordin*
Bmpr	Bone morphogenic protein receptor
six	*sine occulus*

CHAPTER I

INTRODUCTION

The Human Brain is Highly Lateralized

At first glance, the vertebrate body plan appears symmetric. However, anatomical asymmetries are pervasive within the vertebrate lineage. A well-known example of these asymmetries is the lateralized placement of the visceral organs. For example, the heart and pancreas are typically located of the left side of the body while the liver usually resides on the right (Levin, 2005). The presence of brain asymmetries is widespread, although less studied, among vertebrates.

The human brain, for example, exhibits profound anatomical and functional asymmetry. Early attempts to understand the function of left-right (L-R) differences in the cerebral cortex by Sperry and Gazziniga (Sperry, 1961), through examination of “split brain” patients who had undergone transection of the corpus collosum, the chief connection between the two hemispheres of the brain, suggested that the left and right hemispheres of the human brain are specialized in different tasks. It is broadly thought that the left hemisphere is more attuned to processing of higher cognitive functions, such as language (Geschwind and Levitsky, 1968), while the right hemisphere is more efficient at processing visuospatial information (Heilman and Van Den Abell, 1980). These functional lateralities are likely promoted by anatomical asymmetries in brain

structure. It has been hypothesized that the right hemisphere, through locally increased axonal size or density, is capable of higher transmission speeds compared to the left (Miller, 1996). This would lend the right hemisphere the enhanced transmission speed needed for the processing of visual information while allowing expansion of language and thought related areas of the left hemisphere that do not require high speed transmission. Support for this has recently been uncovered in the region of the cortex called the superior longitudinal retroflexus (SLF), a series of axon tracts, which are strongly right lateralized in most individuals (Thiebaut de Schotten et al., 2011). Those with the most right lateralized SLF were better at performing certain visuospatial tasks (Thiebaut de Schotten et al., 2011). The left hemisphere on the other hand seems to be specialized to deal with language. Two of the language processing regions of the brain, Broca's area and Wernicke's area, are typically larger on the left than on the right in most individuals. Unilateral damage to either area can impair the ability to use and understand language (Sun and Walsh, 2006). In addition, disruptions of cortical asymmetries not only lead to difficulties in processing language but also have been linked to schizophrenia and autism (Hasan et al., 2011; Lo et al., 2011). Thus, as with asymmetries in the chicken visual pathway and the mouse hippocampus, human brain asymmetries serve to influence brain function. While new forms of imaging have enabled the analysis of subtle, structural asymmetries in human subjects, direct experimental evidence for the origin and function of most anatomical brain lateralities remains scarce. As a result, many scientists have turned to vertebrate model systems to better

understand the formation and function of anatomical left-right asymmetries.

Brain Asymmetry in Vertebrates Model Systems: Form and Function

Lateralites the in projections of the avian visual pathway are well documented (Concha et al., 2012). For example, in the domestic chicken (*Gallus gallus*), there are Left-Right (L-R) differences in the thalamofugal visual pathway. Normally, the lateral geniculate nucleus in the left side of the thalamus sends more axonal projections to the hyperpallium than the right side of the thalamus (Koshiba, 2003 and Rogers 1999). Typically, chickens use their right eye to distinguish between food and other objects, like pebbles, during feeding while the left eye is used for analyzing unfamiliar objects and potential predators (Rogers, 2008). Chickens with normal L-R lateralization in the thalamofugal pathway can feed (discriminate between food and non-food) and detect predators simultaneously (Dharmaretnam and Rogers, 2005). Chickens with disturbed thalamofugal laterality struggle to feed and respond to predators suggesting that this asymmetry improves the efficiency in processing visual information (Dharmaretnam and Rogers, 2005) and perhaps improves their chances of survival.

In mouse (*Mus musculus*), the hippocampus is emerging as a model to study how molecular and anatomical asymmetries influence normal brain function. In the mouse brain, populations of CA1 pyramidal neurons are located on both the left and right side of the hippocampus. These CA1 neurons receive synaptic inputs originating from CA3 pyramidal neurons on both the ipsilateral and

contralateral sides (Wu et al., 2005). However, the axons extending from CA3 neurons exhibit structural and molecular differences between the left and right sides. Synapses from right-sided CA3 neurons express a higher level of Glutamate receptor subunit R1 (GluR1) than left-sided neurons, which predominantly express NMDA receptor type 2B (NR2B) (Kawakami et al., 2003; Shinohara et al., 2008). These lateralities appear to be genetically determined as *iv* mutant mice, which contain a mutation in *left-right dynein*, lack asymmetric expression of NR2B (Goto et al., 2010). Additionally, right-originating axons have a greater post-synaptic density and larger spine head volume on average as compared to the left-derived axons (Shinohara et al., 2008). Larger spine head volumes have been linked to long-term potentiation (LTP), a crucial memory forming process that allows a synapse to increase its response to electrical stimuli over time (Park et al., 2004; Park et al., 2006; Bruel-Jungerman et al., 2007; Kopec et al., 2007). Interestingly, although spine head volumes and post-synaptic densities are greater in right-originating CA3 neurons, it has been shown that the right hippocampus, which receives less robust synapses from the left sided CA3 neurons, is more efficient than the left in governing spatial memory (Goto et al., 2010). Additionally, stimulation of left sided CA3 neurons produced more robust LTP than the right-sided stimulation suggesting a right bias in certain kinds of memory (Kohl et al., 2011). Finally, *iv* mutants display delays in acquisition of spatial memory and deficits in maintaining working memory (Goto et al., 2010) suggesting these asymmetries are genetically encoded.

The Zebrafish Epithalamus as A Model for Vertebrate Brain Asymmetries

Despite their pervasiveness among vertebrates, little is currently known about the molecular mechanisms that govern the formation of lateralized brain structures. Due to its external development, tractable genetics, and comparatively simple brain, the zebrafish (*Danio rerio*) has been an ideal model system to study nervous system development. Recently, the zebrafish epithalamus, a forebrain region that exhibits robust molecular and anatomical asymmetries, is becoming the focus of increased study because it is strongly lateralized and is the nexus of control for diverse functions such as secretion of the sleep-promoting hormone melatonin as well as stress based fear responses (Agetsuma et al., 2010; Falcon et al., 2010; Lee et al., 2010). The epithalamus consists of a medially located pineal complex and two pairs of habenular nuclei (dorsal and ventral) flanking either side of the midline (Borg et al., 1983; Butler and Hodos, 1996; Amo et al., 2010). The pineal complex can be further subdivided into a pineal organ, which secretes melatonin in response to circadian stimuli, and an accessory structure called the parapineal organ that is usually located on the left side of the brain (Borg et al., 1983). The pineal organ, being directly photoreceptive in zebrafish, is comprised of rod and cone photoreceptors as well as associated projection neurons (Cau et al., 2008; Quillien et al., 2011). The parapineal organ is a cluster of 10-12 neurons that migrate leftward from the anterior midline of the pineal anlage to abut the developing left, dorsal habenula (Gamse et al., 2003; Snelson et al., 2008c). The emergence of the parapineal strongly correlates with the induction of other epithalamic asymmetries. The

zebrafish dorsal habenular nuclei are notable for exhibiting robust anatomical and molecular asymmetries between the left and right sides (Concha et al., 2000; Gamse et al., 2003; Gamse et al., 2005). The left lateral dorsal habenular nucleus is larger and contains a denser field of neuropil as compared to the right lateral habenular nuclei. This full elaboration of these asymmetries among the habenular nuclei depends on the parapineal, which resides next to and innervates the left lateral habenular nucleus (Concha et al., 2000; Concha et al., 2003; Gamse et al., 2003). In mutants where the parapineal does not form, the habenular nuclei develop more symmetrically with the left lateral habenular nucleus more closely resembling the right in gene expression and neuropil density (Snelson et al., 2008c). The disruption in asymmetry between the left and right alters the efferent projections from the habenular nuclei to the interpeduncular nucleus (IPN) in the midbrain. Normally, the left dorsal habenula sends the majority of its axons to the dorsal subnucleus of the IPN while the right dorsal habenula projects chiefly to the ventral subnucleus of the IPN (Gamse et al., 2005). In larvae that lack a parapineal organ both left and right dorsal habenula project mainly to the ventral IPN (Snelson et al., 2008c). The behavioral implications of disrupted L-R asymmetries in the habenula and the subsequent erroneous targeting of the IPN have not been described. However, it has been shown that zebrafish with reversed habenular laterality (right lateral habenula larger than the left) exhibit decreased exploratory behaviors (Barth et al., 2005; Facchin et al., 2009) and, perhaps, reversed eye use preferences (Barth et al., 2005). Thus, the formation of the parapineal organ is a decisive event in the

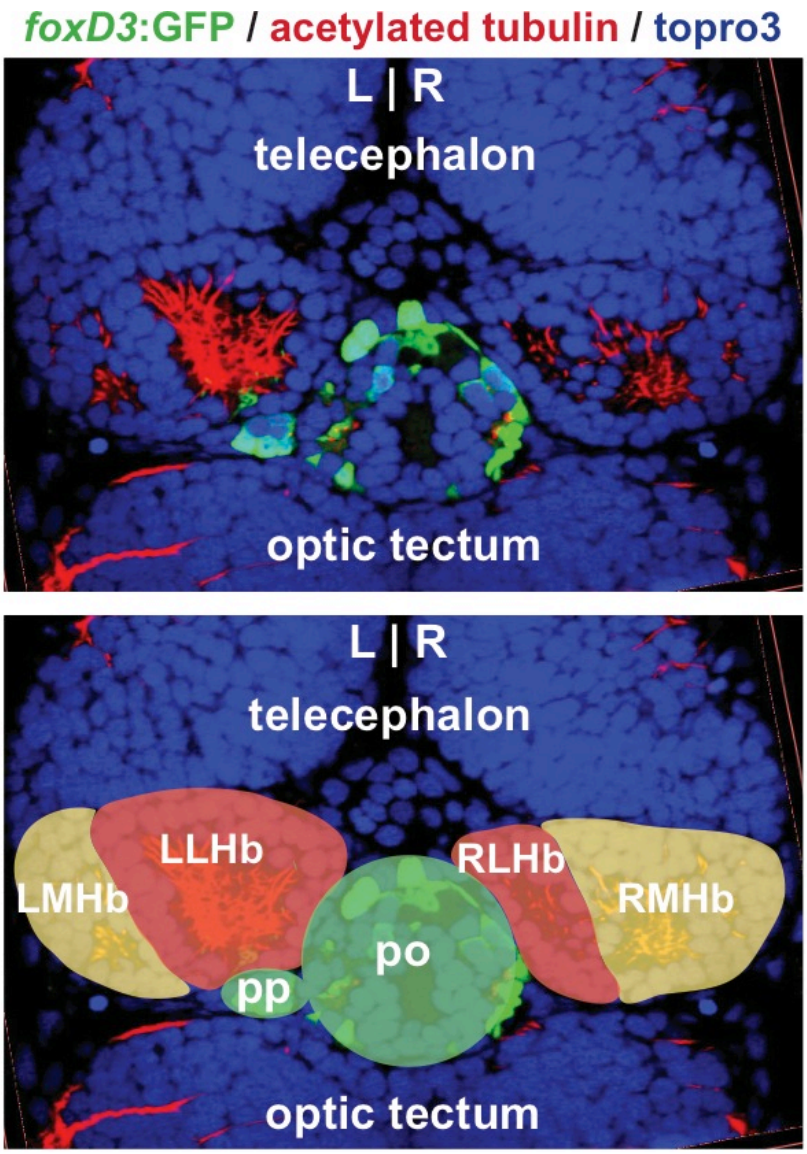

Figure 1. The zebrafish epithalamus exhibits robust Left-Right (L-R) asymmetry. The medially located pineal complex is composed of the pineal organ (po) and the parapineal organ (pp). The parapineal organ is almost always found on the left side of the brain. The pineal complex is flanked by the habenular nuclei. L-R asymmetry is present among the lateral and medial subunits of the habenular nuclei. The left lateral habenula (LLHb) is larger than the right lateral habenula (RLHb). Conversely, the right medial habenula (RMHb) is larger than the left medial habenula (LMHb)

creation of an L-R asymmetric epithalamus, which is likely instrumental in governing aspects of normal zebrafish behavior. The zebrafish epithalamus offers, perhaps, the best opportunity to study how these anatomical and molecular asymmetries could form within the vertebrate brain. Understanding the formation of these asymmetries and their roles in governing normal behavior might be broadly applicable to other vertebrates.

Formation of the Zebrafish Pineal Complex

The zebrafish pineal complex arises during development from a region of the neural plate fated to become diencephalon, which is a subdivision of the embryonic forebrain just posterior to the future telencephalon and just anterior to the developing midbrain (Woo and Fraser, 1995; Staudt and Houart, 2007) (Fig. 2). Fate mapping of late gastrulation embryos by approximately 10 hours post fertilization (hpf) and transplantation assays have revealed that diencephalic progenitors are already regionally patterned within the neural plate prior to neural keel formation (Staudt and Houart, 2007). At this stage, the epithalamic progenitors that will become the pineal complex are located in two, bilateral domains on the lateral margins of the neural plate just posterior to the preoptic area and anterior to the future tegmentum (Masai et al., 1997; Staudt and Houart, 2007). The earliest indication of pineal complex progenitors is the expression of floating head (*flh*), a homeodomain transcription factor (Masai et al., 1997; Snelson et al., 2008a). *flh* expression is first detectable in the forebrain at 80-90% epiboly (approximately 9 hpf) in bilateral domains on the neural plate in a region

consistent with the location of the pineal complex progenitors in diencephalic fate maps. The anterior limit of the pineal complex anlage is governed by Wnt/β-catenin signaling. In strong mutants for Axin1, a key component of the β-catenin destruction complex, ectopic *flh* expression extends anteriorly into the forebrain (Masai et al., 1997). The dorsal-ventral (D-V) limits of the pineal complex depend on precise levels of Bone Morphogenic Protein (Bmp). Moderate loss of Bmp2b activity expands the *flh* expression domain ventrally while a more complete loss of Bmp activity strongly reduces *flh* expression (Barth et al., 1999). As the neural plate folds to form the neural rod by approximately 12-somite stage (approximately 14 hpf), the two lateral *flh* expressing domains fuse to form a medial pineal complex anlage (Snelson et al., 2008a). Previous data suggests that parapineal precursor cells are likely specified prior to the 15-somite stage from a common group of progenitors called the pineal complex anlage (Masai et al., 1997; Snelson et al., 2008a). Parapineal precursor cells are likely specified bilaterally of the pineal complex anlage as a small parapineal organ still forms on both the left and right side of the brain when neural tube closure does not occur (Lu et al., 2013). In addition to the parapineal, the pineal complex anlage gives rise to the projection neurons, rod photoreceptors, and cone photoreceptors of the pineal organ (Masai et al., 1997; Cau and Blader, 2009; Quillien et al., 2011). All pineal complex cell types undergo their final mitotic division in a similar time span between 15 and 24 hpf (Cau et al., 2008; Snelson et al., 2008c). The generation of the proper numbers of the four different cell types (parapineal, pineal rod photoreceptor, pineal cone photoreceptor, and pineal projection

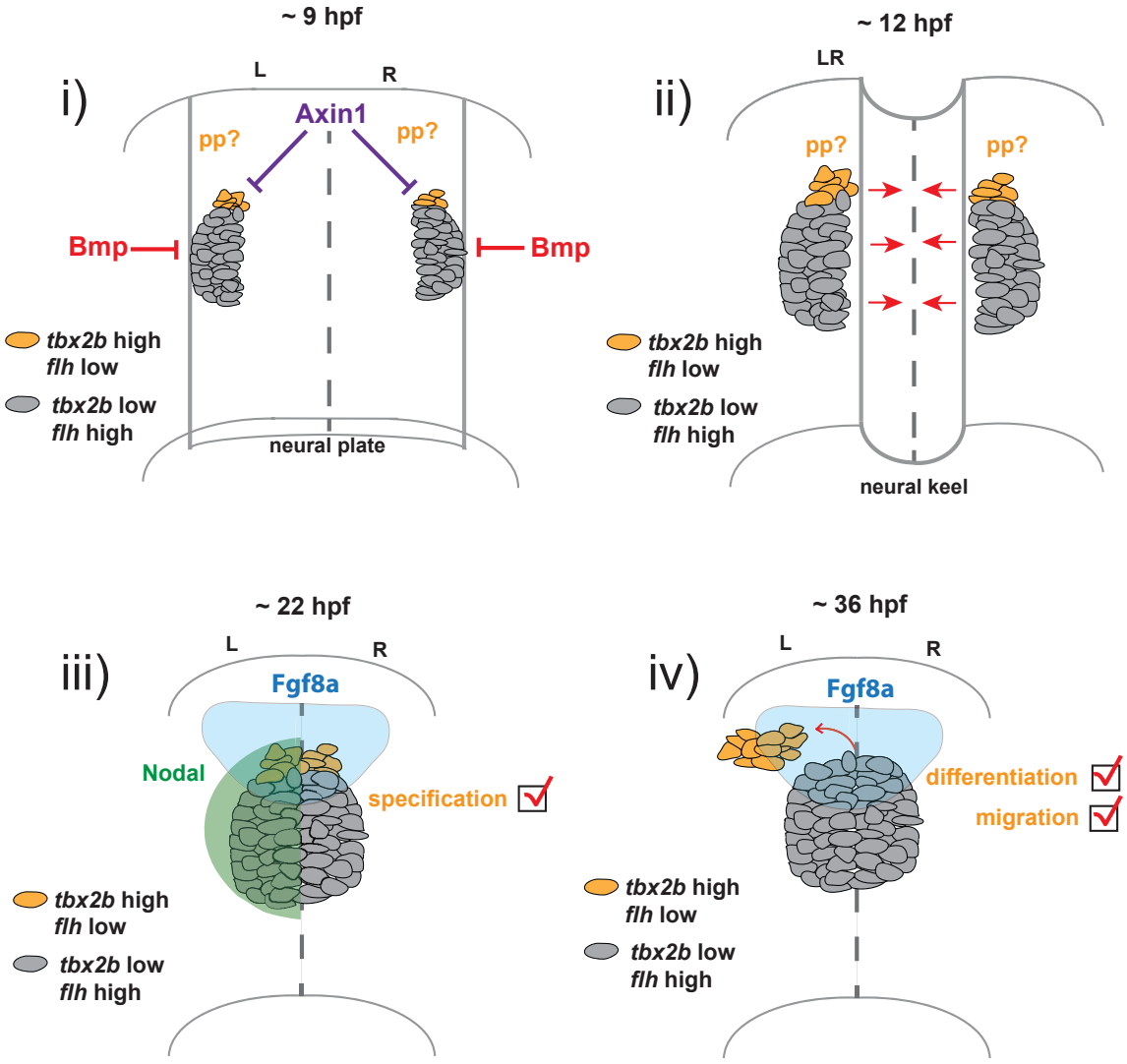

Figure 2. Pineal complex development. i) Pineal complex progenitors arise from a *flh* expressing domain on the lateral edges of the neural plate at approximately 90% epiboly (9 hpf). The *flh* positive domain is positioned mediolateraly by Bmp activity and anteriorly by Wnt activity. Some parapineal precursors might be specified by this time due to initiation of *tbx2b* expression in the anterior pineal complex anlage. ii) As neural keel formation progresses, the "two halves" that will become the pineal complex anlage are brought closer together. *tbx2b* is maintained in the pineal complex suggesting some parapineal precursors have been formed. iii) By approximately 22 hpf, the pineal complex anlage has fused. Left sided Nodal signaling is also occurring in the epithalamus. *fgf8a* expression is evident in the anterior epithalamus. Parapineal precursors are post mitotic suggesting specification has occurred. iv) Continued expression of *fgf8a* in the epithalamus encourages migration of differentiated parapineal cells.

neuron) from the pineal complex anlage depends on the activity of two different transcription factors, T-box containing transcription factor 2b (Tbx2b) and Floating head (Flh), as well as input from the Notch and Bmp pathways (Masai et al., 1997; Cau et al., 2008; Snelson et al., 2008a; Snelson et al., 2008c; Quillien et al., 2011). In *flh* mutants, neurogenesis in the pineal organ is dramatically reduced, resulting in a small pineal organ with less than half the number of projection neurons and photoreceptors of wild-type (WT) individuals (Masai et al., 1997; Cau and Wilson, 2003; Carl et al., 2007; Snelson et al., 2008a). However, *flh* mutants develop a parapineal organ with an appropriate number of cells (Snelson et al., 2008a). The Bmp and Notch pathways coordinately regulate the decision between photoreceptor and projection neuron cell fates (Cau et al., 2008; Quillien et al., 2011). Parapineal cell fate depends on Tbx2b. In homozygous *tbx2b*^{c144} mutants, parapineal formation is disrupted but pineal neurogenesis appears mostly intact with the number of photoreceptors and projection neurons in the pineal organ similar to WT (Snelson et al., 2008a; Snelson et al., 2008c). Tbx2b mutants seem to specify fewer parapineal precursors; additionally, the few remaining parapineal neurons fail to migrate away from the midline (Snelson et al., 2008c). The directionality of the migration of parapineal cells seems to be largely governed by Nodal and Fibroblast growth factor (Fgf) signaling. The Nodal pathway is well known for L-R patterning of the vertebrate mesoderm leading to asymmetric placement of internal organs. In zebrafish, the expression of *nodal-related 2* (*ndr2*), also known as *cyclops* (*cyc*), is initiated on the left side of the epithalamus during late somitogenesis

(approximately 20-24 hpf) (Rebagliati et al., 1998; Concha et al., 2000; Liang et al., 2000). This left-sided Nodal expression effectively biases parapineal cell migration to the left in better than ninety percent of wild-type larvae (Concha et al., 2003; Gamse et al., 2003) but has no apparent impact on parapineal cell number (Concha et al., 2003). One putative model suggests that left sided Nodal activity leads to precocious neurogenesis in the left habenular precursors relative to the right, which somehow attracts the migrating parapineal cells (Roussigne et al., 2009). Disruptions in left sided Nodal signaling leads to randomization of the parapineal organ, which will emerge on the left or right side of the brain with equal frequency (Concha et al., 2003). It is possible that parapineal randomization could be driven by early habenular neurogenesis that occurs earlier in one habenula (either left of right) stochastically. This process also seems to involve Fgf8a, which in the absence of Nodal signaling, can lead the parapineal away from the midline (Regan et al., 2009).

tbx2b and *flh* are both expressed around 10 hpf which is quite early in pineal complex. Also, pineal organ neurogenesis fails by approximately 17 hpf in *flh* mutants resulting in fewer pineal cells (Masai et al., 1997; Snelson et al., 2008a). Additionally, most parapineal precursors appear to be born by 15 hpf suggesting they have already been specified by this point (Snelson et al., 2008a). Taken together, this suggests that pineal and parapineal fate has somewhat diverged by about 17 hpf. However, the earliest indicator of parapineal formation is the migration of the parapineal cells away from the midline and out of the pineal organ anlage (Gamse et al., 2003; Snelson et al., 2008c). As a result, we

sought to identify factors involved during later stages of parapineal development. One candidate(s) for involvement in parapineal cell formation is the Fgf pathway. Fgf ligands and receptors are expressed in the epithalamus of zebrafish and other vertebrates (Crossley and Martin, 1995; Crossley et al., 1996; Reifers et al., 1998; Reifers et al., 2000; Echevarria et al., 2003). Previous work has shown that Fgf8a can promote migration of the parapineal away from the dorsal midline (Regan et al., 2009). However, a role for Fgf signaling in controlling cell fates within the pineal complex anlage was not examined.

Fgfs have well documented roles in the regional pattering, cell division and survival, and migration during vertebrate neurogenesis (Guillemot and Zimmer, 2011). In both the hindbrain and the telencephalon, certain Fgf ligands are thought to act as a morphogens, acting at a distance from the site of expression and generating a signaling gradient that specifies different neuronal fates based on the levels of Fgf signaling (Sansom and Livesey, 2009); (Nakamura et al., 2008). Reducing Fgf signaling in the mid-hindbrain boundary leads to progressive loss of the cerebellum. Likewise, ectopic Fgf signaling in the midbrain causes expansion of the anterior hindbrain at the expense of midbrain structures.

Recently, evidence for a role for Fgf signaling in the epithalamus has emerged. In mice, knocking out Fgf8 results in near complete loss of the dorsal habenular nuclei, as well as most of the pineal organ (Martinez-Ferre and Martinez, 2009). Similarly, *fgf8a*^{ti282a}, a strong hypomorphic *fgf8a* mutant, exhibits deficits in differentiated habenular neurons and neuropil (Regan et al., 2009). Fgf8 knockout mice exhibit deficits in many epithalamic cell types including the

pineal organ and the habenular nuclei (Martinez-Ferre and Martinez, 2009). If Fgf signaling could specify different cell types based on level of activity, then a more complete loss of Fgf8a might reveal additional roles for Fgf signaling in governing cell fate in the pineal complex.

In addition to Fgf signaling, Bmp activity also works to specify pineal photoreceptors while inhibiting the formation of projection neurons. Bmp and Fgf are often involved in pattering the same tissues. Therefore, these two signaling pathways may act to regulate the formation of the parapineal organ. To test if Fgf signaling had a role, in addition to influencing migration, in governing parapineal fate we analyzed the effects of loss and gain of Fgf function on parapineal cells. We found that Fgf signaling influences the cell fate choice among specified parapineal precursors. If Fgf activity is reduced, either through mutation of small molecule inhibition of Fgf receptors, cells that have been specified by Tbx2b to give rise to the parapineal organ become pineal cone photoreceptors instead. This binary cell fate decision occurs does not involve Bmp activity. Reducing Bmp activity in *fgf8a*^{x15} mutants cannot suppress the loss of differentiated parapineal cells or the ectopic increase in cone cell number. Preliminary data suggests that LIM-homeobox (Lhx) transcription factors 2b and 9 are responsive to Fgf signaling. Also, over-expressing Lhx9 can partially rescue parapineal cell number in *fgf8a* mutants. In total, our total suggests that Fgf signaling governs parapineal differentiation by inducing the expression of *lhx2b* and *lhx9*.

CHAPTER II

FGF SIGNALING GOVERNS DIFFERENTIATION OF PARAPINEAL CELLS IN ZEBRAFISH

Preface

Portions of this chapter were accepted for publication in the *Journal of Visualized Experiments* under the name “Lineage labeling of zebrafish cells with laser uncagable fluorescein dextran” by Clanton et al. 2011 (vol. 50, doi: 10.3791/2672) and in the journal *Development* under the name “Fgf signaling governs cell fate in the zebrafish pineal complex” by Clanton et al. 2012 (vol.140, pg. 323-32).

Introduction

In most vertebrates analyzed, Fgf8 and Fgf17 are expressed in both the rostral and the mid-hind brain organizing centers, which are brain regions crucial for neural patterning during brain development (Sansom and Livesey, 2009). Similarly, Fgf8 is required for the proper development of the epithalamus in the mouse. Fgf8 knock out mice exhibit the loss of most cells of the habenula and much of the pineal organ (Martinez-Ferre and Martinez, 2009). Contrary to the epithalamic phenotype seen when Fgf8 is lost in the mouse, the pineal complex is largely intact in *fgf8a* mutant zebrafish suggesting the role of Fgf signaling may only be evolutionarily conserved with regards to habenular development

(Martinez-Ferre and Martinez, 2009; Regan et al., 2009). To further investigate the role for Fgf in the pineal complex, we performed gain-and loss-of-function experiments in zebrafish. We found that Fgf signaling is required between 18 and 30 hpf to ensure parapineal cell formation. However, excess Fgf signaling was insufficient to produce supernumerary parapineal cells. When Fgf signaling was reduced, there was an increase in the number of pineal cone photoreceptors at the expense of parapineal cells. Data obtained from the combined loss of Flh and Fgf8a, as well as cell fate analysis, revealed that the cells of the anterior pineal complex anlage, which give rise to the parapineal organ in wild-type larvae, instead produced cone photoreceptors in *fgf8a* mutants. Epistasis analysis with Tbx2b revealed that both genes are required for parapineal cells to differentiate but only *fgf8a* is required to prevent their differentiation as cone photoreceptors. We conclude that, unlike its typical morphogenic role in brain patterning, Fgf signaling acts permissively on bipotential parapineal precursors to resolve a cell fate decision between parapineal and cone cell fate.

Methods

Zebrafish

Zebrafish were raised at 28.5°C on a 14/10 hour light/dark cycle and staged according to hpf. The following wild-type, mutant, and transgenic fish lines were used: AB** (Walker, 1999),* *fgf8a*^{x15} (Kwon and Riley, 2009), *tbx2b*^{c144} (Snelson et al., 2008c), Tg[*foxd3*:*GFP*]^{zf104} (Gilmour et al., 2002), Tg[*hsp70*:*fgf8a*]^{b1193} (Hans et al., 2007), and Tg [*flh*BAC:*kaede*]^{vu376} (Clanton et al., 2013). For 18 hpf

SU5402 treatments, embryos were raised for approximately 10-12 hours at 25°C.

in situ hybridization

Whole-mount RNA *in situ* hybridization was performed as described previously (Gamse et al., 2003), using reagents from Roche Applied Bioscience. RNA probes were labeled using fluorescein-UTP or digoxingenin-UTP. To synthesize antisense RNA probes, pBS-*otx5* (games 2002) and pBS-*gfi1.2* (Dufourcq et al., 2004) were linearized with SacII and transcribed with T3 RNA polymerase; pBSII SK-*fgfr4* with EcoRI and T7 polymerase; pCRII-*fgfr3* with SpeI and T3 polymerase; pCRII-*fgfr2* with EcoRV and SP6 polymerase; pCRII-*fgfr1* with HindIII and T7 polymerase; pBSII SK-*erm* with NotI and T7 polymerase; pENTR-D-Topo-*sox1a* with NotI and T7 polymerase. Anti-sense probe for *fgf17* was transcribed from pME18S-*fgf17* (Open Biosystems) by amplifying the open reading frame of *fgf17* from the plasmid with primers (5'-TCCTCAGTGGATGTTC-3') and (5'-TAATACGACTCACTATAGGG-3'). The reverse primer contains a T7 binding sequence that facilitates antisense probe transcription from the PCR product (Thisse and Thisse, 2008). Embryos were incubated at 70°C with probe and hybridization solution containing 50% formamide. Hybridized probes were detected using alkaline phosphatase-conjugated antibodies (Roche) and visualized by 4-nitro blue tetrazolium (NBT) (Roche) and 5-bromo-4-chloro-3-indolyl-phosphate (BCIP) (Roche) staining for single labeling, or NBT/BCIP followed by iodonitrotetrazolium (INT) and BCIP staining for double labeling. In fluorescent *in situ* hybridization, staining was developed in a 1:1 ratio of fast red tablet (Sigma) to fast red buffer (0.1M Tris

pH8.2, 0.4M $NaCl_2$) at 37°C. Antibody labeling of fluorescent *in situ* was carried out using 1:500 of rabbit anti-GFP (Torrey Pines) or 1:500 of rabbit anti-Kaede (MBL). Secondary labeling was done with 1:300 anti rabbit Alexa 488 (Invitrogen).

Cloning

Full-length *sox1a* transcript was cloned from total RNA from 24 hpf AB* embryos dissolved in Trizol (Invitrogen). Total cDNA was made from phenol-chloroform purified total RNA with random hexamer (Applied Biosystems) priming and Superscript III reverse transcriptase (Invitrogen). *sox1a* transcript was amplified using the following primers: Fw-CACCACTGGCTACAGGAGCGAAAA with the 5' CACC sequence to facilitate entry into pENTR-D-Topo vector (Invitrogen); Rv-CAGAAACGCTGTCAGGATCA. Amplified product was agarose gel purified with Wizard SV Gel and PCR clean up system (Promega). Purified *sox1a* transcript was inserted into pENTR-D-Topo vector via Topo-TA cloning reaction and transformed into One Shot Top10 cells (Invitrogen) on ampicillin containing agar plates overnight at 37°C. Bacterial containing colonies containing construct were expanded and the plasmid was harvested using Pure Yield Plasmid Midi Prep System (Promega).

Cryosectioning

After whole mount *in situ* hybridization, embryos were embedded in 1.5% agarose, 5% sucrose media. Blocks containing embedded embryos were excised, equilibrated overnight at 4°C in 30% sucrose, and frozen using 2-methylbutane chilled with liquid nitrogen. Frozen blocks were sectioned with a Leica CM1850 cryostat at a thickness of approximately 10-12μM.

Whole mount antibody labeling

Embryos and larvae were fixed in AB fixative (4% paraformaldehyde, 0.3mM $CaCl_2$, 4% sucrose, 1X PBS) for either 4 hours at room temperature (25°C) or overnight at 4°C with rocking. Samples were rehydrated with three successive 5-minute washes with 1XPBSTx (1X PBS, 0.01% Triton X100) and four 20-minute washes with deionized water. Samples were blocked one hour at room temperature in 10% AB block (10% sheep serum, 1mg/mL Bovine Serum Albumin in 1X PBSTw). Samples were incubated with primary and secondary antibodies in 2% AB block overnight with rocking at 4°C. Excess antibody was washed off with 1XPBSTx. Primary antibodies used: 1:1000 rabbit anti-GFP (Torrey Pines), 1:1000 rabbit anti-Kaede (MBL), 1:500 mouse anti-ZPR1(Arrestin3a) (Developmental Studies Hybridoma Bank), 1:500 mouse anti-Opsin1 (Developmental Studies Hybridoma Bank), 1:200 mouse anti-HuC/D (Invitrogen). Secondary antibodies used: 1:300 Alexa 488 goat anti-rabbit (Invitrogen), 1:300 Alexa 568 goat anti-mouse (Invitrogen). Embryo nuclei were counterstained with TOPRO-3 (Invitrogen). All confocal images were taken with Zeiss LSM 510 microscope and processed using Improvision Velocity software.

Heat Shock Conditions

Embryo clutches containing both heterozygous Tg[*hsp70l:fgf8a*]^{b1943} transgenic embryos and their non-transgenic siblings (still in their chorions) were placed in a 2mL microcentrifuge tube (35-40 embryos/tube). Approximately 2mL of pre-warmed egg water containing 0.3% PTU was added per tube. Tubes were incubated in a 37°C water bath then removed and emptied into a dish in a 28.5°C

incubator. *fgf8a* was induced by single heat shock treatment at different intervals from approximately 12-somites stage to 30 hpf, or by multiple short heat shocks at 37°C between 18-somites stage and 30 hpf. In addition, continuous low-temperature heat shock for six hours or 15 hours was performed as above, but at lower temperatures (30°C or 32°C).

Caged fluorescein injection, uncaging, and detection

One-cell stage Tg[*foxd3*:*GFP*]^{zf104}; Tg[*flh*BAC:*Kaede*]^{vu376} double transgenic embryos were injected with 0.5nL of a 1% DMNB-caged fluorescein-dextran solution. Caged fluorescein dextran was synthesized as previously described (Clanton et al., 2011). Injected embryos were kept in the dark until laser uncaging was performed. Embryos were anesthetized with 4% tricaine and mounted in 0.8% agarose in egg water containing 1XPTU. Fluorescein was uncaged using 10-20 pulses of a 365 nm laser (Spectra Physics) on a Leica 6000M compound microscope fitted with a 40x water immersion objective. Embryos were fixed overnight at 4°C in AB fix and dehydrated with 100% MeOH overnight at -20°C. Embryos were re-hydrated in successive, five-minute washes of decreasing MeOH/increasing 1XPBT concentration. Samples were permeabilized with 10μg/μl of Proteinase K (Roche Applied Biosciences) and re-fixed for 20 minutes in AB fix. Embryos were blocked in 1XPBTxS (1XPBS, 10% Sheep serum and BSA, 0.01% DMSO) for one hour at room temperature. Embryos were incubated primary and secondary antibodies in 1XPBTxS overnight at 4°C. Excess antibodies were removed with washes in 1XPBTX. Primary antibodies used: 1:500 rabbit anti-GFP (Torrey Pines), 1:250 mouse anti-ZPR1 (Developmental

Studies Hybridoma Bank), 1:500 goat anti-fluorescein (Invitrogen). Secondary antibodies used: 1:300 Alexa 488 donkey anti-rabbit (Invitrogen), 1:300 Alexa 568 donkey anti-mouse (Invitrogen), and 1:300 Alexa 633 donkey anti-goat (Invitrogen).

Morpholino Injection

Embryos were injected at the one cell stage. The following morpholinos were used in this study: *tbx2b* splice blocking morpholino (5'-AAAATATGGGTACATACCTTGTCGT-3') (Snelson et al., 2008c); *flh* MO (5'-AATCTGCATGGCGTCTGTTTAGTCC-3').

Inhibitor Treatments

For *in situ* hybridizations and whole mount antibody labeling, we incubated embryos in their chorions in 12μM SU5402 (Calbiochem and Tocris) dissolved in 0.3% DMSO in egg water in 1XPTU in the dark. Control embryos were treated with 0.3% Dimethyl sulfoxide (DMSO) in parallel with their SU5402 treated siblings. 6μM SU5402 (Calbiochem and Tocris) dissolved in 0.3% DMSO in egg water in 1XPTU in the dark. Control embryos were treated with 0.15% Dimethyl sulfoxide (DMSO) in parallel with their SU5402 treated siblings. For lineage labeling, dechorionated embryos were treated with 8μM SU5402 (we found that dechorionated embryos were more sensitive to the drug treatment). For these experiments, control embryos were treated with 0.2% DMSO.

Results

Fgf Ligands, Receptor, and a Target Gene are Expressed in the PinealComplex Anlage

Previous work showed that *fgf8a* and *fgf17*, two ligands in the Fgf family, are expressed in the epithalamus (Reifers et al., 1998; Reifers et al., 2000; Itoh, 2007; Jovelin et al., 2007; Regan et al., 2009). However, the expression of these ligands has not been analyzed relative to molecular markers of the pineal complex anlage at stages beyond 24 hpf. To accurately detect the expression of Fgf pathway components within the epithalamus at a high resolution by confocal microscopy, we used fluorescent *in situ* hybridization (FISH) in combination with immunofluorescence. The transgenes, Tg[*foxd3*:*GFP*]^{zf104} (Gilmour et al., 2002) and Tg[*flh*BAC:*Kaede*]^{vu376} (Clanton et al., 2013) together label all cells of the pineal complex anlage and its derivatives, the pineal organ and parapineal organ. In contrast to *fgf8a* and the *fgf receptors*, transcripts for *fgf17* and *erm* (*ets related molecule*), which is a downstream transcriptional target of Fgf signaling (Roehl and Nusslein-Volhard, 2001), are not abundant enough to permit traditional FISH methods (Clay and Ramakrishnan, 2005). Thus, the expression of these genes was detected with two-color chromogenic *in situ* hybridization.

At 24hpf, *fgf8a* expression encompasses the anterior pineal complex with slight enrichment at the midline (Fig.3A). An optical cross section reveals that *fgf8a* expression extends 2-3 cell diameters inside the anterior pineal complex (Fig.3A'). At 30 hpf, *fgf8a* continues to be expressed in the anterior pineal complex, including the parapineal cells that are beginning to separate from the pineal complex anlage (Fig 3B and 3B'). At this time significant expression of

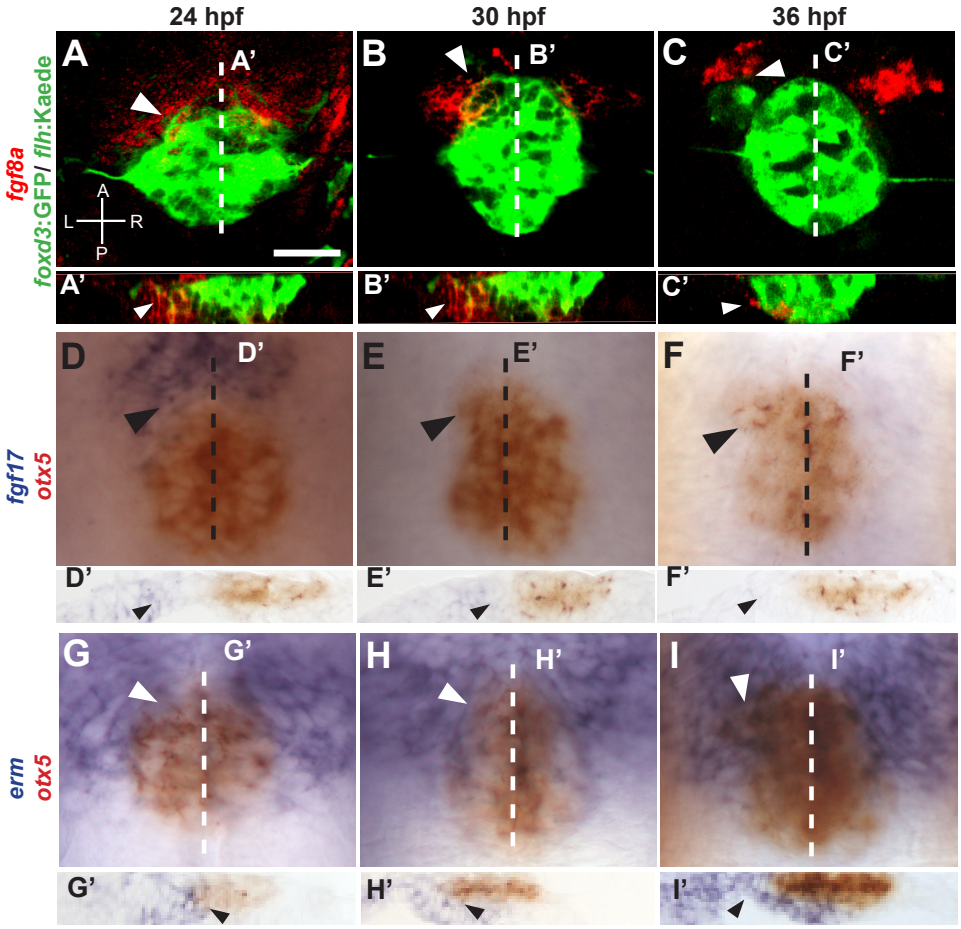

Figure 3. Fgf components are expressed in the epithalamus during parapineal formation. (A-C) *fgf8a* (red) is expressed in the anterior pineal complex (white arrows) of *foxd3*:GFP/*flhBAC*:Kaede (green) expressing embryos during parapineal development. Dashed line indicates the plane of section. (A'-C') Optical cross sections. *fgf8a* is expressed in the ventral region of the anterior pineal complex anlage (white arrows). (D-F) Dorsal views of *in situ* hybridizations of *fgf17* (blue) relative to the pineal complex (*otx5*, red). *fgf17* is expressed in the anterior pineal complex (black arrows) at 24 hpf, but is almost gone by 30 and 36 hpf. Dashed line indicates plane of sectioning. (D'-F') Cryosections show that *fgf17* expression is evident in the region ventral to the anterior pineal complex anlage (black arrows) at 24 hpf. (G-I) Dorsal views of *in situ* hybridization of *erm* (blue) relative to the pineal complex anlage (*otx5*; red). *erm* expression shows that Fgf signaling activity is high in the anterior pineal complex (white arrows). White dashed lines indicate the plane of sectioning. (white arrows). (G'-I') Cryosections of i*n situ* hybridizations of *erm*. *erm* is detected in the anterior pineal complex anlage at all stages (black arrows). Scale bar in A: 25 micrometers.

fgf8a is also present in cells found directly to the left and right sides of the anterior pineal complex, which are probably habenular precursor cells (Concha et al., 2003) (Fig. 3B). By 36hpf, *fgf8a* is mostly excluded from the migrating parapineal, and is expressed primarily in cells anterior and lateral to the pineal complex, likely the habenular precursor cells (Fig.3C and3C').

Like *fgf8a*, *fgf17* is expressed in the anterior one-third of the pineal complex indicated by *otx5* expression (Gamse et al., 2002) (Fig.3D,D'). A longitudinal cryosection shows that *fgf17* transcripts are present within the anteriormost several cell diameters of the pineal complex anlage (Fig.3D'). However, at 30 hpf and 36 hpf, *fgf17* expression is almost undetectable in the epithalamus, with only a low level of transcript visible in a few cells near the pineal complex (Fig.3E,E',F,F'). In summary, *fgf17* and *fgf8a* are both expressed in anterior pineal complex anlage where parapineal cells are present at 24 hpf (Concha et al., 2003), but only *fgf8a* persists in parapineal precursors at 30 hpf. Fgf signaling is necessary and sufficient to induce expression of the gene *erm*, making it a convenient readout of Fgf signaling (Roehl and Nusslein-Volhard, 2001). The expression of *erm* in the pineal complex anlage is very robust at the anterior-most aspect, where parapineal precursors are located, indicating that these cells are responding to high levels of Fgf signaling at 24, 30, and 36hpf (Fig. 3G,G',H,H',I,I').

Once secreted, Fgf ligands can bind to and activate any of four Fgf receptors (Bottcher and Niehrs, 2005). To identify which receptors could transduce Fgf8a and Fgf17 signals in the epithalamus, we examined the

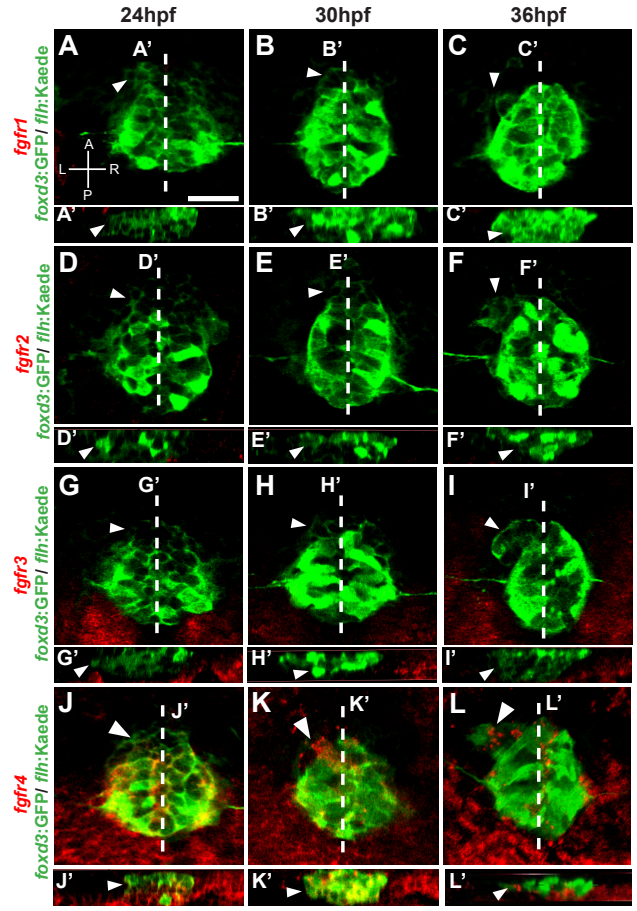

Figure 4. *fgfr4* is the only fgf receptor expressed in the epithalamus during parapineal formation. (A-C) Dorsal views of the embryos expressing both *foxd3*:GFP and *flh*BAC:Kaede at 24 hpf, 30 hpf, and 36 hpf. The white dashed line indicates approximate plane of section with approximate position of parapineal precursors labeled (white arrows). (A'-C') Confocal sections through the pineal complex of *foxd3*:GFP/*flh*BAC:Kaede expressing embryos at 24 hpf, 30 hpf, and 36 hpf. (D-F) Dorsal views of the embryos expressing both *foxd3*:GFP and *flh*BAC:Kaede at 24 hpf, 30 hpf, and 36 hpf. The white dashed line indicates approximate plane of section. (D'-F') Confocal sections through the pineal complex of *foxd3*:GFP/*flh*BAC:Kaede expressing embryos at 24 hpf, 30 hpf, and 36 hpf. (G-I) Dorsal views of the embryos expressing both *foxd3*:GFP and *flh*BAC:Kaede at 24 hpf, 30 hpf, and 36 hpf. The white dashed line indicates approximate plane of section. (G'-I') Confocal sections through the pineal complex of *foxd3*:GFP/*flh*BAC:Kaede expressing embryos at 24 hpf, 30 hpf, and 36 hpf. (J-L). Confocal projections show *fgfr4* (red), a likely receptor for Fgf ligands in the epithalamus, is expressed within the pineal complex anlage (*foxd3*:GFP/*flh*BAC:Kaede) including the anterior portion (white arrows). (J'-L') Optical cross sections of the pineal complex show *fgfr4* expression in the pineal complex anlage even near parapineal precursors (white arrows). Scale bar in A: 25 micrometers

expression of all four *fgf receptor* (*fgfr*) genes. *fgfr1*, *fgfr2*, and *fgfr3* were not highly expressed in the vicinity of the pineal complex between 24 and 36 hpf (Fig. 4A-4I, Fig. 4A'-1I'). However, non-fluorescent *in situ* hybridizations showed that *fgfr1* transcripts are expressed diffusely throughout the brain (data not shown). In addition, *fgfr3* is expressed more posteriorly and ventrally in the diencephalon, but not in the pineal complex anlage between 24 and 36 hpf (Fig. 4G-4I, 4G'-4I'). We did detect *fgfr4* expression in the pineal complex between 24 and 36 hpf. Therefore, *fgfr4* is the likely receptor for Fgf8a and Fgf17 during parapineal development.

Attenuating Fgf Signaling Disrupts Parapineal Formation

To quantify the effect of Fgf8a loss on parapineal development, we examined the expression of *sex determining Y-box 1a* (*sox1a*) and *growth factor inhibited 1.2* (*gfi-1.2*) expression in *fgf8a*^{x15}, a null allele of *fgf8a* (Kwon and Riley, 2009). Since *sox1a* expression in the epithalamus had not previously been examined in detail, we characterized its expression during time points relevant to parapineal development. In WT, *sox1a* expression can first be reliably detected at approximately 26 hpf in a few cell in the anterior pineal complex anlage (Fig. 5A). By 28 hpf, *sox1a* is expressed in a cluster of cells spanning the midline of the anterior pineal complex (Fig.5B), similar to the placement of parapineal cell precursors at 24 hpf (Concha et al., 2003; Clanton et al., 2013). The *sox1a* expressing cells are found clearly to the left of the midline at 36 hpf; by 48 hpf, *sox1a* is co-expressed with Tg[*foxd3*:GFP]^{zf104} in a group of cells to the left of

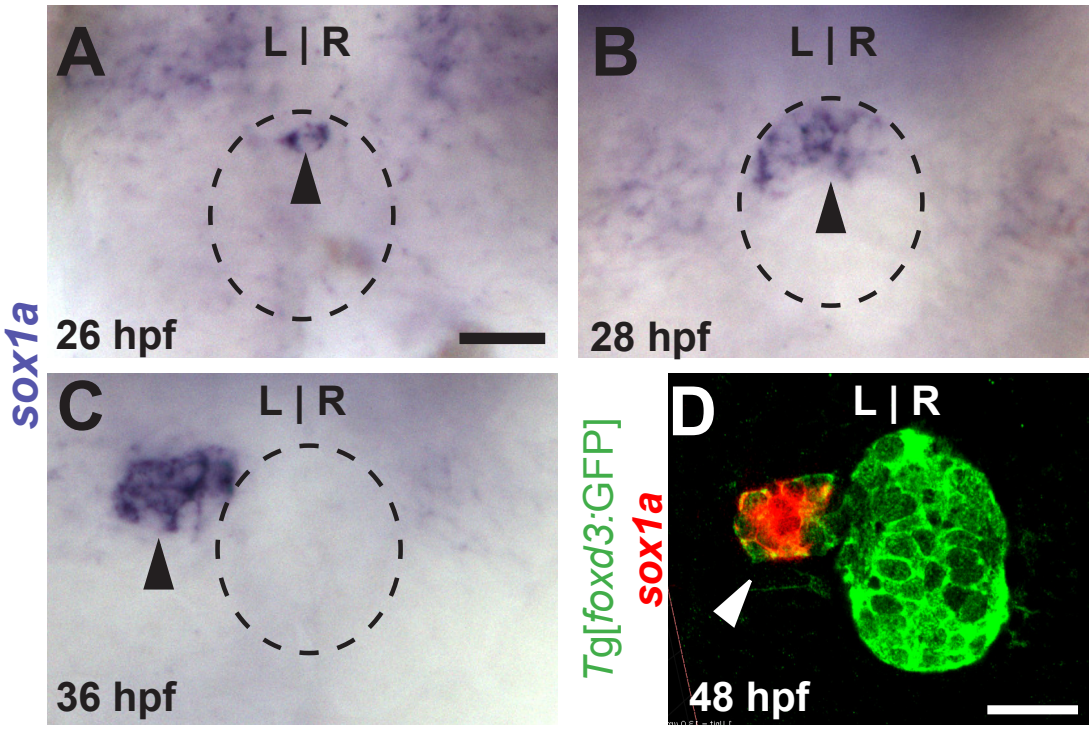

Figure 5. *sox1a* is expressed in parapineal cells near their time of differentiation. All images are from dorsal view**.** (A) *sox1a* expression (black arrow) in WT pineal complex anlage (dotted circle). (B) A cluster of *sox1a* expressing cells are in anterior pineal complex anlage at 28 hpf WT embryos. (C) By 36 hpf, *sox1a* expression is present to the left of the pineal anlage suggesting it is indeed expressed in parapineal cells. (D) Confocal slice of 48 hpf WT larvae showing co-localization of *sox1a* (white arrow) and Tg[*foxd3*:GFP] confirming *sox1a* is expressed in parapineal cells. (Scale bar in A: 20 micrometers. Scale bar B: 25 micrometers. Scale bar in C: 20 micrometers.

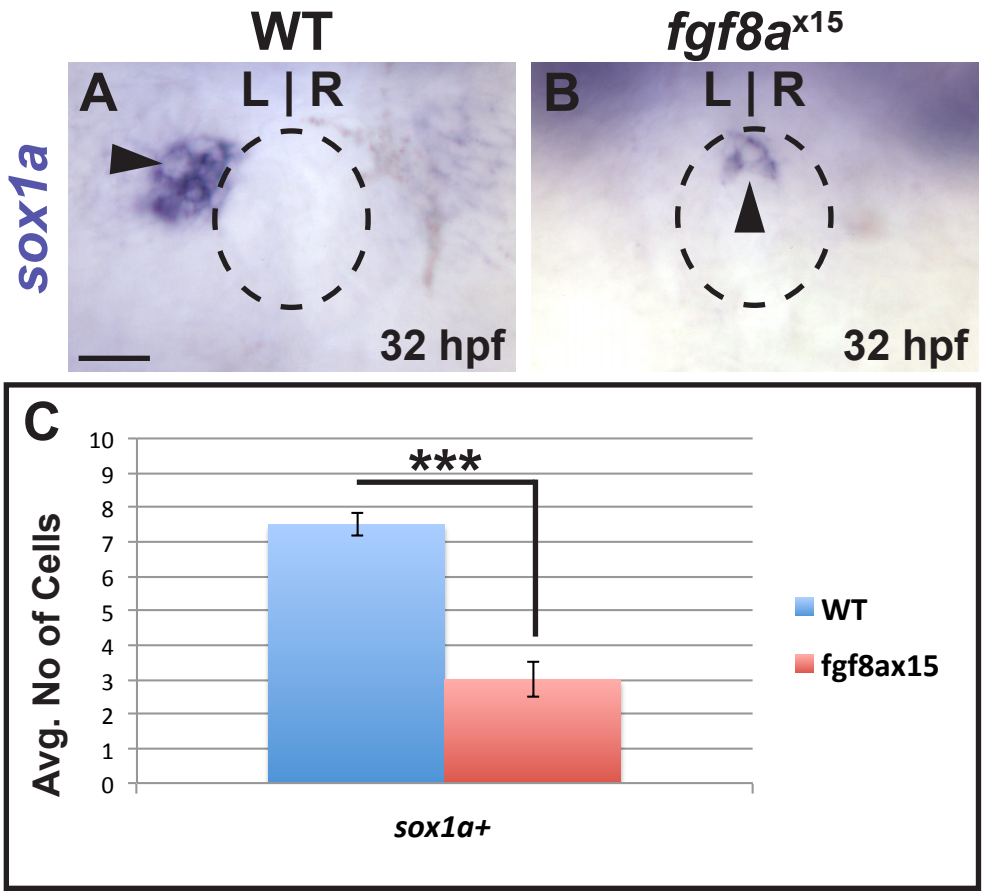

Figure 6. *fgf8a*^{x15} mutants have fewer newly differentiated parapineal cells. (A,B) *sox1a* expression (black arrows) in WT and *fgf8a*^{x15} mutants at 32 hpf. (C) Graph quantifying the number of *sox1a* expressing cells in WT and *fgf8a*^{x15} mutants at 32 hpf. and *fgf8a*^{x15} mutants have significantly reduced numbers of *sox1a* expressing cells (***p<0.0005 by t-test). Error bars represent S.E.M. Scale bar in A: 20 micrometers.

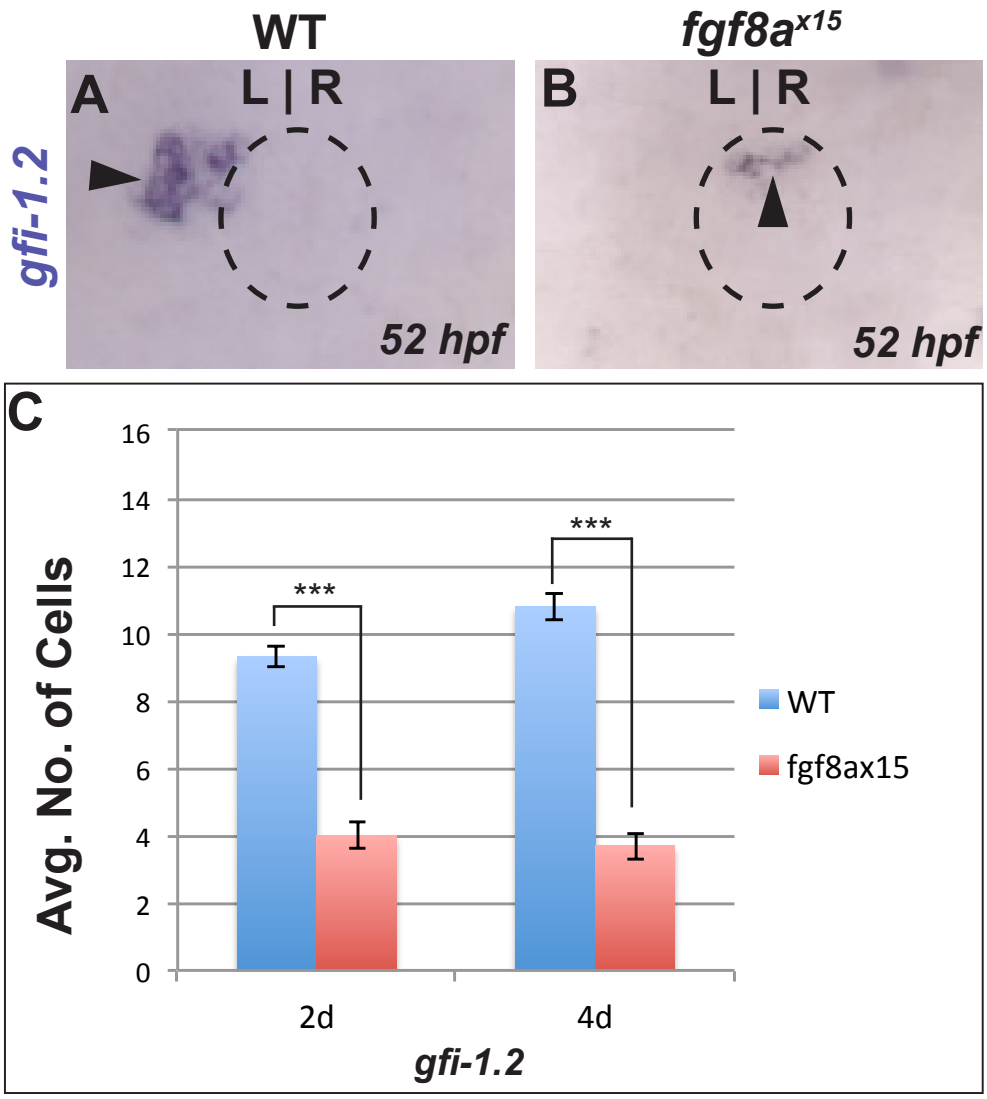

Figure 7. Loss of Fgf signaling results in fewer mature parapineal cells. (A,B) Dorsal views of 52 hpf wild-type and *fgf8a*^{x15} mutant embryos labeled with *gfi-1.2*, which is expressed in parapineal cells (black arrows). (C) The number of *gfi-1.2* expressing cells was quantified in wild-type and *fgf8a*^{x15} mutant larvae at 52 and 96 hpf. *fgf8a*^{x15} mutants displayed a significant reduction in parapineal cell number compared to WT. (***p=<0.0005 by t-test). Scale bar in A= 25 micrometers

the pineal complex, similar to *gfi-1.2* (Fig.5C,D). Thus, we conclude that *sox1a* is expressed specifically in parapineal cells just prior to migration and may be indicative of parapineal differentiation. Like *sox1a*, *gfi-1.2* expression in the epithalamus is restricted to the parapineal and is not present in other pineal complex cells (Dufourcq et al., 2004). However, *gfi-1.2* is not expressed in the parapineal until approximately 45 hpf (unpublished observations N.H de Borsetti), well after the parapineal cells have migrated away from the pineal complex anlage suggesting that it is expressed only in mature parapineal cells. At 32 hpf, *fgf8a*^{x15} mutants have fewer than half the number of *sox1a*-positive as WT embryos (3.0±0.5;n=17 and 7.5±0.3;n=16 respectively) (Fig.6A,B,C). Reduced expression of the early parapineal marker *sox1a* in *fgf8a*^{x15} mutants supports the idea that Fgf signaling is required for specification or differentiation of parapineal fate.

In wild-type embryos at 52 hpf, the parapineal is a distinct cluster of 9-12 cells (average 9.3±0.3, n=23) that is located to the left side of the pineal organ (Fig.7 A,C). *fgf8a*^{x15} mutants, by contrast, exhibit an almost sixty percent reduction in the number of *gfi-1.2* expressing cells (4.0±0.4; n=27) (Fig.7B,C). In addition, the remaining *gfi-1.2* expressing cells are located within the pineal organ and do not form a distinct parapineal organ, indicating that Fgf signaling is also required for parapineal cell migration to the left side of the brain, as previously reported (Regan et al., 2009). To eliminate the possibility that the reduction in the number of *gfi-1.2* expressing cells in *fgf8a*^{x15} mutants is simply a delay in parapineal formation, we also examined parapineal formation at 96 hpf.

The reduction of parapineal cells persists in *fgf8a*^{x15} mutants compared to wild-type siblings with an average of 3.7±0.4 (n=18) and 10.8±0.4 (n=18) cells respectively (Fig.7C) indicating that the mutants never develop the proper number of parapineal cells.

Expression of *fgf8a* is found in the epithalamus from approximately 20 hpf through 72 hpf (Fig.3 and data not shown). Previous work had shown that Fgf signaling is needed between 24 and 44 hpf for parapineal migration (Regan et al., 2009). To establish a temporal requirement for Fgf signaling in production of parapineal cells, we used SU5402, a small molecule that blocks Ras/MAPK activation by Fgf receptors (Mohammadi et al., 1997), to abrogate Fgf signaling at different intervals between 18 and 36 hpf. While all treatment regimens reduced the number of parapineal cells, blocking Fgf activity between 18 and 30hpf proved the most effective in reducing parapineal cell number (Fig.8E). Embryos treated with SU5402 between 18 to 24 hpf had an average of 1.8±0.6 (n=16) *gfi-1.2*-expressing cells compared to 10.3±0.4 (n=14) in control embryos. Likewise, blocking Fgf signaling between 24-30hpf resulted in an average of 1.8±.5 (n=18) for SU5402 treated embryos compared to 9.9±0.5 (n=16) parapineal cells in control embryos (Fig.8A,B,E). However, blocking Fgf signaling later, between 30 to 36 hpf results in a more modest reduction in parapineal cell number with inhibitor treated embryos having 6.2±0.6 (n=18) parapineal cells compared to 10.3±0.5 (n=16) for control embryos (Fig.8E). Although the average number of *gfi-1.2* expressing cells in this treatment approached WT, most remaining parapineal cells failed to migrate very far form the midline similar to

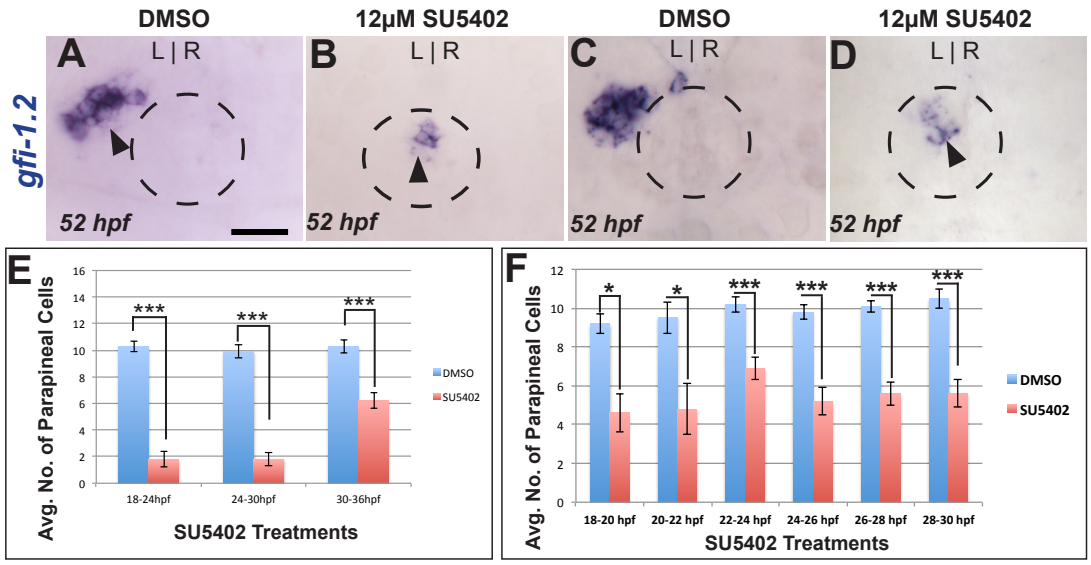

Figure 8. Conditional loss of Fgf signaling results in fewer parapineal cells. (A,B) Dorsal views showing expression of *gfi-1.2* (black arrows) in wild-type larvae at 52 hpf that were treated between 24-30 hpf with either DMSO or SU5402, a small molecule inhibitor of Fgf signaling. (C-D) Dorsal views of *gfi-1.2* expression (black arrows) 52 hpf wild-type larvae treated with SU5402 and DMSO from 24-26 hpf. (E) The number of *gfi-1.2* expressing cells was quantified at 52 hpf for the following SU5402 and DMSO treatments: 18-24 hpf; 24-30 hpf; 30-36 hpf. Severe reductions in parapineal cell numbers were observed in 18-24 hpf and 24-30 hpf treatments, but milder reductions for 30-36 hpf treatments. (***p=<0.0005 by t-test). (F) The number of *gfi-1.2* expressing cells was quantified at 52 hpf for the following DMSO and SU5402 treatments: 18-20 hpf; 20-22 hpf; 22-24 hpf; 24-26 hpf; 26-28 hpf; 28-30 hpf.(***p<0.0005, *p<0.05 by t-test). Scale bar in A= 25 micrometers

earlier treatments. To further hone the time point when Fgf is required during parapineal development, we performed an array of two-hour treatments between 18 and 30 hpf. Inhibiting Fgf signaling even in shorter intervals resulted in significantly reduced parapineal cell numbers at every case (Fig.8,B,C,F): 18-20 hpf (DMSO 9.2±0.5, n=13; SU5402 4.6±1.0, n=13); 20-22 hpf (DMSO 9.5±0.8, n=8; SU5402 4.8±1.3, n=10); 22-24 hpf (DMSO 10.2±0.4, n=17; SU5402 6.9±0.6, n=20); 24-26 hpf (DMSO 9.8±0.4, n=20; SU5402 5.2±0.7, n=15); 26-28 hpf (DMSO 10.1±0.3, n=27; SU5402 5.6±0.6, n=23); 28-30 hpf (DMSO 10.5±0.5, n=13; SU5402 5.6±0.7, n=14). However, the reduction is less severe in these treatments than the six-hour treatments (Fig.8E). All together, these data suggests that Fgf signaling is required over a broad time frame from 18 to 30 hpf to ensure formation of the correct number of parapineal cells. This encompasses the period following parapineal specification but before parapineal migration.

Parapineal Differentiation Does Not Depend on Parapineal Cell Migration

It is possible that the paucity in parapineal cell number is secondary to parapineal migration. By migrating away from the pineal complex, it is possible that specified parapineal precursors escape an “anti-parapineal” signal near the midline. To address this possibility, we moderated the dose of SU5402 used to inhibit Fgf signaling and assayed for parapineal position using *sox1a* expression which is efficiently labeled using FISH, relative to the medially positioned pineal complex indicated by Tg[*foxd3*:GFP]^{zf104} expression. Treating embryos with 6μM SU5402 (one half of the dose used above), resulted in reduced migration of

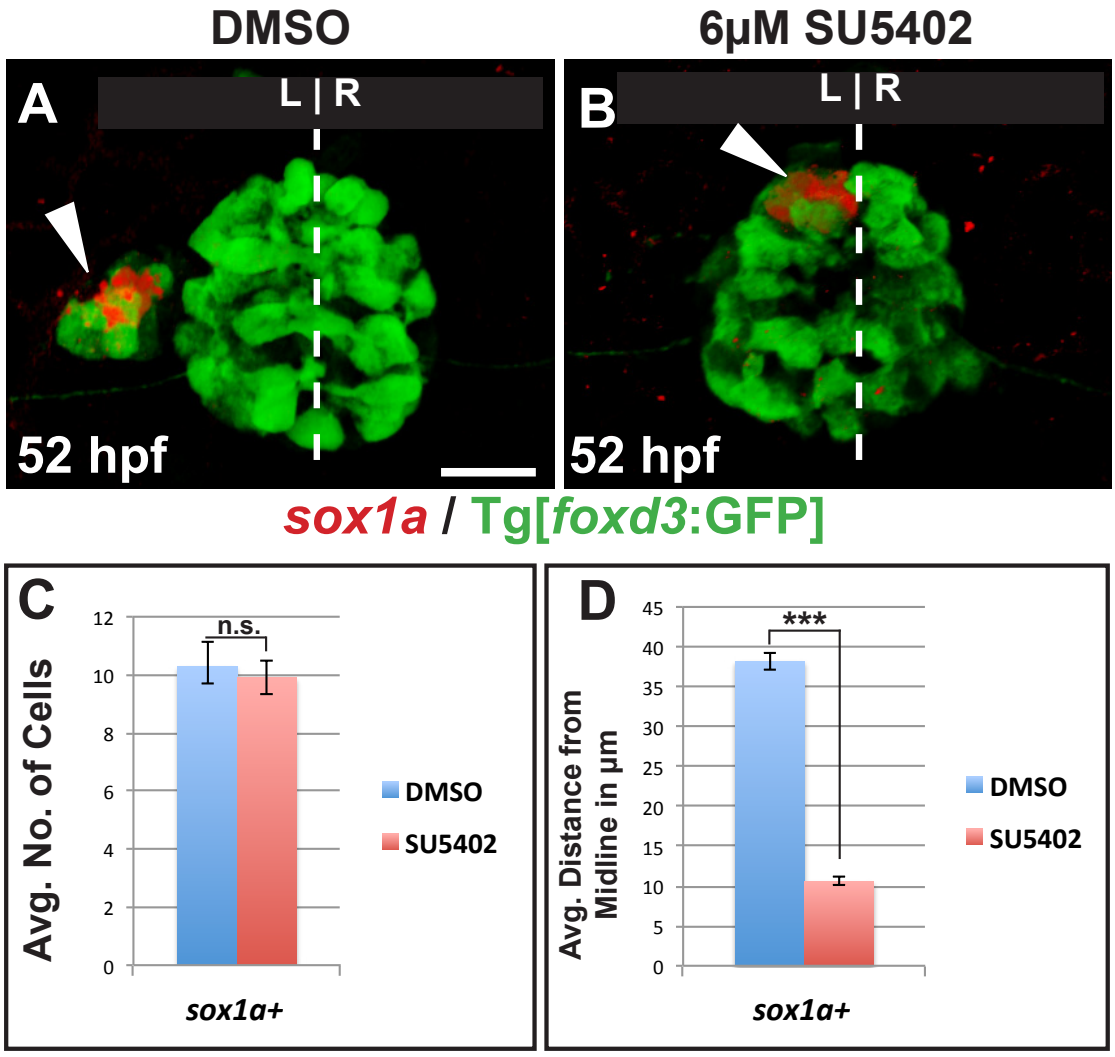

Figure 9. Parapineal differentiation is not dependent on migration.(A,B) 3D reconstructions of the pineal complex of a DMSO and 6μM SU5402 treated larvae at 52 hpf. The parapineal (white arrows) fails to migrate away from the midline (dotted line) in SU5402 treated larvae. (C) Graph quantifying the number of *sox1a*- expressing cells. The number of *sox1a*-expressing cells is unchanged between DMSO and SU5402 treated embryos (D) Graph quantifying the distance of parapineal cell migration. Parapineal cell migration is greatly attenuated in SU5402 treated larvae (***$p<0.0005$ by t-test). Error bars represent S.E.M. n.s. indicates not significant. Scale bar in A: 25 micrometers.

parapineal cells, but did not significantly alter parapineal cell number. Embryos treated with 6μM SU5402 had an average of 9.9±0.8 (n=12) parapineal cells as compared to 10.3±0.6 (n=7) for control embryos (Fig.9C). However, 6μM SU5402 treatment greatly affected the migration of parapineal cells which only moved an average of 10.6±0.6 μm (n=116 *sox1a* positive cells) from the midline as indicated by the center of Tg[*foxd3*:GFP]^{zf104} expression (Fig.9B,D). The parapineal cells in DMSO treated embryos moved leftward more than three times as far with average of 38.2±1.1μm (n=73 cells) (Fig.9A,D). These data suggest that parapineal differentiation is not dependent on migration.

Conditional Expression of Fgf8a is Not Sufficient to Induce Parapineal Cells or Rescue Parapineal Defects in *fgf8a*^{x15} Mutants

Since Fgf8a is necessary for parapineal cell generation, we next tested if Fgf8a is sufficient to produce additional parapineal cells. We conditionally over-expressed Fgf8a using the Tg[*hsp70l:fgf8a*]^{b1193} transgenic line, in which *fgf8a* transcription is induced by elevated temperature (Hans et al., 2007). Based on the temporal requirement for Fgf signaling as determined by our SU5402 treatments, we induced *fgf8a* expression at 24 hpf for thirty minutes and examined *gfi1.2* expression at 52 hpf. If Fgf8a were sufficient to specify parapineal cells, we would predict an increase in the number of *gfi-1.2* positive cells in *fgf8a* over-expressing embryos as compared to non-transgenic siblings. However, we detected no significant difference in parapineal cell number in *hsp70l:fgf8a* transgenic embryos relative to their non-transgenic siblings

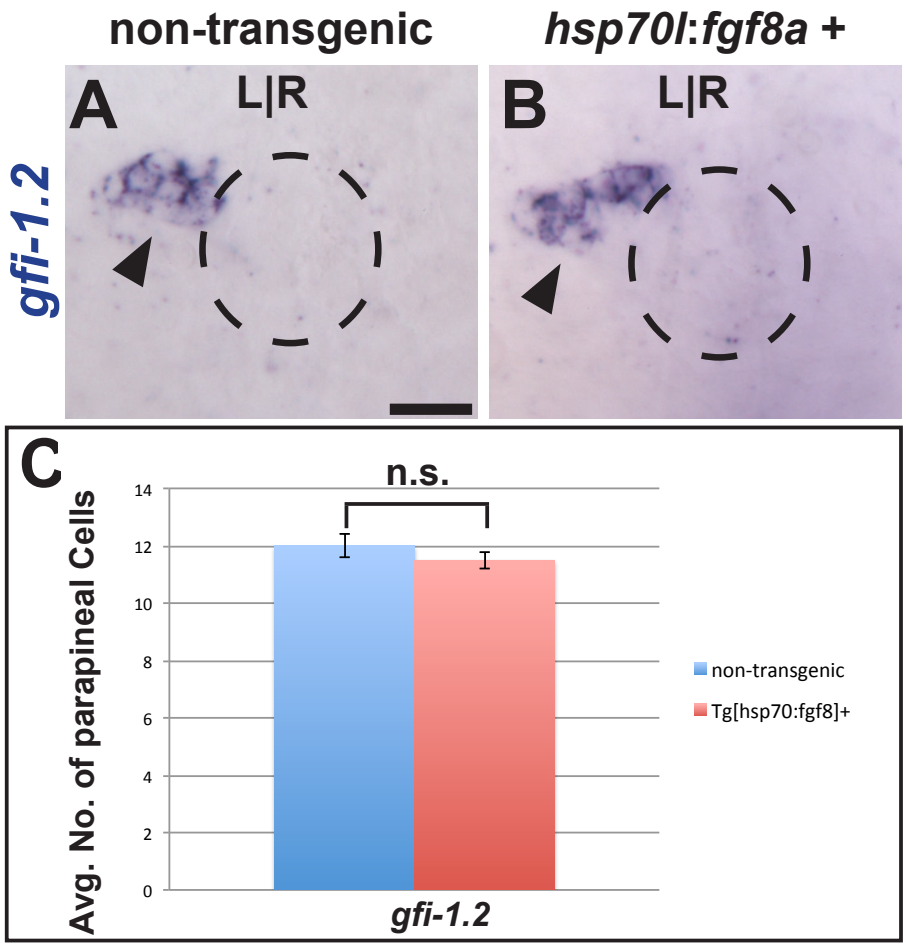

Figure 10. Fgf8a overexpression is not sufficient to induce supernumerary parapineal cells. (A,B) Dorsal view of non-transgenic and Tg[*hps70*l:*fgf8a*]^{b193} larvae at 52hpf that were heat shocked for 30 minutes at 24 hpf and labeled with *gfi-1.2* (black arrows). (C) Graph quantifying the number of *gfi-1.2* expressing cells. Scale bar in A: 25 micrometers.

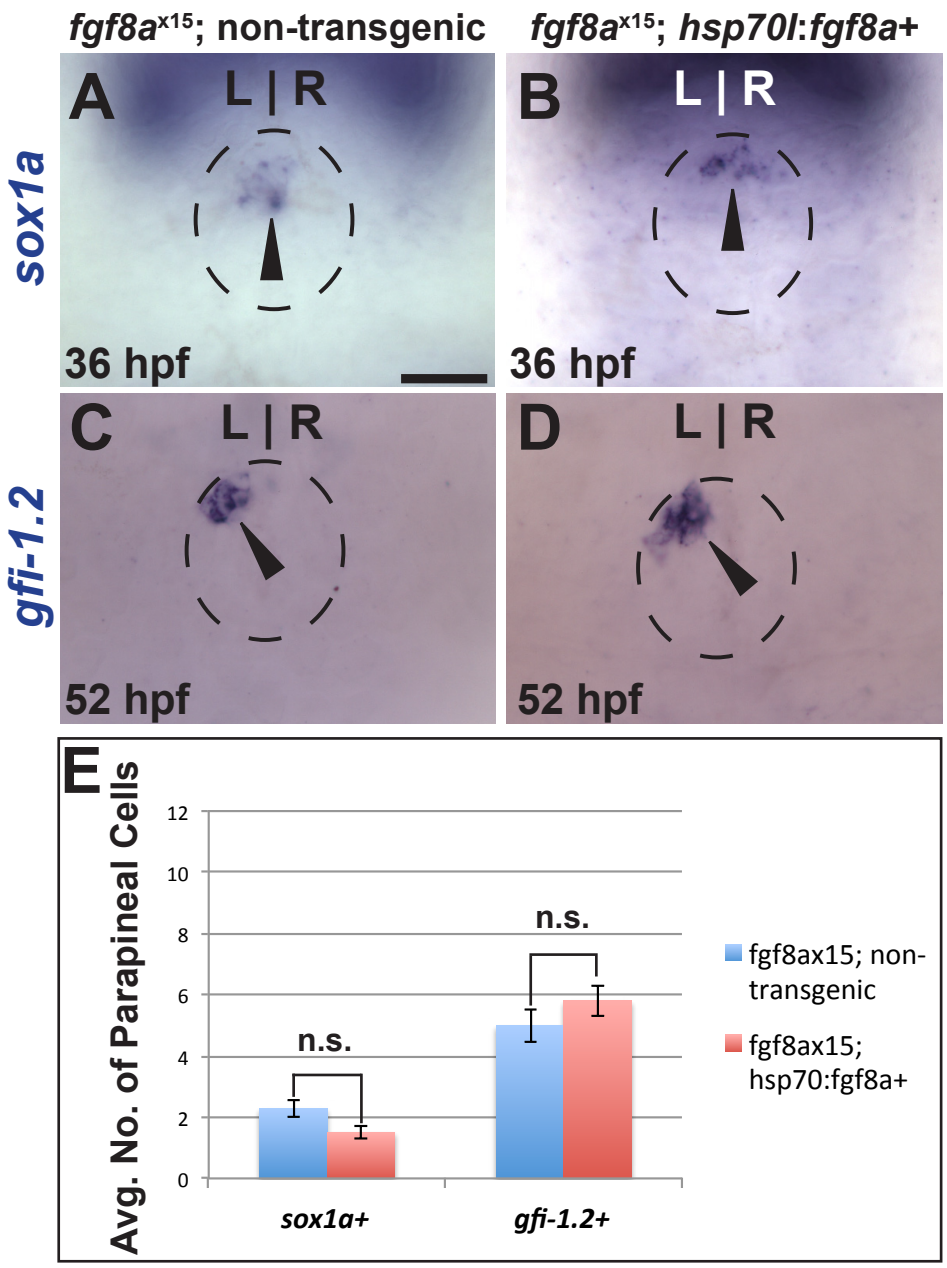

Figure 11. Fgf8a over-expression cannot rescue parapineal cell number defects in *fgf8a*^{x15} mutants. (A,B) Dorsal views *sox1a* expression (black arrowheads) in *fgf8a*^{x15} mutants with and without the Tg[*hsp70l:fgf8a*]^{b1198} transgene at 36 hpf (C,D) Dorsal views *gfi-1.2* expression (black arrowheads) in *fgf8a*^{x15} mutants with and without the Tg[*hsp70l:fgf8a*]^{b1198} transgene 52 hpf. Dashed line encircles the pineal complex anlage in A-D. (E) Graph quantifying the number of *sox1a* and *gfi-1.2* expressing cells in *fgf8a*^{x15} mutants with and without the Tg[*hsp70l:fgf8a*]^{b1198} transgene. (F) Graph quantifying the number of Tg[foxd3:GFP] and Arr3a positive cells in *fgf8a*^{x15} mutants with and without the Tg[*hsp70l:fgf8a*]^{b1198} transgene. Error bars represent S.E.M. n.s. indicates not significant. Scale bar in A: 20 micrometers.

(*hsp70l:fgf8a* transgenic larvae: average of 11.5±1.0.3 (n=17) *gfi-1.2* expressing cells; non-transgenic controls: 12±0.4 (n=12) cells) (Fig.10A,B,C). Similar results were obtained when *fgf8a* was induced by single heat shock at other points in development, by multiple heat shocks, or by continuous lower-temperature heat shock (see Materials and Methods). From these results, we conclude that excess Fgf signaling is insufficient to induce additional pineal complex precursor cells to become parapineal cells.

In addition to attempting to induce parapineal cells, we also tried to rescue the parapineal cell deficit in *fgf8a*^{x15} mutants by over-expression of *fgf8a*. As with the above over-expression experiments in wild-type embryos, we induced *fgf8a* expression at 24 hpf with a thirty minute heat shock. To assess the rescue of an early maker of parapineal differentiation, we analyzed *sox1a* expression at 36 hpf in non-transgenic and *fgf8a* over-expressing mutants. We found that non-transgenic *fgf8a*^{x15} mutants had an average of 2.3±0.3 (n=12) *sox1a* positive cells while *fgf8a* over-expressing mutants had 1.5±0.2 (n=10) cells. This suggests that we cannot rescue early parapineal differentiation by *fgf8a* over-expression (Fig.11A,B, E). Not surprisingly, we were also unable to rescue *gfi-1.2* expression with the additional of *fgf8a.* Non-transgenic *fgf8a*^{x15} mutants averaged 5.0±0.5 (n=24) *gfi-1.2* expressing cells and *fgf8a* over-expressing *fgf8a*^{x15} mutants with 5.8±0.5 (n=22) *gfi-1.2* positive cells (Fig.11C,D,E). All together, these data suggests that we cannot rescue either the early parapineal differentiation defects or later parapineal maturation problems in *fgf8a*^{x15} mutants by the addition of Fgf8a. We noted that the *hsp70l*:*fgf8a* transgenic line was

capable of both inducing the near-ubiquitous expression of *fgf8a*, as well as *erm*, a transcriptional target of Fgf signaling, suggesting that we were activating Fgf/MAPK pathway via Fgf8a overexpression (data not shown). However, the induction of *erm* expression seems to occur outside of the known sites of *fgf receptor* expression which lie in distinct regions of the brain at this stage (Fig.4 and (Ota et al., 2010). This indicates that our method of Fgf8a overexpression might not fulfill a precise physiological mechanism required for parapineal cell formation.

Reduced Fgf Activity Leads to a Selective Increase in Cone Cell Number

During embryogenesis, Fgf signaling can change cell fate, promote cell division, and increase cell survival (Bottcher and Niehrs, 2005; Thisse and Thisse, 2005). Therefore, the deficit of parapineal cells seen in *fgf8a*^{x15} mutants and SU5402-treated embryos could result from alterations of cell fate or reductions in the total number of pineal complex cells. To distinguish between these possibilities, we counted the total number of pineal complex cells, as well as the number of each cell type. The pineal complex is composed of rod photoreceptors, cone photoreceptors, projection neurons, and parapineal cells (Fig.12A) (Butler and Hodos, 1996; Masai et al., 1997; Concha et al., 2000; Cau et al., 2008; Snelson et al., 2008c). With the exception of rod cells, all pineal complex cells express Tg[*foxd3*:GFP]^{zf104} at 52 hpf. Thus, by counting cells that express either Tg[*foxd3*:GFP]^{zf104} or Opsin-1 (which labels only rod photoreceptors), we can quantify the total number of pineal complex cells. The morphology of the pineal

organ is largely unaltered in *fgf8a*^{x15} mutants as compared to wild-type siblings (Fig.12B-E), although it was slightly wider in some mutants. However, *fgf8a*^{x15} mutant larvae do not have a distinct parapineal organ (Fig.12C,E), consistent with data that the remaining *gfi-1.2* expressing cells in *fgf8a*^{x15} mutants remain within the pineal anlage. Despite having fewer *gfi-1.2* expressing cells, the total number of Tg[*foxd3*:GFP]^{zf104} positive cells in *fgf8a*^{x15} mutants is not significantly different from wild-type larvae (average of 57.8±1.2; n=12 and 55.4±1.3; n=10 cells respectively) at 52 hpf (Fig.13A,B,C) or 96 hpf (average of 57.3±1.0; n=14 and 56.9±1.2; n=14) (Fig.13D,E,F)

To look for changes in cell fate, we analyzed three other pineal complex cells subtypes. Rod photoreceptors are characterized by the expression of Rhodospin (Opsin-1) in their outer segment, which projects into the lumen of the pineal organ (Concha et al., 2000). At 96 hpf, there is no significant difference in the number of rod photoreceptors between *fgf8a*^{x15} mutants and wild-type siblings (average of 21.4±1.4, n=19 and 20.0±1.4, n=19 cells respectively) (Fig.12B,C). The number of projection neurons, which express HuC/D at 52 hpf (Cau et al., 2008), is unchanged in *fgf8a*^{x15} mutants with an average of 26.8±0.7 (n=11) cells compared to 25.4±0.8 (n=12) cells for wild-type larvae (Fig.12D,E). Unlike rods and projection neurons, the number of cone photoreceptors, labeled by Arrestin 3a (Arr3a) (also known as Zpr1 and Fret43) (Larison and Bremiller, 1990; Masai et al., 1997; Ile et al., 2010) is significantly different between *fgf8a*^{x15} mutants and WT. At 52 hpf, wild-type larvae had an average of 23.2±0.8 (n=10) cells expressing Arr3a (Fig.13D,C). Arr3a expression was only observed in the

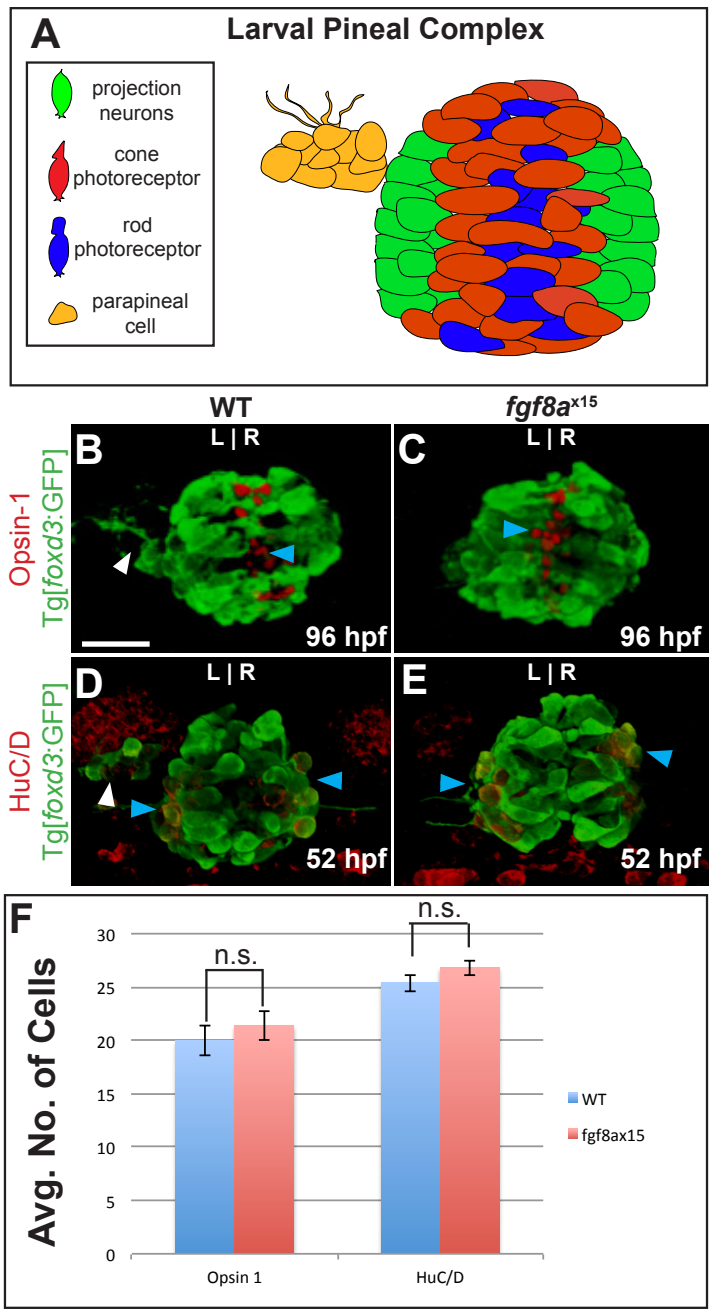

Figure 12. *fgf8a* mutants show no change in the number of rod cells or projection neurons. All images are dorsal views of confocal 3D reconstructions. WT larvae were co-labeled with *foxd3*:GFP and either Opsin-1 (rod photoreceptors outer segment) at 96 hpf or HuC/D (projection neurons) at 52 hpf. (A) Schematic of WT pineal complex at 52 hpf. (B) WT larvae exhibiting a parapineal (white arrow) and rod photoreceptors (blue arrow). (C) *fgf8a*^{x15} mutants have no parapineal organ but still form rod photoreceptors (blue arrow). (D) WT embryos with visible parapineal (white arrow) and projection neurons (blue arrows). (E) *fgf8a*^{x15} mutants still develop projection neurons (blue arrows). (F) Graph quantifying rod cells and projection neurons. n.s. indicates not significant. Error bars indicate S.E.M. Scale bar in A: 25 micrometers.

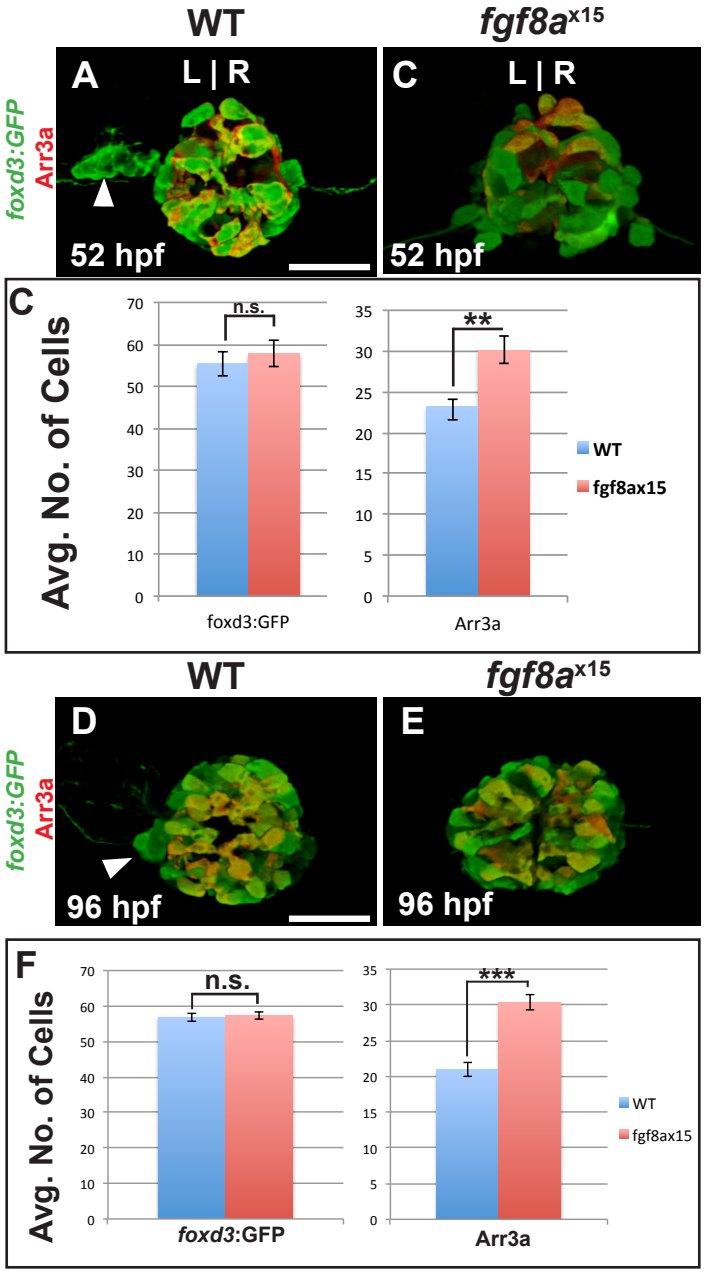

Figure 13. *fgf8a*^{x15} mutants have a selective increase in pineal cone cells. All images are dorsal 3D confocal projections larvae labeled with Tg[*foxd3*:GFP] and Arr3a. (A,B) Compared to WT, *fgf8a*^{x15} mutants do not have an obvious parapineal (white arrow) at 52 hpf. (C) Graph quantifying the number of Tg[*foxd3*:GFP] and Arr3a expressing cells. (D,E) Dorsal views of WT and *fgf8a*^{x15} mutants labeled with Tg[*foxd3*:GFP] and Arr3a. (F) Graph quantifying the number of Tg[*foxd3*:GFP] and Arr3a expressing cells. Error bars indicate S.E.M. n.s. indicates not significant. (***p<0.0005; **p<0.005 by T-test). Scale bar=25μM.

pineal organ and was never seen in the parapineal of WT (Fig.13A). *fgf8a*^{x15} mutants have an average of 30.1±1.7 (n=12) cone cells (Fig.13B,C). The average increase of approximately 7 cone cells in *fgf8a*^{x15} mutants relative to WT is comparable to the decrease in *gfi-1.2*-expressing cells (Fig.7C). Similar to the reduction in *gfi-1.2* expressing cells, this concomitant increase in cone cells is not resolved over time. At 96 hpf, *fgf8a*^{x15} mutant larvae have an average 30.4±1.1 (n=14) compared to 21.0±1.0 (n=14) for WT (Fig.13D,E,F). Taken together, these data show that the total number of pineal complex cells is unchanged in *fgf8a*^{x15} mutants compared with their wild-type siblings, arguing against a role for Fgf8a in governing cell proliferation or cell survival in the pineal complex. However, *fgf8a*^{x15} mutants do exhibit an increase specifically in cone photoreceptor number that mirrors the decrease in the number of parapineal cells.

Given that blocking Fgf activity with a high concentration of SU5402, a small molecule of inhibitor of Fgf receptor activity, could lead to a similar reduction in the number of parapineal cells, we decided to see if blocking Fgf activity in this way could also yield an increase in Arr3a positive cells. After inhibiting Fgf signaling between 24 and 30 hpf, we counted the number of Tg[f*oxd3*:GFP] and Arr3a positive cells. At 52 hpf, SU5402 treated larvae and DSMO treated controls had similar number of Tg[f*oxd3*:GFP] expressing cells (58.3±0.8; n=8 and 57.6±1.8; n=7 respectively) at 52 hpf (Fig.14A,B,C). Similar to *fgf8a*^{x15} mutants, SU5402 treated larvae showed a significant increase in the number of Arr3a positive cells compared with control larvae (17.9±1.1; n=7 and 27.0±2.5; n=6 cells respectively) (Fig.14A,B,C).

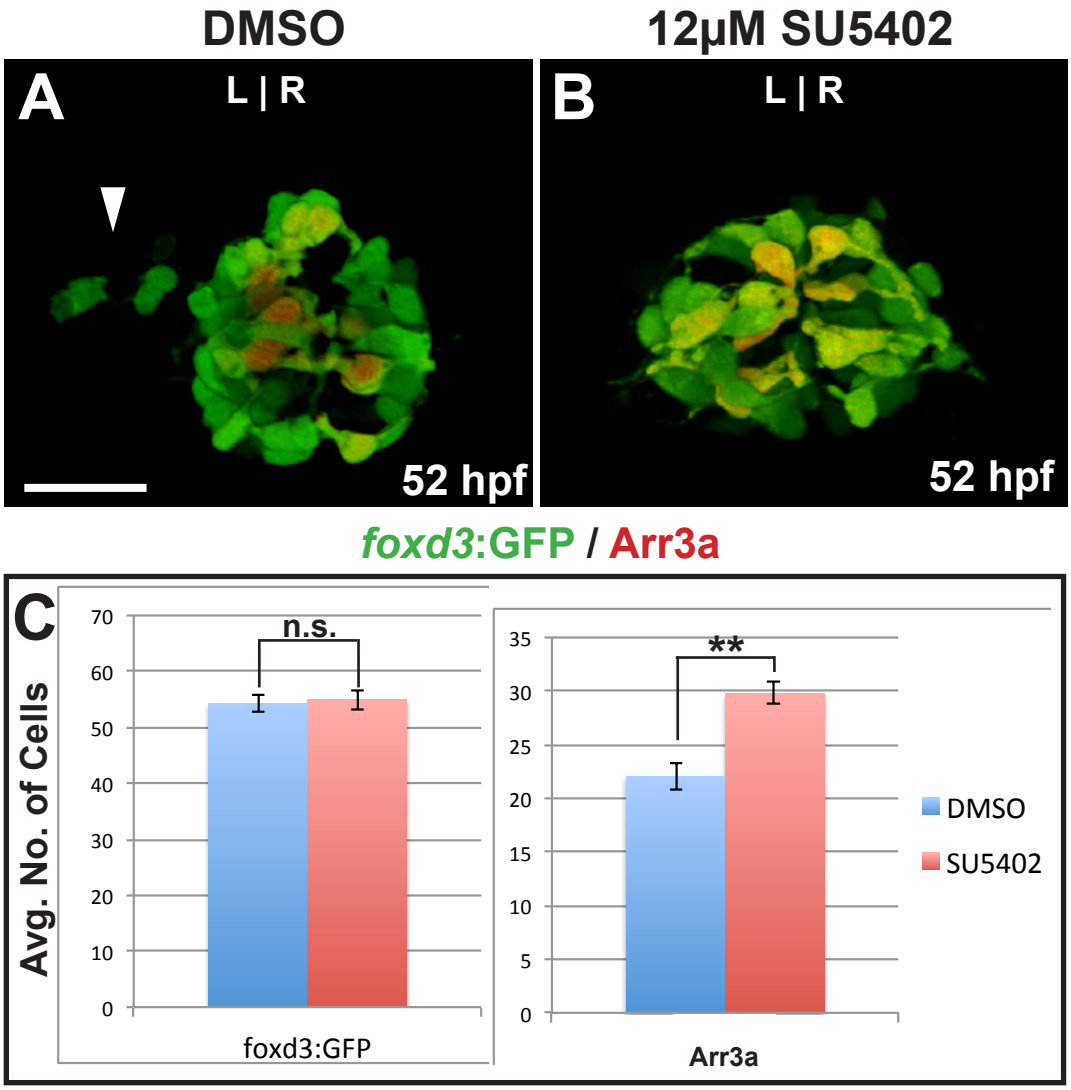

Figure 14. Ectopic increase in cone cells persist in SU5402 treated larvae. (A,B) Dorsal views of DMSO and SU5402 treated embryos at 52 hpf labeled with Tg[*foxd3*:GFP] and Arr3a. SU5402 treated embryos lack obvious parapineal (white arrow). (C) Graph quantifying the number of Tg[*foxd3*:GFP] and Arr3a cells in 52 hpf larvae treated with DMSO or 12μM SU5402 from 24-30hpf. Scale. (**p<0.005 by t-test). Error bars represent S.E.M. n.s. indicates not significant. Scale bar in B: 25 micrometers.

Parapineal Precursors Give Rise to Cone Cells in *fgf8a*^{x15} Mutants

Because the number of cone cells is increased and the number of parapineal cells is decreased in *fgf8a*^{x15} in similar numbers, we hypothesized that parapineal precursors were differentiating instead as cone photoreceptors. To test this hypothesis, we analyzed the effect of the loss of Flh in *fgf8a* mutant embryos as well as performing cell fate analysis in the pineal complex.

One possible explanation for the *fgf8a*^{x15} mutant phenotype in the pineal complex (decreased number of parapineal neurons but increased pineal cone cells) is that there is a simply an expansion of cone photoreceptors masking the loss of parapineal cells. To delineate the source of the supernumerary cone cells (pineal precursors versus parapineal precursors), we knocked down Flh in *fgf8a* mutants. The transcription factor Flh is required for neurogenesis in the developing pineal organ. In *flh*-depleted embryos, there is a drastic reduction in the number of all pineal organ cell types, including cone photoreceptors (Masai et al., 1997; Cau and Wilson, 2003; Snelson et al., 2008a). However, the number of cells in the parapineal organ in unchanged relative to WT (Snelson et al., 2008a). If the extra cone cells in *fgf8a*^{x15} mutants derive from pineal organ precursors, then depletion of *flh* in *fgf8a*^{x15} mutants would result in a smaller increase in the number of cone cells compare to non-injected controls.

As expected, loss of Flh dramatically reduced the number of pineal complex cells in both *fgf8a*^{x15} mutants and wild-type siblings compared to non-injected larvae. In WT;*flh*^{MO} and *fgf*8a^{x15};*flh*^{MO} embryos at 96 hpf we detected 33±2.0 (n=10) and 34.9±2.2 (n=7) Tg[*foxd3*:GFP]^{zf104} expressing cells respectively

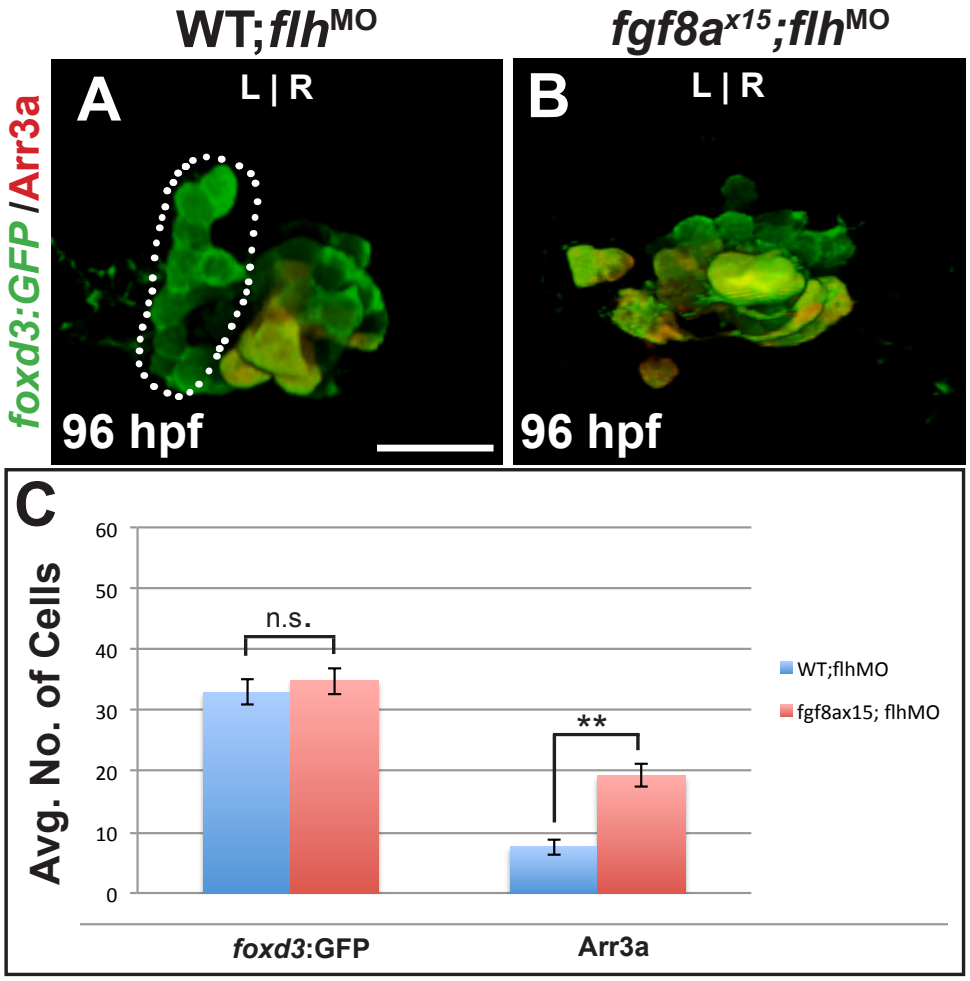

Figure 15. Ectopic cone photoreceptors persist in *flh* depleted *fgf8a*^{x15} mutants. (A,B) Dorsal views of 96 hpf wild-type and *fgf8a*^{x15} mutant embryos injected with *flh* morpholino (*flh*MO) labeled with *foxd3*:GFP (pineal complex) and Arr3a (cone photoreceptors). In WT injected with *flh*MO (WT; *flh*MO), a full-sized parapineal organ (dotted line) is evident, while pineal cells are reduced in number. In *flh*MO injected *fgf8a*^{x15} mutants (*fgf8a*^{x15}; *flh*MO), no parapineal organ is visible. (C) Graph quantifying the total number of pineal complex cells and of cone photoreceptors in WT; *flh*MO and *fgf8a*^{x15}; *flh*MO. The number of *foxd3*:GFP expressing cells is unchanged between *fgf8a*^{x15};*flh*MO and WT;*flh*MO. However, the number of cone photoreceptors in increased *fgf8a*^{x15};*flh*MO relative to WT;*flh*MO larvae. (**p<0.005 by t-test). Scale bar in A: 25micrometers.

(Fig.15A,B,C). WT;*flh*^{MO} larvae have a relatively normal parapineal organ, while *fgf8a*^{x15};*flh*^{MO} larvae lacked an obvious parapineal organ (Fig.6 A,B). We found an elevated number of cone photoreceptors in *fgf*8a^{x15};*flh*^{MO} embryos compared to WT;*flh*^{MO} embryos with 19.3±1.8 (n=10) and 7.6±1.3 (n=7) respectively (Fig.15C). There is an average increase of 11.7 cone cells in *fgf*8a^{x15};*flh*^{MO} compared with WT;*flh*^{MO} siblings. Taken together, the data indicate that depletion of *flh* did reduce the number of ectopic cone cells in *fgf8a* mutants, suggesting that the additional cone cells in *fgf8a*^{x15} mutants are from specified parapineal precursor cells. Additionally, it suggests that these ectopic cone cells do not result from an increase in Flh activity that could, in theory, re-specify the fate of parapineal precursors. The above experiments suggest that parapineal precursors are changing fate to become pineal cone photoreceptors *fgf8a*^{x15} mutants. However, we decided to directly label likely parapineal precursor cells in *fgf8a*^{x15} mutants to determine their cell fate. Fate mapping of the pineal complex indicates that, by 24 hpf, parapineal cells reside in the anterior one third of the pineal complex anlage, seemingly intermingled with precursors of the pineal organ (Concha et al., 2003). To perform cell fate analysis in the pineal complex we optimized existing methods using caged fluorescein dextran, a photoactivatable fluorophore that has been used for lineage labeling in zebrafish embryos (Kozlowski et al., 1997; Concha et al., 2003). Previous efforts focused on using caged fluorescein to determine the developmental origin of small populations of cells or tissues. We combined the ability to selectively label small groups of cells with caged-fluorescein dextran with cell type specific antibody

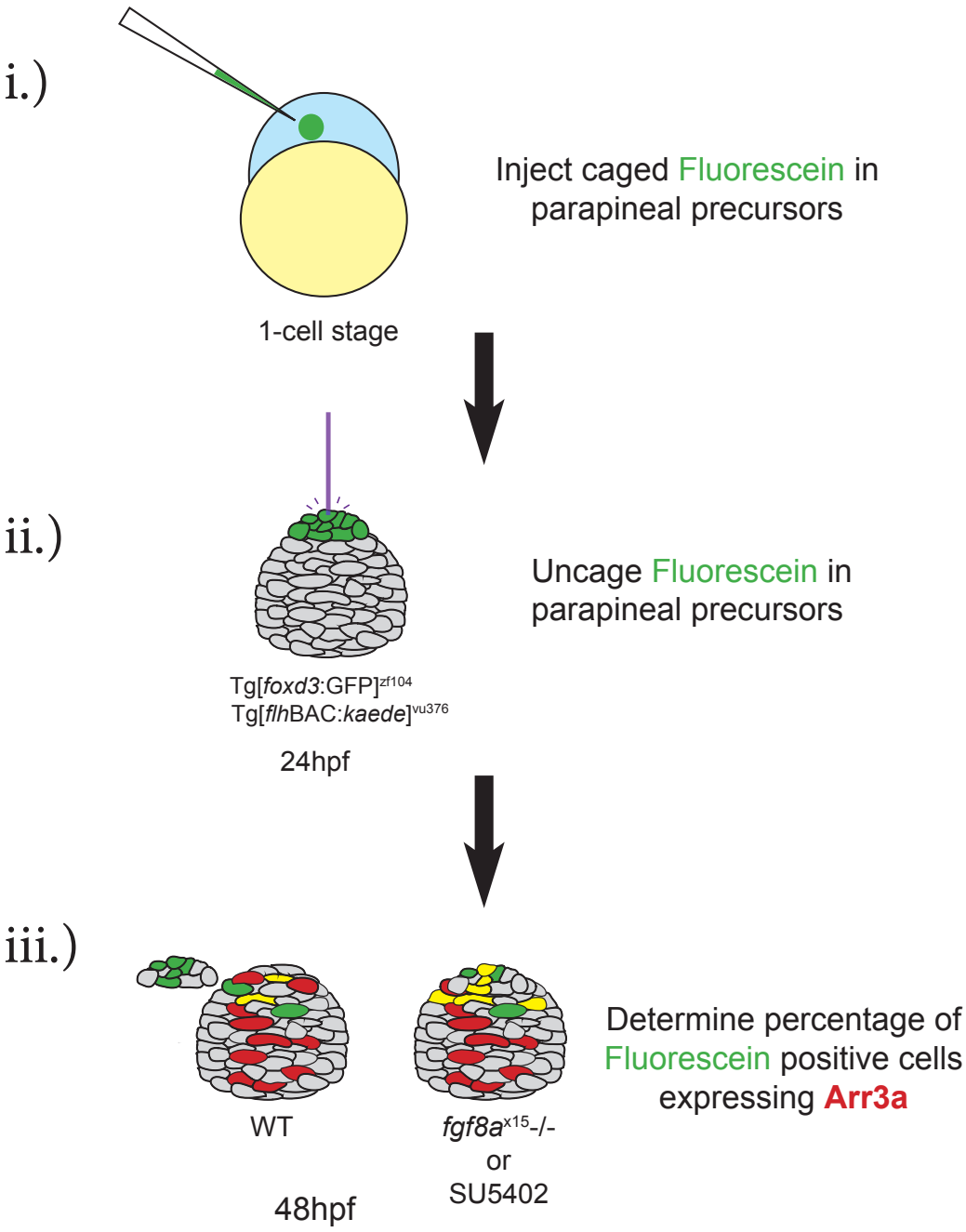

Figure 16. Cell fate analysis of the pineal complex. (i.) Caged fluorescein is injected into 1-cell stage embryos. (ii.) Fluorescein is photoactivated in likely specified parapineal precursors in the anterior pineal complex anlage at 24 hfp. (iii.) At 48 hpf, fluorescein is detected in either WT or *fgf8a*^{x15} mutants and DMSO or SU5402 treated embryo. The percentage of fluorescein positive Arr3a positive pineal cone cells is calculated.

labeling to determine cell fate among specified parapineal precursors. To mark all pineal complex cells from 24 hpf and later, we used the Tg[*foxd3:*GFP]^{zf104} and Tg[*flh*BAC*:*Kaede]^{vu376} transgenes. After injecting caged-fluorescein into one cell stage embryos, we photoactivated fluorescein in 10 to 15 cells of the anterior pineal anlage at 24 hpf in *fgf8a*^{x15} mutants or wild-type siblings and allowed them to develop until 52 hpf (Fig.16). In wild-type embryos, fluorescein labeled parapineal cells were clearly detectable at 52 hpf (Fig.17A,A"). Since the anterior pineal complex anlage does not give rise exclusively to parapineal cells, some cells of the pineal organ (including cone photoreceptors of the pineal) were also labeled (Fig.17A,A"). In WT embryos, only 27%±5.4 (n=14) of fluorescein labeled cells became cone photoreceptors (Fig.17C). However, in *fgf8a*^{x15} mutants, cone photoreceptors made up almost twice as many of the fluorescein labeled cells (48%±4.7, n=14) than in wild-type siblings (Fig.17B,B",C). One explanation for the increase in labeled cone photoreceptors in our lineage labeling experiments is that in *fgf8a*^{x15} mutants, parapineal precursor cells may not reside in the anterior pineal anlage (e.g. if Fgf8a was required for the precursors to migrate to an anterior position following specification somewhere else in the anlage). To exclude this possibility, we performed cell fate analysis of the anterior pineal complex anlage using embryos treated with SU5402 between 24 and 30 hpf. Because Fgf signaling is normal in these embryos up until the time of fluorescein labeling at 24 hpf, the location of the parapineal precursors in these embryos is the same as untreated wild-type. Thus, any difference in cell fate in the anterior

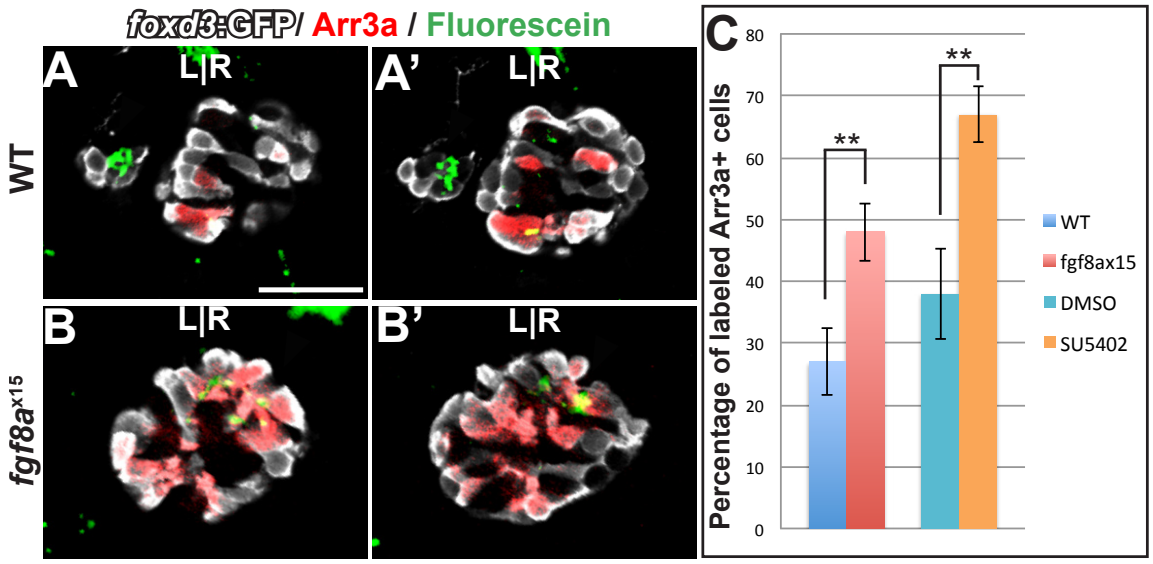

Figure 17. Cell fate analysis of anterior pineal complex indicates that parapineal precursors adopt a cone photoreceptor fate in *fgf8a*^{x15} mutants. (A,A') Dorsal views of serial confocal sections in the pineal complex of wild-type embryos at 52 hpf, following lineage labeling of the anterior pineal complex anlage at 24 hpf. Clusters of parapineal cells labeled with fluorescein are evident (blue arrows). (B,B') Serial confocal sections in *fgf8a*^{x15} mutants at 52 hpf following lineage labeling at 24 hpf. Many of the cells that were labeled in the anterior pineal complex anlage at 24 hpf become cone photoreceptors (blue arrows). (C) Graph quantifying the number of fluorescein labeled cone photoreceptors in wild-type embryos compared to *fgf8a*^{x15} mutants (left bars), and in DMSO-treated controls compared to SU5402 treated embryos (right bars). When Fgf signaling is reduced, a significantly higher percentage of fluorescein labeled cells become cone photoreceptors as compared to controls. (**p<0.005 by t-test). Scale bar in B: 30 micrometers.

pineal complex anlage between SU5402-treated and control embryos is the result of changes in the fate of parapineal precursors, not differences in their location (Fig.17C). In SU5402 treated embryos 67%±4.5 (n=9) of fluorescein labeled cells became cone cells. However, only 38%±7.4 (n=7) of labeled cells in control embryos gave rise to cone cells. These data are very similar to our results using *fgf8a*^{x15} mutants, indicating that the parapineal precursors in mutants likely reside in a similar anterior location in the pineal complex anlage as wild-type embryos. Based on these data, as well as our Flh knock down experiments, we conclude that the additional cone cells in *fgf8a*^{x15} mutants are derived from specified parapineal precursor cells that have incorrectly adopted a cone photoreceptor fate.

Fgf8a and Tbx2b Act During Different Steps of Parapineal Development

As with other cell types in the developing brain, the formation of parapineal neurons likely involves the input of multiple genes to specify the correct number of precursor cells and to maintain the specified state until differentiation. Disruption of either of these steps would result in fewer parapineal cells. Previously, the transcription factor Tbx2b was implicated in parapineal specification (Snelson et al., 2008c). Indeed, *tbx2b*^{c144} mutants and *fgf8a*^{x15} mutants exhibit a strikingly similar phenotype with a reduction in the number of *gfi-1.2* expressing cells and the failure of the remaining cells to migrate toward the left side of the brain.

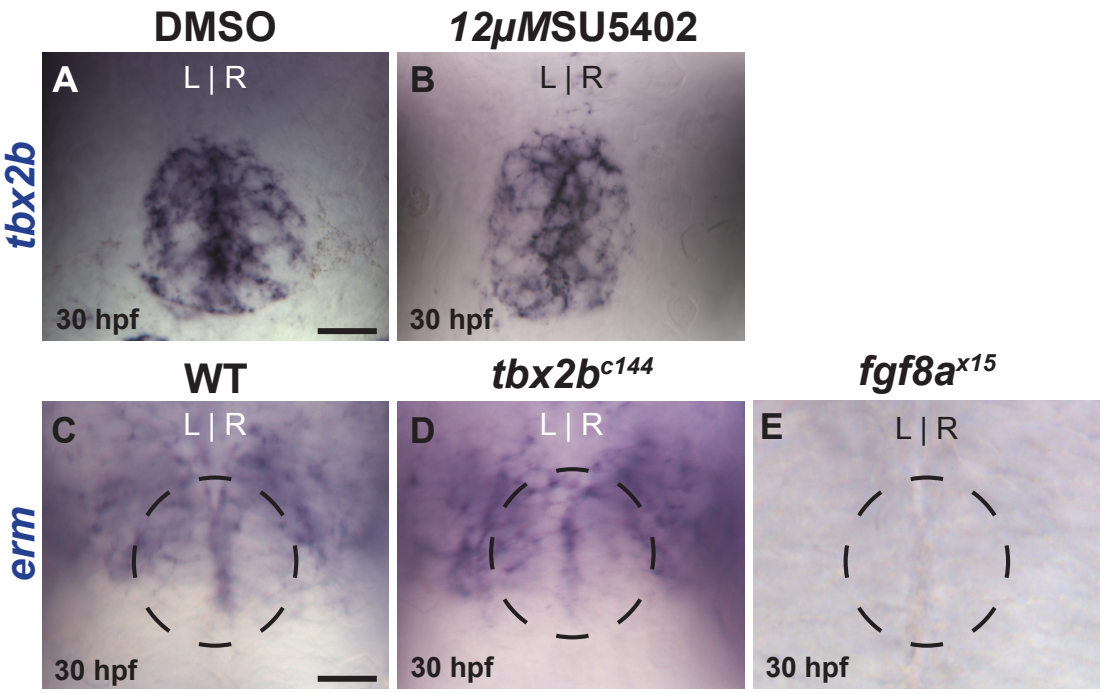

Figure 18. Tbx2b and Fgf8a have no cross-regulatory relationship. (A, B) Dorsal views of DMSO or SU5402 treated embryos labeled with *tbx2b* at 30 hpf. Embryos were treated from 24-30 hpf. (C,D) Dorsal view of *erm* expression in the pineal complex of WT and *tbx2b*^{c144} mutant at 30 hpf. The position of the pineal is indicated by the dashed circle. Scale bar in A and C: 25 micrometers.

Previous work has shown that Fgf8 could activate the expression of *tbx2*, an ortholog to *tbx2b*, in chick nasal mesenchyme (Firnberg and Neubuser, 2002). Therefore, we tested whether a similar regulatory relationship exists between Fgf signaling and Tbx2b in parapineal formation. We blocked Fgf signaling by SU5402 treatment from 24-30 hpf and examined *tbx2b* expression at 30 hpf. We see no change in *tbx2b* transcript level in the epithalamus of SU5402-treated embryos compared to controls (Fig.18A,B). Likewise, we looked at the expression of *erm,* a target gene of Fgf signaling in *tbx2b*^{c144} mutants. At 30 hpf, *erm* expression is similar in *tbx2b*^{c144} mutants and wild-type controls as compared to *fgf8a*^{x15} mutants which exhibits a drastic reduction in erm expression in the epithalamus (Fig.18C,D,E). These data indicates that, in the epithalamus, Fgf8a does not induce *tbx2b* expression nor is Tbx2b required for Fgf activity.

If two genes have a similar mutant phenotype, and the double mutant has an additive phenotype, then the two genes act in independent pathways. To determine whether loss of both *fgf8a* and *tbx2b* have additive effects with respect to parapineal cell number, we analyzed *gfi-1.2* expression in larvae lacking the function of both Fgf8a and Tbx2b at 96 hpf. To knock down Tbx2b, we injected *tbx2b*^{MO} into WT and *fgf8a*^{x15} mutants. As expected, wild-type embryos injected with *tbx2b*^{MO} (WT;*tbx2b*^{MO}) had a drastic reduction in parapineal cells with 3.3±0.7 (n=8) *gfi-1.2* expressing cells compared to non-injected WT siblings (WT;NI) with 10.8±0.4 (n=5) cells (Fig.19A,C,E). Similar to WT;*tbx2b*^{MO} embryos and consistent with our previous results, non-injected *fgf8a*^{x15} mutants

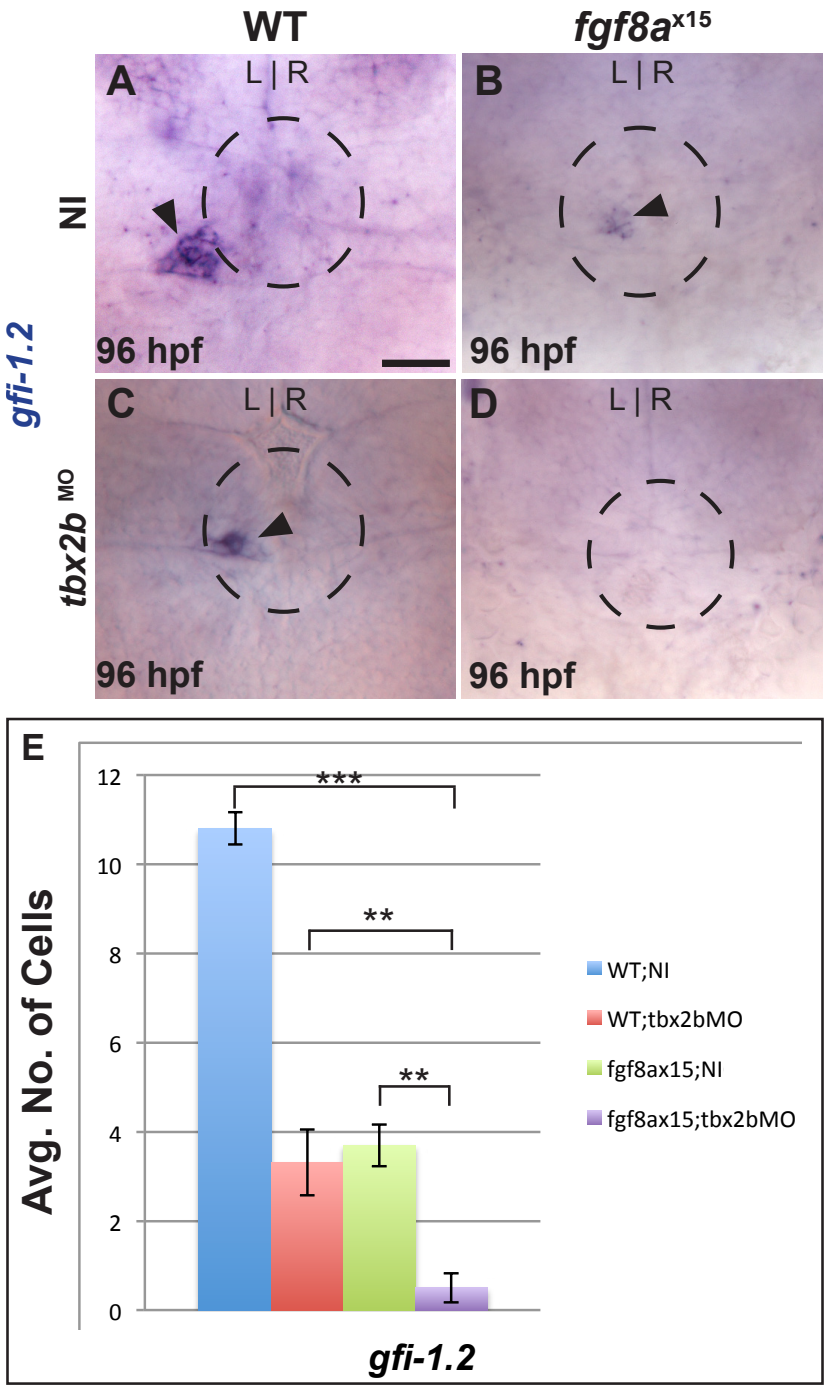

Figure 19. Fgf8a and Tbx2b act additively in the formation of parapineal cells. (A,B) Dorsal views of uninjected wild-type and *fgf8a*^{x15} mutant larvae (WT;NI and *fgf8a*^{x15};NI respectively) at 96 hpf, labeled for *gfi-1.2* to mark parapineal cells (black arrows). (C,D) Dorsal views of wild-type and *fgf8a*^{x15} mutant embryos injected with t*bx2b*^{MO} (WT; t*bx2b*^{MO} and *fgf8a*^{x15}; t*bx2b*^{MO}) at 96 hpf labeled for *gfi-1.2* (black arrows). (E) Graph quantifying the number of *gfi-1.2* expressing cells. Error bars indicate S.E.M. (**p<0.005, ***p<0.0005). Many fewer parapineal cells are detected when *tbx2b* and *fgf8a* are simultaneously reduced than when either is singly depleted. Scale bars in A is 25μM.

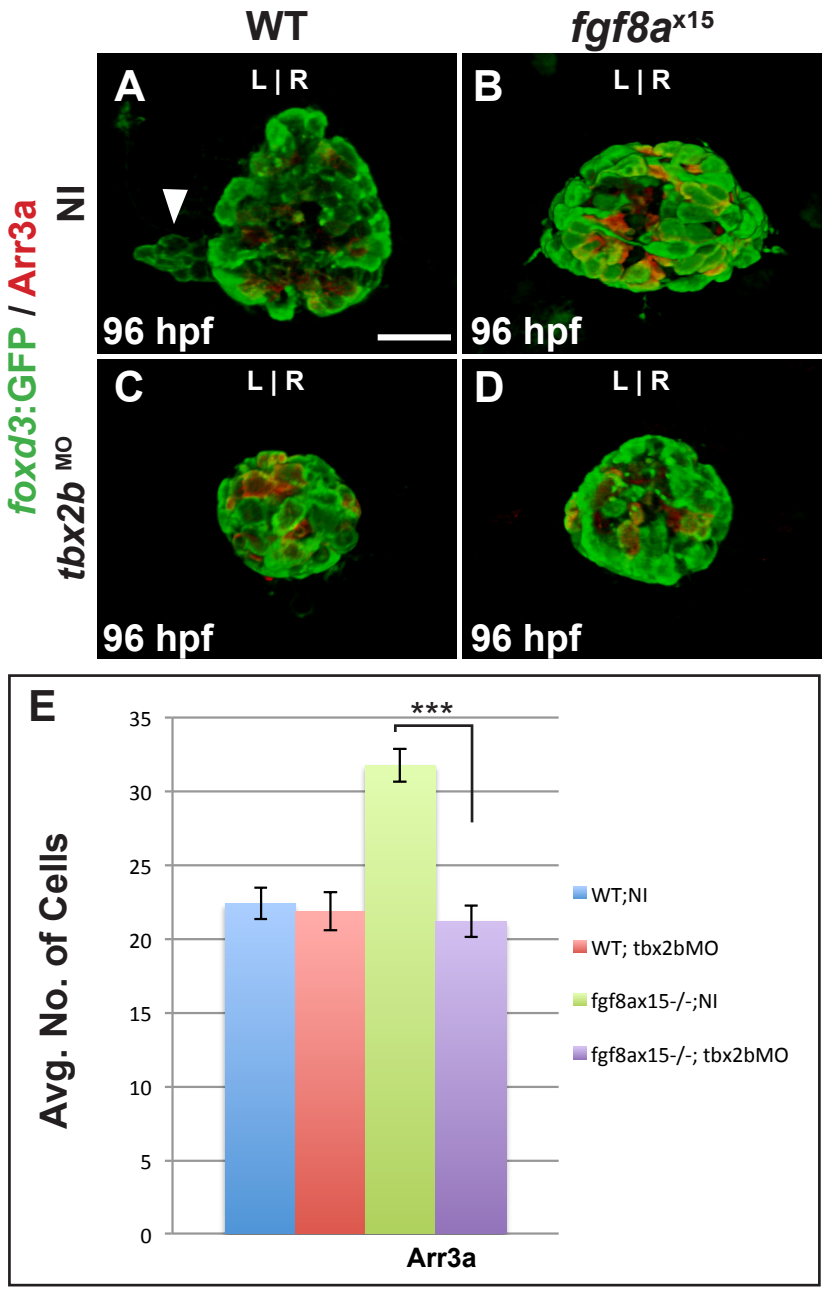

Figure 20. Tbx2b is required to produce the extra cone cells in *fgf8a*^{x15} mutants. (A,B) Dorsal views of confocal slices of WT;NI and *fgf8a*^{x15};NI larvae labeled with *foxd3*:GFP to mark the entire pineal complex and Arr3a to mark cone photoreceptors. (C,D) Dorsal views of confocal slices of WT;*tbx2b*^{MO} and *fgf8a*^{x15} ;*tbx2b*^{MO} larvae labeled with *foxd3*:GFP and Arr3a at 96 hpf. (E) Graph quantifying the number of cone photoreceptors. Tbx2b depletion reduces the number of cone photoreceptors to a level indistinguishable from non-injected WT and *tbx2b* morphants. (***p<0.0005). Scale bars in A and F: 25 micrometers.

(*fgf8a*^{x15};NI) had an average of 3.7±0.5 (n=7) *gfi-1.2* positive cells (Fig.19B,E). However, *fgf8a*^{x15} injected with *tbx2b*^{MO} (*fgf8a*^{x15};*tbx2b*^{MO}) larvae had significantly fewer *gfi-1.2* expressing cells (0.5±0.3; n=8) than either WT;*tbx2b*^{MO} or NI;*fgf8a*^{x15} embryos (Fig.19D,E) suggesting that the loss of both Fgf8a and Tbx2b creates an additive defect with respect to parapineal cell number indicating that these two genes act to generate parapineal cell via separate pathways.

We also examined the phenotype of simultaneously depleting Tbx2b and Fgf8a with respect to cone photoreceptor number. Previous work suggested that, although *tbx2b* mutants had a deficit in *gfi-1.2* positive cells, they lacked the additional cone photoreceptors seen in *fgf8a*^{x15} mutants at 96 hpf (Snelson et al., 2008c). Since *tbx2b* and *fgf8a* mutants had different phenotypes with respect to cone photoreceptor number, we performed epistasis analysis. As before, we used a *tbx2b* morpholino (*tbx2b*^{MO}) to knock down Tbx2b. As expected, Tbx2b depletion did not alter the number of cone cells (Snelson et al., 2008a). The average number of cone cells in WT;NI and WT;*tbx2b*^{MO} were not statistically different with 22.4±1.1 (n=11) and 21.8±1.1 (n=6) cone cells respectively (Fig.20A,C,E).As previously observed, *fgf8a*^{x15};NI larvae exhibited significantly elevated cone cell number with an average of 31.8±1.3 (n=12) (Fig.20B,E). However, *fgf8a*^{x15};*tbx2b*^{MO} larvae had 21.2±1.0 (n=12) cone cells which was significantly fewer than *fgf8a*^{x15};NI larvae and were indistinguishable from WT;NI larvae (Fig.20D,E). These data indicate that regarding cone cell number, the depletion of *tbx2b* is epistatic to mutation of *fgf8a* (Fig.21).

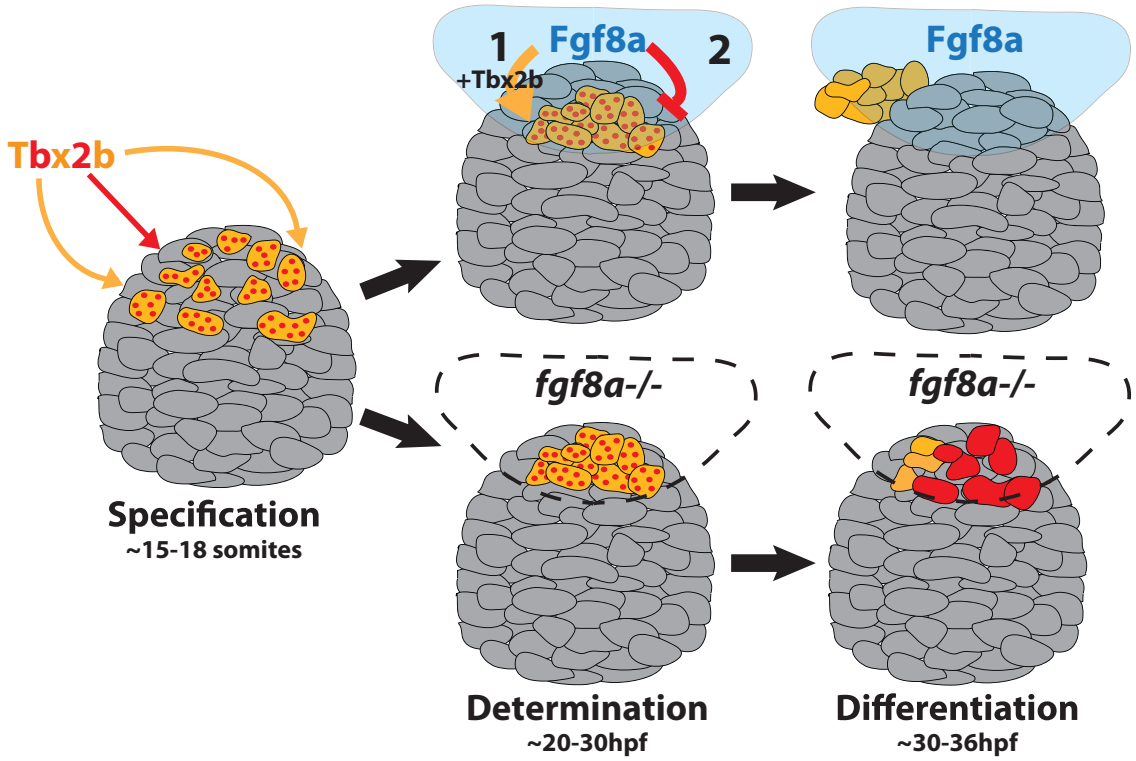

Figure 21. Model: Fgf8a acts on bi-potential parapineal/cone cells to promote parapineal fate and/or inhibit cone photoreceptor fate. The transcription factor Tbx2b specifies cells in the anterior region of the pineal complex anlage (grey) as bi-potential parapineal/cone precursors (red-dotted orange cells). Fgf8a acts on the bipotential cells (orange arrow) 1. in parallel with Tbx2b, to determine them as unipotential parapineal cells (solid orange cells), and 2. by itself (red arrow) to suppress the cone photoreceptor (red cell) differentiation program. In *fgf8a* mutants, a limited number of bipotential parapineal/cone precursor cells are specified as in WT. However, these mutants lack Fgf8a that can either suppress cone cell fate or promote parapineal differentiation. As a result, many of the cone/parapineal precursor cells adopt a cone cell fate.

Discussion

We have shown that Fgf signaling is required during a fate decision by specified parapineal precursors in order for them to form a left-sided parapineal organ. In *fgf8a*^{x15} mutants, there is a significant decrease in the number of parapineal neurons. This deficit in parapineal neurons is accompanied by an increase in the number of pineal cone photoreceptors. By cell fate and mutant analysis we gather that in the absence of Fgf8a, specified parapineal precursor cells adopt a cone photoreceptor fate. However, overexpression of Fgf8a is not sufficient to recruit more pineal complex anlage cells to become parapineal cells. Finally, we find that Fgf8a acts in parallel to the transcription factor Tbx2b to determine parapineal cell number, but downstream of Tbx2b to prevent differentiation of parapineal precursors as cone photoreceptors. Therefore, we propose that cells in the epithalamus are specified by Tbx2b as bipotential precursors that can go on to form parapineal cells or cone photoreceptors. They require Fgf signaling and Tbx2b to differentiate as parapineal cells, and might also require Fgf signaling to prevent differentiation as cone cells (Fig.21).

Perhaps the most confounding of the above results is the lack of rescue of parapineal cell fate by overexpression of Fgf8a. In theory, our model predicts that once specified, parapineal precursor cells respond to Fgf activity by correctly differentiating as parapineal cells and then migrating away from the pineal organ anlage. Providing *fgf8a*^{x15} mutants with exogenous Fgf8a should restore this missing signal and promote correct differentiation of parapineal cells. One

possibility is that Fgf receptor localization might be slightly different in *fgf8a*^{x15} mutants compared to WT. Recent evidence suggests that modulation of Fgf activity could alter the expression of Fgf receptors (Ota et al., 2010).In addition, we noted that heat shock of approximately 30 minutes at 37°C was able to activate near ubiquitous expression of *erm*, a target gene of Fgf signaling, although the expression of *fgf receptors* are not ubiquitous at this stage (data not shown). To us, this suggests that overexpression of Fgf8a causes effects beyond the normal range of physiological levels of Fgf activity. Additionally, overexpression of Fgf8a in wild-type embryos did not alter the migration parapineal cells although Fgf8a is thought to influence the directionality of parapineal cell migration (Regan et al., 2009). Thus, this method of Fgf8a overexpression may not provide the correct level or type of activity to rescue parapineal differentiation or migration in *fgf8a*^{x15} mutants.

If our overexpression experiments are valid, Fgf signaling plays an incredibly permissive role in parapineal differentiation. The inability of Fgf to produce more parapineal cells when overexpressed suggests that parapineal cell production requires multiple steps. According to our data, Fgf signaling is acting primarily on specified parapineal cells in that knocking down tbx2b in fgf8ax15 mutants ablates the ectopic generation of cone cell while further reducing the number of differentiated parapineal cells. This suggests that at least two different pathways are governing parapineal development. One possibility is that the prolonged expression of Tbx2b and the exclusion of Flh in the anterior pineal complex anlage generates a small number of parapineal precursors prior to the

15-somite stage. These precursor cells are then competent to respond to Fgf signaling by differentiating as parapineal neurons, which express *sox1a* and *gfi-1.2*. While this succinct model explains the reduction in parapineal neurons, it fails to fully account for the cell fate switch from specified parapineal precursor to pineal cone cell that occurs when Fgf activity is abrogated. This suggests that the mechanism by which Fgf signaling ensures parapineal differentiation is more complex than presented. Therefore, we sought to uncover why parapineal cells are switching fate. As a result, we examined a possible role for Bmp signaling and Lhx2b and 9, two LIM homeodomain transcription factors, during parapineal development.

Chapter III

FGF SIGNALING DOES NOT REGULATE BMP ACTIVITY DURING PARAPINEAL FORMATION

Introduction

We have shown that Fgf acts during parapineal formation to promote their correct differentiation. In the absence of Fgf signaling, the majority of specified parapineal precursors change their fate to become pineal cone cells. It is possible that these bipotential precursor cells enter a default pathway toward photoreceptor differentiation in the absence of Fgf signaling. Recently published work has shown that Bmp signaling, as well as the Notch pathway, govern cell fate within the pineal organ (Cau et al., 2008; Quillien et al., 2011). The zebrafish pineal organ contains rod and cone photoreceptors in addition to glial-like projection neurons. In Quillien et al. 2011, Bmp signaling, partially though potentiation of Notch activity, is necessary and sufficient to drive pineal cell precursors toward a photoreceptor fate and away from a projection neuron fate. In addition, increased activation of the Bmp pathway can increase the number of photoreceptors, including Arr3a positive cone cells. We have shown that, similar to most pineal precursor cells, specified parapineal precursors are at least bipotential, able to differentiate into parapineal neurons or pineal cone cells depending on Fgf activity. We posited that Bmp, in *fgf8a* mutants, acts on parapineal precursors in *fgf8a* mutants to induce their differentiation as cone

photoreceptors instead. To block Bmp signaling, Fgf could directly repress the expression of Bmp ligand (Furthauer et al., 2004), inhibit Smad activation by phosphorylation of the linker domain (Pera et al., 2003), and/or upregulate the expression of Bmp inhibitors such as Chordin (Branney et al., 2009). We found that the *chordin*, a secreted Bmp inhibitor, is expressed in the anterior epithalamus near parapineal precursor cells. Thus, if inhibition of Bmp activity would be expected to suppress the parapineal defects in *fgf8a*^{x15} mutants. In addition, if *chordin* is link between Fgf8a activity and Bmp inhibition in the anterior pineal complex, then *chordin* mutants should display similar parapineal defects as *fgf8a*^{x15} mutants. Finally, if Fgf signaling negatively regulates Bmp activity in the pineal complex anlage, we would expect ectopic phosphorylated Smad, an indicator of Bmp activity, when Fgf signaling is attenuated. To test these hypotheses, we analyzed parapineal differentiation in *chordin* mutants, inhibited Bmp activity in *fgfa*^{x15} mutants, and examined Bmp activity in the pineal complex when Fgf signaling is attenuated.

Methods

Zebrafish

Zebrafish were raised at 28.5°C on a 14/10 hour light/dark cycle and staged according to hpf. The following wild-type, mutant, and transgenic fish lines were used: AB* *(Walker, 1999), chd*^{tt250} (Hammerschmidt et al., 1996), *fgf8a*^{x15} (Kwon and Riley, 2009), Tg[*foxd3*:GFP]^{zf104} (Gilmour et al., 2002), Tg[*hsp70l*:dnXla.Bmpr1a-GFP]^{w30} (Pyati et al., 2005).

In situ hybridization

Whole-mount RNA *in situ* hybridization was performed as described previously (Gamse et al., 2003), using reagents from Roche Applied Bioscience. RNA probes were labeled using fluorescein-UTP or digoxygenin-UTP. To synthesize antisense RNA probes, pBS-*otx5* (Gamse et al., 2002); and pBS-*gfi1.2* (Dufourcq et al., 2004) were linearized with SacII and transcribed with T3 RNA polymerase; pENTR-D-Topo-*sox1a* with NotI and T7 polymerase; pBSK-*chordin* (Miller-Bertoglio et al., 1997) with SpeI and T7 polymerase. Embryos were incubated at 70°C with probe and hybridization solution containing 50% formamide. Hybridized probes were detected using alkaline phosphatase-conjugated antibodies (Roche) and visualized by 4-nitro blue tetrazolium (NBT) (Roche) and 5-bromo-4-chloro-3-indolyl-phosphate (BCIP) (Roche) staining for single labeling, or NBT/BCIP followed by iodonitrotetrazolium (INT) and BCIP staining for double labeling.

Whole mount antibody labeling

Embryos and larvae were fixed in AB fixative (4% paraformaldehyde, 0.3mM $CaCl_2$, 4% sucrose, 1X PBS) for either 4 hours at room temperature (25°C) or overnight at 4°C with rocking. Samples were rehydrated with three successive 5-minute washes with 1XPBSTx (1X PBS, 0.01% Triton X100) and four 20-minute washes with deionized water. Samples were blocked one hour at room temperature in 10% AB block (10% sheep serum, 1mg/mL Bovine Serum Albumin in 1X PBSTw). Samples were incubated with primary and secondary antibodies in 2% AB block overnight with rocking at 4°C. Excess antibody was

washed off with 1XPBSTx. Primary antibodies used: 1:1000 rabbit anti-GFP (Torrey Pines), 1:500 mouse anti-ZPR1(Arrestin3a) (Developmental Studies Hybridoma Bank), 1:100 rabbit anti-phosphorylated Smad1 (gift from C.V. Wright Lab). Secondary antibodies used: 1:300 Alexa 568 goat anti-rabbit (Invitrogen), 1:300 Alexa 488 goat anti-mouse (Invitrogen). Embryo nuclei were counterstained with TOPRO-3 (Invitrogen). All confocal images were taken with Zeiss LSM 510 microscope or Leica TSC-200 and processed using Improvision Velocity software.

Heat Shock Conditions

Embryo clutches containing both heterozygous transgenic Tg[*hsp70l*:dnXla.Bmpr1a-GFP]^{w30} embryos and their non-transgenic siblings (still in their chorions) were placed in a 2mL microcentrifuge tube (35-40 embryos/tube). Approximately 2mL of pre-warmed egg water containing 0.3% PTU was added per tube. Tubes were incubated in a 37°C water bath then I removed and emptied into a dish in a 28.5°C incubator. DN-Bmpr1a expression was induced by single heat shock treatment at 24 hpf for 30 minutes at 37°C.

Results

Fgf Signaling Does Not Regulate Bmp Activity Via Chordin

Chordin, as well as other members of the Chordin family of molecules, are mportant in the negative regulation of Bmp activity (Zakin and De Robertis, 2010). Once secreted, Chrodin binds to extracellular Bmp ligands preventing them from binding to Bmp receptors and activating downstream pathway components

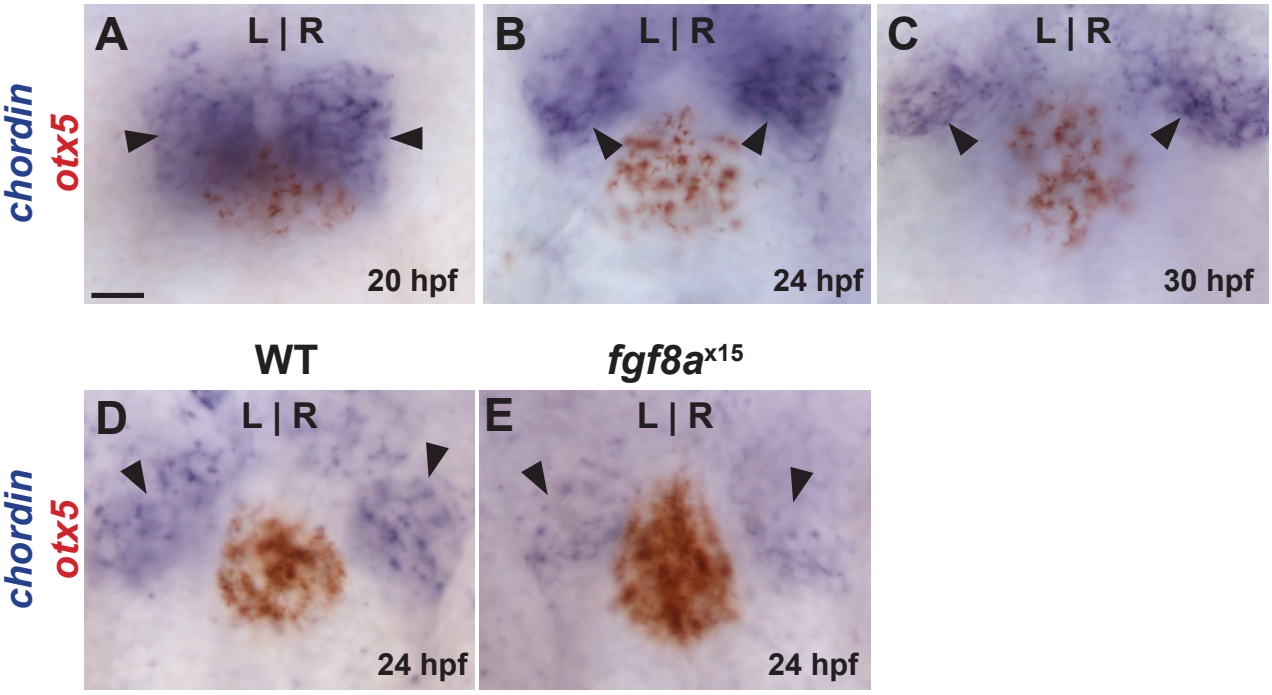

Figure 22. *chordin* is expressed in or near the epithalamus during parapineal organ development and exhibits reduced *chordin* expression in *fgf8a* mutants. (A) In 20 hpf WT embryos, *chordin* (blue) is expressed near the anterior pineal complex anlage indicated by *otx5* expression (red). (B,C) *chordin* continues to be expressed in two domains near the pineal complex at 24 and 30 hpf. (D,E) As compared to WT siblings, *chordin* expression is reduced in f*gf8a*^{x15} mutants at 24 hpf. Scale bar in A= 25 micrometers.

(Zakin and De Robertis, 2010). As such, Chordin can act at a distance from the initial source of expression. We found *chordin* to be expressed just anterior to the pineal complex anlage at 20, 24, and 30 hpf (Fig.22A,B,C) in WT embryos. The expression of *chordin* in or near the epithalamus during parapineal development suggests that it could be involved in the negative regulation of Bmp activity in the pineal complex. Additionally, *chordin* expression appears to be moderately decreased in *fgf8a*^{x15} mutants at 30 hpf (Fig.22D,E). Also, the reduction of *chordin* in *fgf8a*^{x15} mutants suggests that excessive Bmp activity could be responsible for the parapineal defects.

If Fgf signaling governs parapineal cell differentiation through regulation of *chordin*, then the loss of Chordin should produce similar parapineal defects seen in *fgf8a*^{x15} mutants. Thus, we analyzed parapineal cell number, as well as cone cell number, in *chordin*^{tt250} (*chd*^{tt250}) mutants. At 52 hpf, the number of *gfi-1.2* expressing cells in *chd*^{tt250} mutant is reduced by approximately 60% compared to WT (4.3±1.0;n=18 and 9.5±0.6;n=8 respectively) (Fig.23A,B,C). This reduction in parapineal cells closely resembles the phenotype seen when Fgf signaling is attenuated. To further explore the possible connection between Fgf signaling and Chordin, we examined Tg[*foxd3*:GFP]^{zf104} and Arr3a expression in *chd*^{tt250} mutants. Like *fgf8a*^{x15} mutants, *chd*^{tt250} mutants exhibit a lack of an obvious external parapineal with a few GFP expressing cells near the pineal organ in several mutants (Fig.24A,B). *chd*^{tt250} mutants have 44.4±2.9 (n=7) compared to WT with 56.1±2.2 (n=8) (Fig.24C) suggesting the *chd*^{tt250} mutation leads to fewer total pineal complex cells. Similarly, the number of cone cells is also significantly

reduced in *chd*^{tt250} mutants compared to WT (14.4±1.3; n=7 and 18.9±2.2; n=8 respectively). These data suggest that reduction in parapineal cells in *chd*^{tt250} mutants is likely the product of an overall reduction in pineal complex cell number and does not result from reduced Fgf/increased Bmp actvity. Indeed, the severity in the reduction of parapineal cells was variable with some *chd*^{tt250} mutants having no parapineal cells and others closely resembling WT. We attribute this variability to variation in penetrance in certain aspects of the *chd*^{tt250} mutant phenotype. Chordin is key in the patterning of the anterior axis early in embryonic development (Hammerschmidt et al., 1996). *chd*^{tt250} mutants show different degrees of ventralization, the loss of head structures and the expansion of ventrally derived tissues, in our hands. Thus, many *chd*^{tt250} mutants seem to exhibit a smaller head with as reduced pineal complex, which confounds easy analysis of potential cell fate changes.

Inhibition of Fgf Signaling Does Not Expand Bmp Activity

If Fgf signaling is directly governing Bmp activity during parapineal formation, then there should be higher levels of activated Smad1 in the anterior pineal complex when Fgf activity is attenuated. The binding of extracellular Bmp ligands to membrane bound Bmp receptors culminates in the phosphorylation and activation of Smad1/5/8 that can translocate to the nucleus and regulate transcription of target genes (Ramel and Hill, 2012). As such, analyzing the levels of phosphorylated Smad (pSmad) is a valid method for accessing Bmp activity. We examined pSmad1 in the pineal complex in embryos treated with SU5402 at

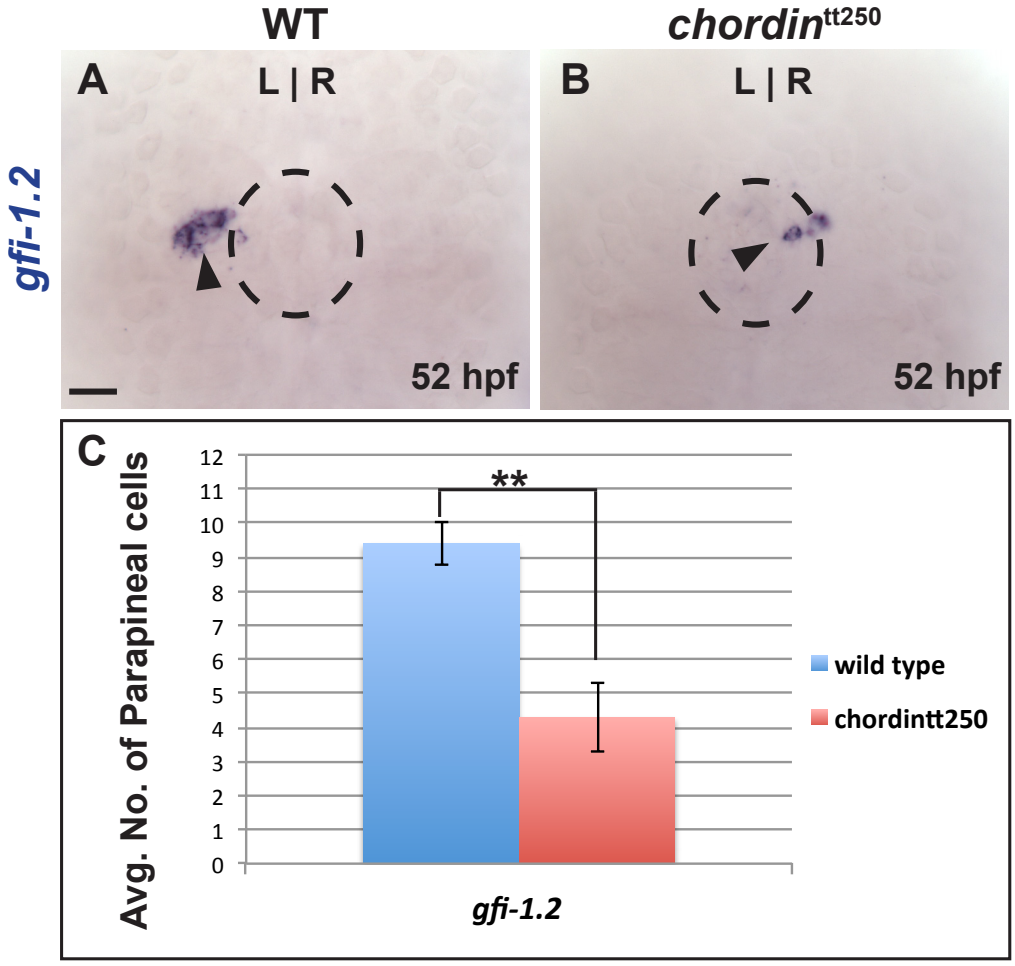

Figure 23. *chordin*^{tt250} mutants display a reduced number of differentiated parapineal cells. (A,B) As compared to WT siblings, *chordin* mutants show significant reductions in parapineal cells as indicated by *gfi-1.2* expression (black arrows) at 96 hpf. The approximate location of the pineal complex is indicated by black dashed circle. (C) Graph quantifying the number of parapineal cells in WT and *chordin*^{tt250} mutants. Error bars indicate S.E.M. (**p<0.005 by t-test). Scale bar in A =25 micrometers.

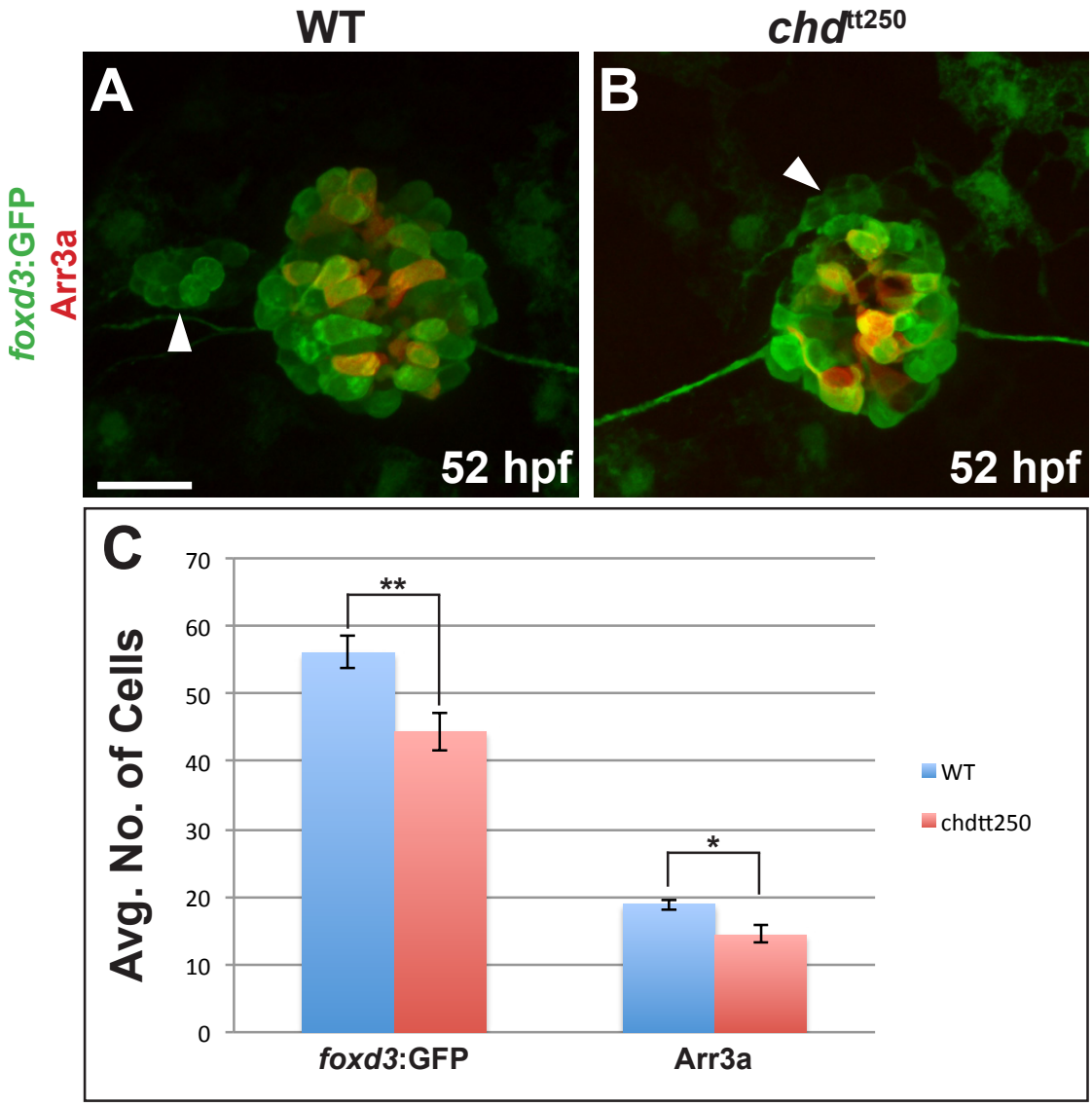

Figure 24. *chordin*^{tt250} (*chd*^{tt250})mutants show deficits in pineal complex cells. All images are dorsal 3D confocal reconstructions of the pineal complex labeled with Tg[*foxd3*:GFP] and Arr3a at 52 hpf. (A,B) In WT larvae, the parapineal is clearly visible on the left side (white arrow) while many *chd*^{tt250} mutants show only a putative parapineal cells near the anterior pineal anlage (white arrow). (C) Graph quantifying the number of Tg[*foxd3*:GFP] and Arr3a expressing cells. Error bars indicate S.E.M. (*p<0.05; **p<0.005 by t-test). Scale bar in A= 25 micrometers.

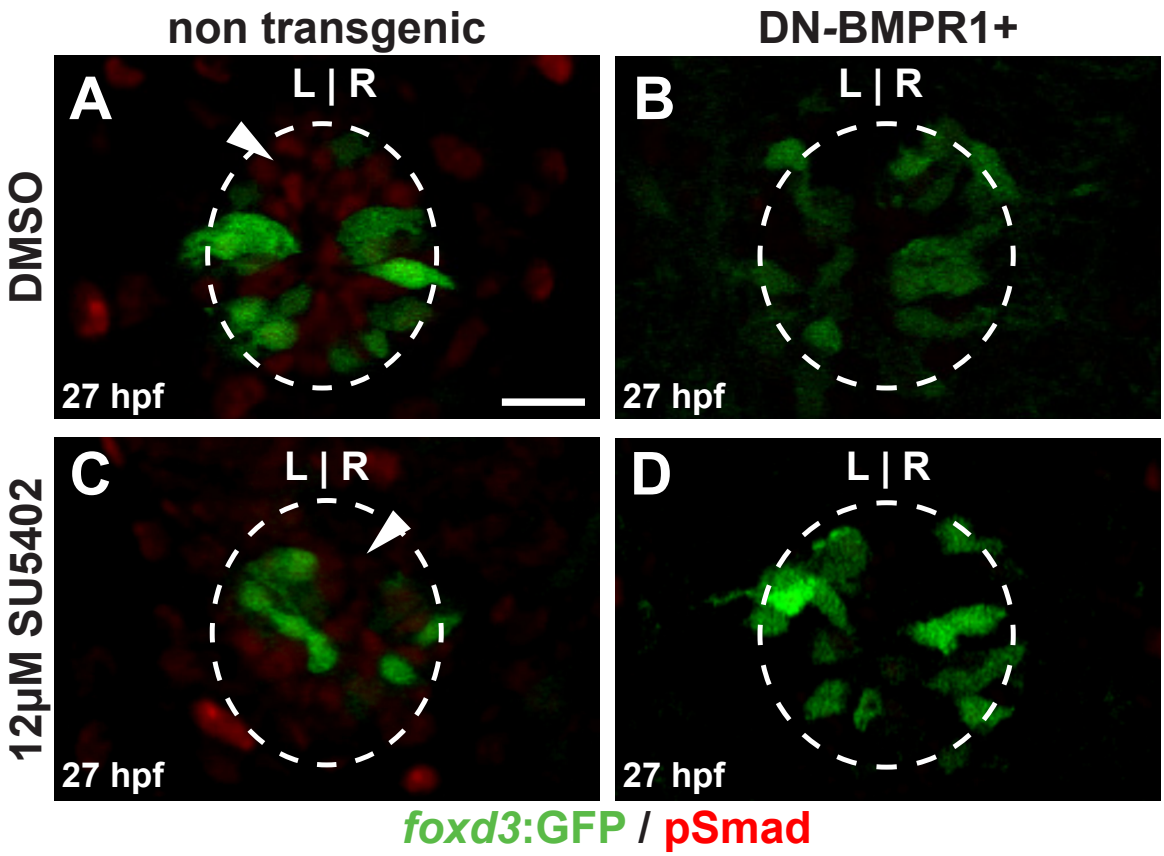

Figure 25. Inhibition of Fgf signaling does not increase Bmp activity in the pineal complex. All images are dorsal views of confocal slices of larvae labeled for Tg[*foxd3*:GFP] and phosphorylated Smad (pSmad) at 27 hpf. The approximately location of the pineal complex is indicated with a dashed circle. (A) In WT embryos treated with DMSO from 24-27 hpf, there are several cell with detectable levels of pSmad in the anterior pineal complex (white arrow). (B) Larvae treated 12μM SU5402 from 24-27 hpf show several pSmad positive cells in the anterior pineal complex (white arrow). (B,D) Expression of a dominant negative Bmp receptor effectively ablates pSmad labeling in DMSO and SU5042 treated larvae confirming the validity of pSmad labeling. Scale bar in A= 25 micrometers.

approximately 24 hpf for 3 hours. There was no obvious difference in pSmad1 labeling in SU5402 and control treated embryos (Fig.25 A,C). As a control, we suppressed Bmp activity by expressing by a dominant negative Bmp receptor (DN-Bmpr1) via the Tg[*hsp70l*:dnXla.Bmpr1a-GFP]^{w30} transgenic line. We induced expression of the DN-Bmpr1 by a heat shock of 30 minutes starting approximately at 23.5 hpf. At 27 hpf, there was no detectable pSmad1 in either SU5402 or DMSO treated embryos in DN-Bmpr1 expressing larvae (Fig.25B,D) confirming that the DNBmpr1 worked as expected.. These data suggest that Fgf signaling does not regulate Bmp signaling in the pineal complex.

Inhibition of Bmp Activity Cannot Suppress Parapineal Defects in *fgf8a* Mutants

If excessive Bmp signaling is changing the fate of parapineal precursors in *fgf8a*^{x15} mutants then inhibiting Bmp signaling in these mutants should restore parapineal differentiation. Based on the SU5402 treatment regimens, we induced the expression of a DN-Bmpr1 at 24 hpf in *fgf8a*^{x15} mutants and analyzed parapineal cell number at 52 hpf. Suppression of Bmp signaling in *fgf8a*^{x15} mutants failed to increase the number of *gfi-1.2* expressing cells with DN-Bmpr1 positive mutants having 3.5±1.0 (n=6) cells and non transgenic *fgf8a*^{x15} mutants having 3.9±0.7 (n=8) cells (Fig.26A,B,C.). Likewise, suppression of Bmp signaling in mutants failed to increase the number of *sox1a* positive cells at 36 hpf with DN-Bmpr1 expressing mutants having 2.7±0.7 (n=7) and non transgenic mutants having 2.0±0.9 (n=6) (Fig.26D).

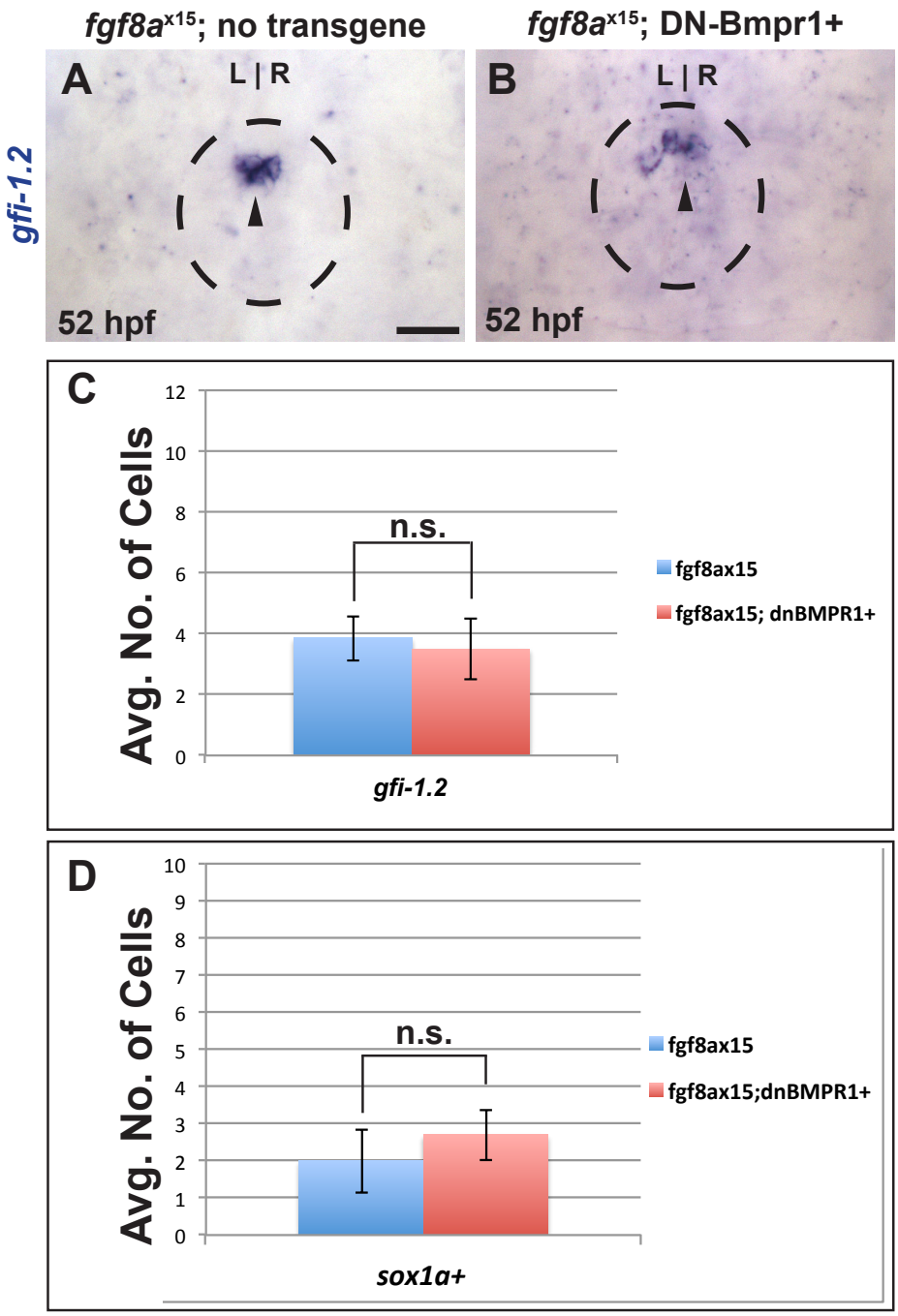

Figure 26. Bmp inhibition cannot rescue parapineal deficits in *fgf8a*^{x15} mutants. (A) Dorsal view of 52 hpf non-transgenic *fgf8a*^{x15} mutant labeled with *gfi-1.2* (black arrow). (B) Dorsal view of 52 hpf *fgf8a*^{x15} mutant expressing a dominant negative Bmp receptor (DN-Bmpr1) labeled with *gfi-1.2* (black arrow). (C) Graph quantifying the number of mature parapineal cells expressing *gfi-1.2*. (D) Graph quantifying the number of cells expressing *sox1a*, a marker likely expressed in newly differentiated parapineal cells. Error bars indicate S.E.M. n.s. indicates not significant. Scale bar in A= 25 micrometers.

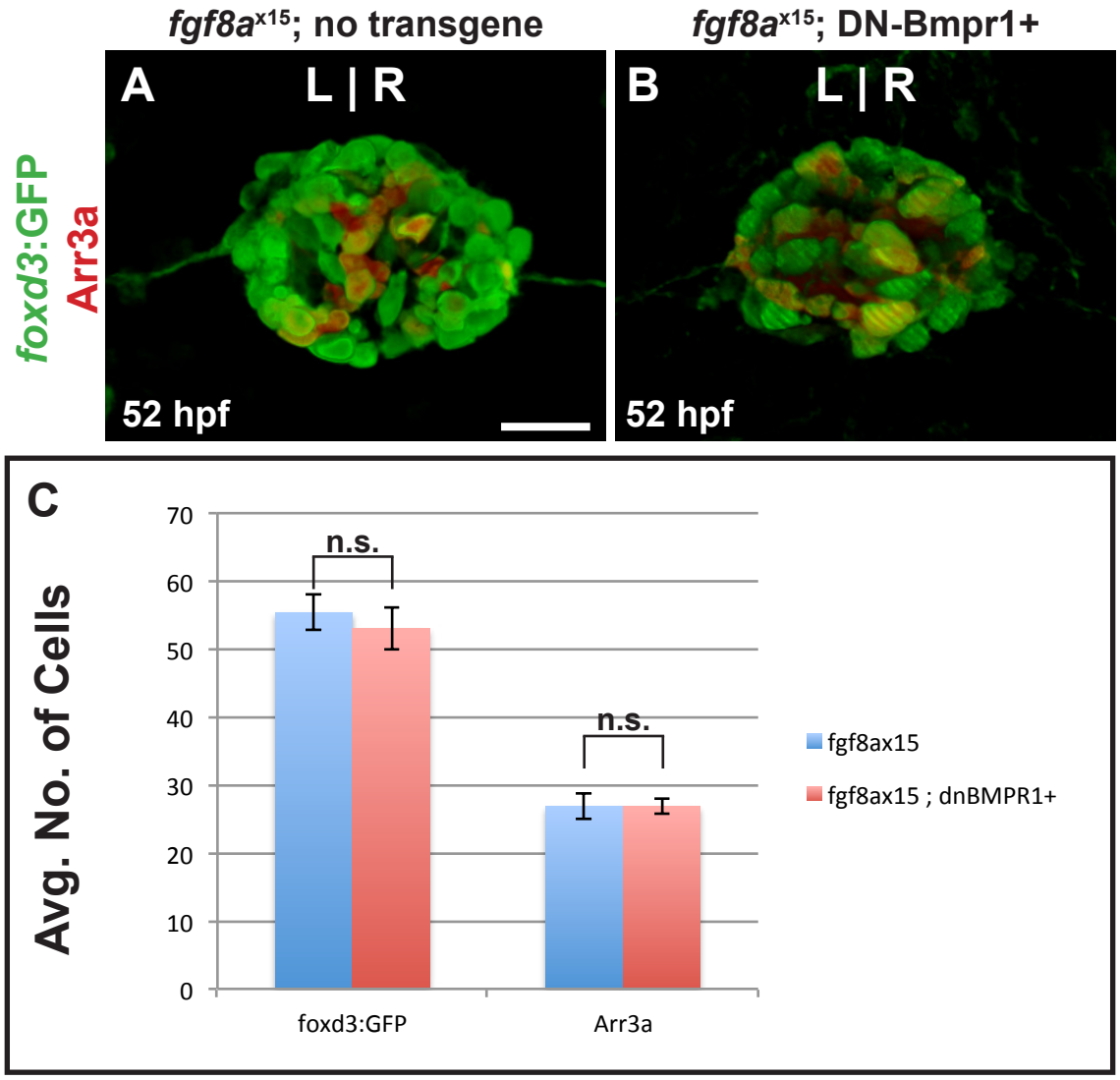

Figure 27. Inhibition of Bmp signaling cannot suppress ectopic cone cells in *fgf8a*^{x15} mutants. (A) Dorsal view of 3D confocal projection of non transgenic *fgf8a*^{x15} mutant labeled with Tg[*foxd3*:GFP] and Arr3a at 52 hpf. (B) Dorsal view of 3D confocal projection of *fgf8*^{ax15} mutant expressing a dominant negative Bmp receptor (DN-Bmpr1) labeled with Tg[*foxd3*:GFP] and Arr3a at 52 hpf. (C) Graph quantifying the number of Tg[*foxd3*:GFP] and Arr3a expressing cells. Error bars indicate S.E.M. n.s. indicates not significant. Scale bar in A= 25micrometers.

Similarly, there is no change in the number of Tg[*foxd3*:GFP]^{zf104} and Arr3a expressing cells when Bmp signaling is inhibited in *fgf8a*^{x15} mutants. Mutants expressing the DN-Bmpr1 transgene had 53.0±3.1 (n=8) Tg[*foxd3*:GFP]^{zf104} expressing cells compared to 55.0±2.5 (n=8) for non transgenic mutants (Fig.27A,B,C). Likewise, the number of cone cells is not different between non-transgenic mutants and mutants expressing the DN-Bmpr1 transgene (26.9±1.9; n=8 and 26.9±1.1; n=8 respectively) (Fig.27C).

Discussion

Published data suggests that Bmp2a is a key factor in specifying photoreceptors in the pineal organ (Quillien et al., 2011). We hypothesized that Bmp might also cause the cell fate change from parapineal to cone photoreceptor that is seen in *fgf8a*^{x15} mutants. However, we now think this is not the case for a several reasons. First, our hypothesis predicts that Bmp activity should be elevated in the anterior pineal complex when Fgf signaling is attenuated. However, after treatment with SU5402, a powerful inhibitor of Fgf activity, pSmad1 levels seem unchanged compared to control embryos. Second, reducing Bmp activity would be expected to suppress some of the cell fate defects seen in *fgf8a*^{x15} mutants. However, expression of a dominant negative Bmp receptor was unable to prevent the formation of ectopic cone cells in these mutants, much less restore parapineal cell number. Finally, the expression of *chordin*, a secreted Bmp antagonist, seems to be responsive to Fgf signaling providing a possible mechanism for the regulation of Bmp activity in the epithalamus. However,

although the phenotype of *chordin*^{tt250} mutants is superficially similar to *fgf8a*^{x15} mutants, closer investigation reveals significant differences. While the number of differentiated parapineal cells is drastically reduced in *chordin* mutants (Fig.23), this phenotype was extremely variable in penetrance. Additionally, the overall number of pineal complex cells, including Arr3a positive cone cells, is reduced in *chordin* mutants, which is not seen in *fgf8a*^{x15} mutants. We postulate that the parapineal cell deficits in *chordin* mutants are driven by earlier axial patterning defects which reduces the overall numbers of pineal complex progenitor cells and not the result of increased Bmp activity brought on by reduced Fgf signaling. Thus, Fgf signaling operates through a distinct mechanism that does not involve Bmp signaling.

CHAPTER IV

FGF SIGNALING MIGHT GOVERN PARAPINEAL DIFFERENTIATION THROUGH REGULATION OF LHX2B AND LHX9

Introduction

In Chapters II and III, we have shown that Fgf signaling regulates parapineal cell differentiation and that the cell fate defects resulting from reduced Fgf activity are likely independent of Bmp signaling. In the absence of Bmp involvement, we were without a suitable mechanism to explain the cell fate changes seen in Fgf deficient larvae. Therefore we investigated two good candidates for governing parapineal cell fate, are the LIM homeobox transcription factors 2b (Lhx2b) and Lhx9. In *Xenopus laevis*, the expression of Xlhx2 and Xlhx9, orthologs to zebrafish Lhx2b and Lhx9, are expressed in the diencephalon (Atkinson-Leadbeater et al., 2009). Furthermore, Xlhx9 is regulated by Fgf signaling (Atkinson-Leadbeater et al., 2009). In the zebrafish, Lhx2b was found to be downstream of Fgf signaling during guidance of the optic nerve across the midline (Seth A and Culverwell J, 2006). In addition, both *lhx2b* and *lhx9* are expressed in the pineal complex (Ando et al., 2005). Orthologs of Lhx2b and Lhx9 in other vertebrates have been implicated in various developmental processes such as axon guidance (Marcos-Mondejar et al., 2012), cell differentiation (Kolterud et al., 2004; Peukert et al., 2011) and specification (Berghard et al., 2012). We hypothesize that Lhx2b and Lhx9 could be acting

redundantly downstream of Fgf signaling during parapineal formation. To explore the involvement of Lhx2b and Lhx9 in parapineal formation we need to assess parapineal and cone cell number in Lhx2b and Lhx9 deficient larvae. In addition, if Lhx2b and Lhx9 are key effectors of Fgf mediated parapineal cell differentiation, then we would expect that loss of *lhx2b* and/or *lhx9* function would result in loss of parapineal cells and that overexpression of these transcription factors to rescue parapineal defects in *fgf8a*^{x15} mutants.

Methods

Zebrafish

Zebrafish were raised at 28.5°C on a 14/10 hour light/dark cycle and staged according to hpf. The following wild-type, mutant, and transgenic fish lines were used: AB* *(Walker, 1999),* *fgf8a*^{x15} (Kwon and Riley, 2009), Tg[*foxd3*:GFP]^{zf104} (Gilmour et al., 2002), Tg[*flhBAC*:Kaede]^{vu376} (Clanton et al., 2013), *lhx2b*^{b700} (Seth A and Culverwell J, 2006).

in situ hybridization

Whole-mount RNA *in situ* hybridization was performed as described previously (Gamse et al., 2003), using reagents from Roche Applied Bioscience. RNA probes were labeled using fluorescein-UTP or digoxygenin-UTP. To synthesize antisense RNA probes: pENTR-D-Topo-*lhx2b* (Seth A and Culverwell J, 2006) with Not1 with T7; pCRII-Topo-*lhx9* (Ando et al., 2005) with HindIII and T7; pBS-*gfi1.2* (Dufourcq et al., 2004) were linearized with SacII and transcribed with T3 RNA polymerase. Embryos were incubated at 70°C with probe and hybridization

solution containing 50% formamide. Hybridized probes were detected using alkaline phosphatase-conjugated antibodies (Roche) and visualized by 4-nitro blue tetrazolium (NBT) (Roche) and 5-bromo-4-chloro-3-indolyl-phosphate (BCIP) (Roche) staining for single labeling, or NBT/BCIP followed by iodonitrotetrazolium (INT) and BCIP staining for double labeling. In fluorescent *in situ* hybridization, staining was developed in a 1:1 ratio of fast red tablet to fast red buffer (0.1M Tris pH8.2, 0.4M $NaCl_2$) at 37°C. Antibody labeling of fluorescent *in situ* was carried out using 1:500 of rabbit anti-GFP (Torrey Pines) or 1:500 of rabbit anti-Kaede (MBL). Secondary labeling was done with 1:300 anti rabbit Alexa 488 (Invitrogen).

Inhibitor Treatments

For *in situ* hybridizations and whole mount antibody labeling, we incubated embryos in their chorions in 12μM SU5402 (Calbiochem and Tocris) dissolved in 0.3% DMSO in egg water in 1XPTU in the dark. Control embryos were treated with 0.3% Dimethyl sulfoxide (DMSO) in parallel with their SU5402 treated siblings.

Cloning

Full-length contructs for *in situ* hybridization probes for *lhx2b* and *lhx9* transcripts were cloned from total RNA from 28 hpf AB* embryos dissolved in Trizol (Invitrogen). Total cDNA was made from phenol-chloroform purified total RNA with random hexamer (Applied Biosystems) priming and Superscript III reverse transcriptase (Invitrogen). *lhx2b* transcript was amplified using the following primers: Fw-CACCTCAGACCGATCAGACACTGC with the 5' CACC sequence to

facilitate entry into pENTR-D-Topo vector (Invitrogen); Rv-TGCAGTGGGCTAAAATGATG. *lhx9* transcript was using the following primers: Fw-GAACGGACGGGAGACAACTA and Rv-TCCAGGCCACTTGACACTCC. *lhx2b* PCR product was amplified with Phusion polymerase (NEB). *lhx9* PCR product was treated for 10 minutes at 72°C with Go Taq polymerase (Promega) to add TA overhangs. *lhx2b* and *lhx9* products were agarose gel purified with Wizard SV Gel and PCR clean up system (Promega). Purified *lhx2b* transcript was inserted into pENTR-D-Topo vector via Topo cloning reaction. *lhx9* transcript was inserted into pCRII-Topo vector via Topo TA cloning. Purified *lhx2b* and *lhx9* products were transformed into One Shot Top10 cells (Invitrogen) on ampicillin containing agar plates overnight at 37°C. Bacterial containing colonies containing construct were expanded and the plasmid was harvested using Pure Yield Plasmid Midi Prep System (Promega). To make mRNA expression constructs, we cloned *lhx2b* and *lhx9* into pCS2+ Gateway plasmid (pCS2+ backbone with att1 and att2 sites just inside the multiple cloning site to facilitate Gateway cloning reactions). *lhx9* we amplified using the following primers: Fw-CACCAATTCCACCGGCTTAATATGG with a CACC overhang to allow entry into pENTR-D-Topo and Rv-TCCAGGCCACTTGACACTCC. *lhx9* PCR product was purified and cloned into pENTR-D-Topo as described above. *lhx2b* and *lhx9* were flipped from pENTR-D-Topo into pCS2+Gateway via a gateway cloning reaction catalyzed by LR Clonase II Plus (Invitrogen) overnight at room temperature. *lhx2b*-pCS2+Gateway and *lhx9*-pCS2+Gateway were transformed into Top10 cells and harvested as described above. For mRNA transcription *lhx2b*-

pCS2+Gateway was linearized with NotI and *lhx9*-pCS2+Gateway was linearized with KpnI. The linearized fragments were purified with phenol chloroform and precipitated with 100% EtOH. Sense mRNA was transcribed with Sp6 mMessage mMachine Kit (Ambion).

mRNA injection

lhx9 mRNA diluted to the desired concentration with nuclease-free water and phenol red. Approximately 1nL was injected into zebrafish embryos between 1 and 4 cell stage. Injected embryos were raised at 28.5°C.

Results

lhx2b and *lhx9* are Expressed in the Pineal Complex During Parapineal Formation

While both *lhx2b* and *lhx9* are known to be expressed in the zebrafish epithalamus (Ando et al., 2005), their expression was not described in detail in the pineal complex. We performed fluorescent *in situ* hybridization for *lhx2b* and *lhx9* in embryos carrying both the Tg[*foxd3*:GFP]^{zf104} and Tg[*flh*BAC:Kaede]^{vu376} transgenes to highlight the pineal complex anlage. At 24 hpf, expression of both *lhx2b* and *lhx9* is enriched in the anterior and midline of the pineal complex (Fig.28A,B). Importantly, parapineal precursors are located in the anterior one-third of the pineal complex at 24 hpf within the domain of strong *lhx2b* and *lhx9* expression. By 30 hpf, *lhx2b* and *lhx9* remain enriched in the anterior pineal complex including the emerging parapineal cells (Fig.28C,D). The expression of these two transcription factors make them ideal candidates for being involved in

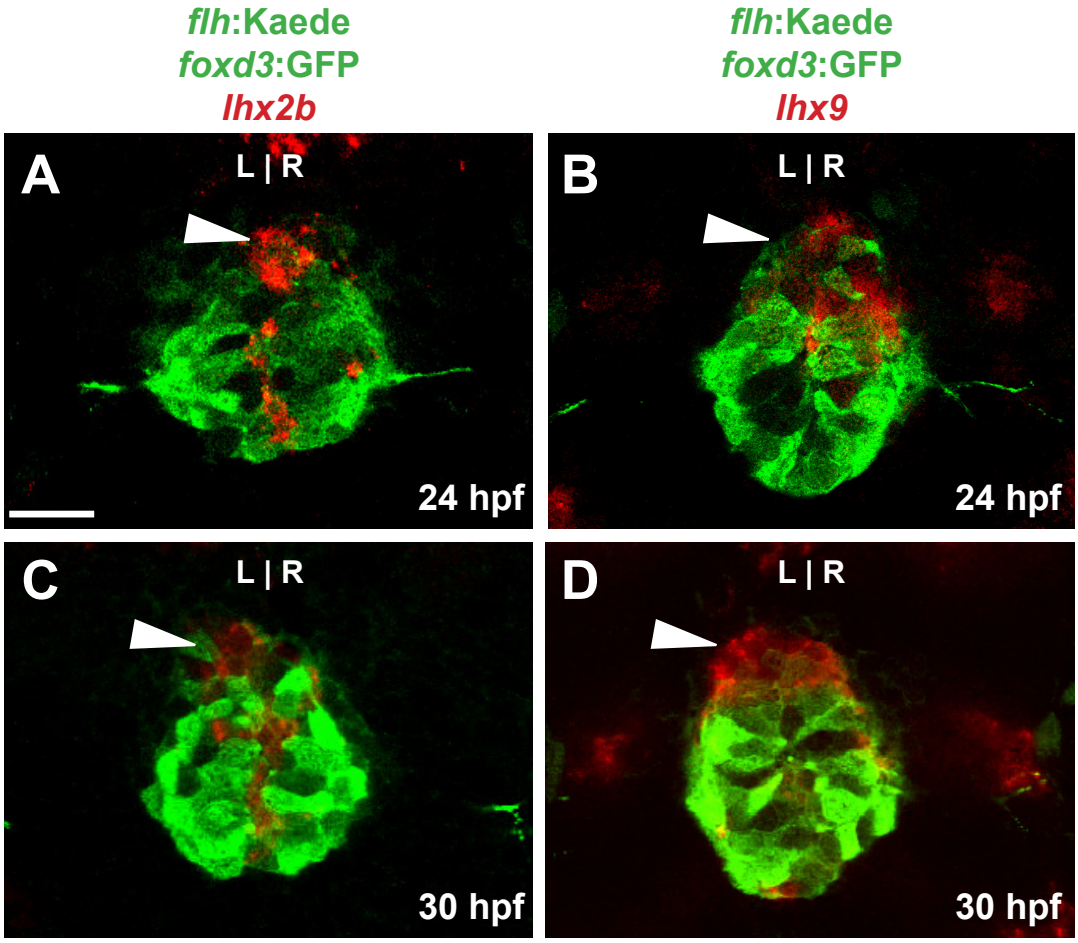

Figure 28. *lhx2b* and *lhx9* are expressed in the anterior pineal complex during parapineal formation. All images are dorsal view of confocal slices of embryos labeled with Tg[*foxd3*:GFP] and Tg[*flh*:Kaede] to indicate the pineal complex. (A,C) *lhx2b* is expressed in the anterior pineal complex at 24 and 30 hpf in what is migrating parapineal cells (white arrow in C). (B,D) *lhx9* is expressed in the anterior pineal complex at 24 and 30 hpf in what is appears to be parapineal precursor cells (white arrow in D). Scale bar in A=25 micrometers.

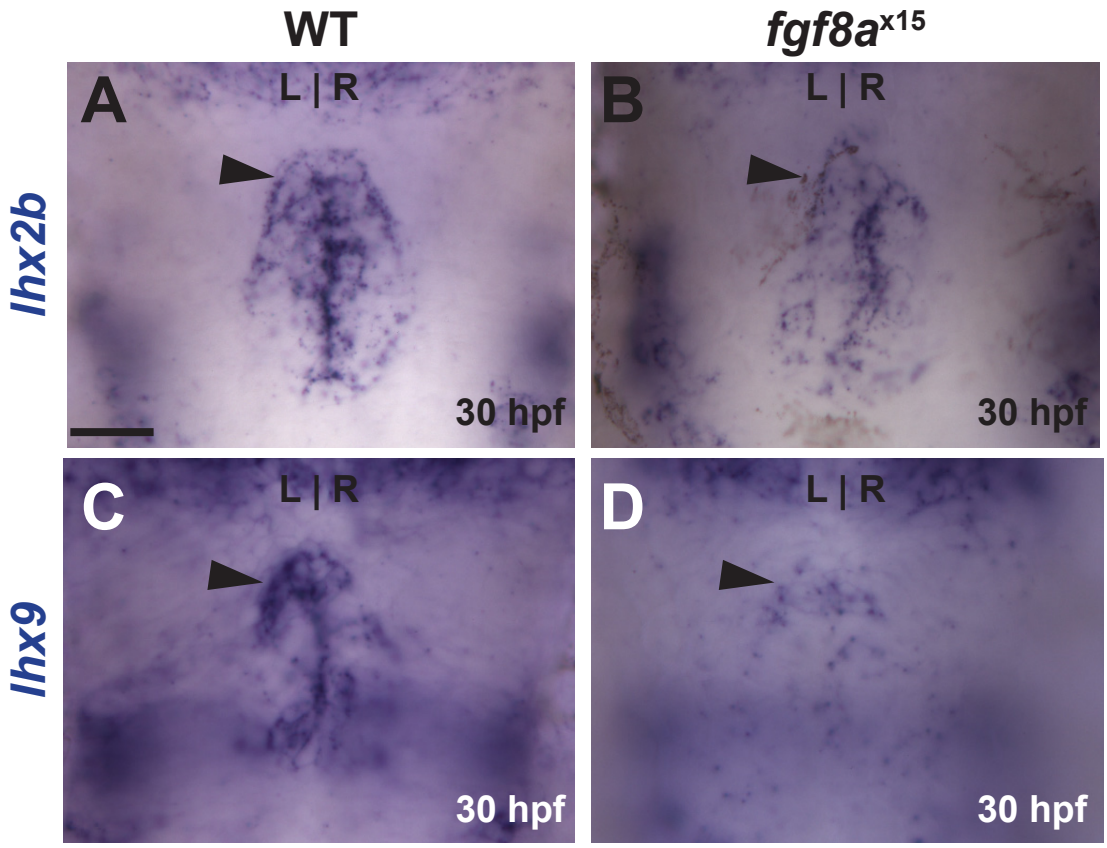

Figure 29. *lhx2b* and *lhx9* expression is reduced in *fgf8a*^{x15} mutants. All images are dorsal views of 30 hpf larvae. (A) In 30 hpf, *lhx2b* expression is strong in the anterior pineal complex (black arrow). (B) *lhx2b* expression is reduced in the anterior pineal complex anlage (black arrow) in *fgf8a*^{x15} mutants. (C) In 30 hpf, *lhx9* expression is strong in the anterior pineal complex (black arrow). (D) *lhx9* expression is relegated to a few cells in the anterior pineal complex (black arrows). Scale bar in A= 25 micrometers.

parapineal formation.

The Expression of *lhx2b* and *lhx9* is Regulated by Fgf Signaling

Previous data suggested that the expression of *lhx2b* (in zebrafish) and *lhx9* (in *Xenopus*) is responsive to Fgf signaling (Seth A and Culverwell J, 2006; Atkinson-Leadbeater et al., 2009). To confirm that Fgf activity can govern the expression of *lhx2b* and *lhx9* in the zebrafish pineal complex, we examined the expression of the these two transcription factors when Fgf signaling is attenuated. At 30 hpf, *fgf8a*^{x15} mutants exhibit reduced expression of *lhx2b* as compared to WT (Fig.29A,B). This loss of expression is especially acute in the anterior pineal complex in the region of the parapineal precursors (black arrow Fig.29B). Similarly, *lhx9* is reduced in *fgf8a*^{x15} mutants (Fig.29C,D). As further conformation that Fgf signaling could control the expression of *lhx2b* and *lhx9* at relevant time points during parapineal formation, we analyzed expression in embryos treated with 12μM SU5402 between 24 and 30 hpf. At 30 hpf, *lhx2b* expression was drastically reduced in SU5402 treated embryos as compared with controls (Fig.30A,B). Likewise, the expression of *lhx9* was reduced to only a few cells at the midline and the anterior pineal complex (Fig.30C,D). Taken together, these data strongly suggests that Fgf signaling governs the expression of both *lhx2b* and *lhx9* in the pineal complex.

Lhx2b and Lhx9 Might Play a Role in Parapineal Formation

To explore the potential role of Lhx2b during parapineal formation, we

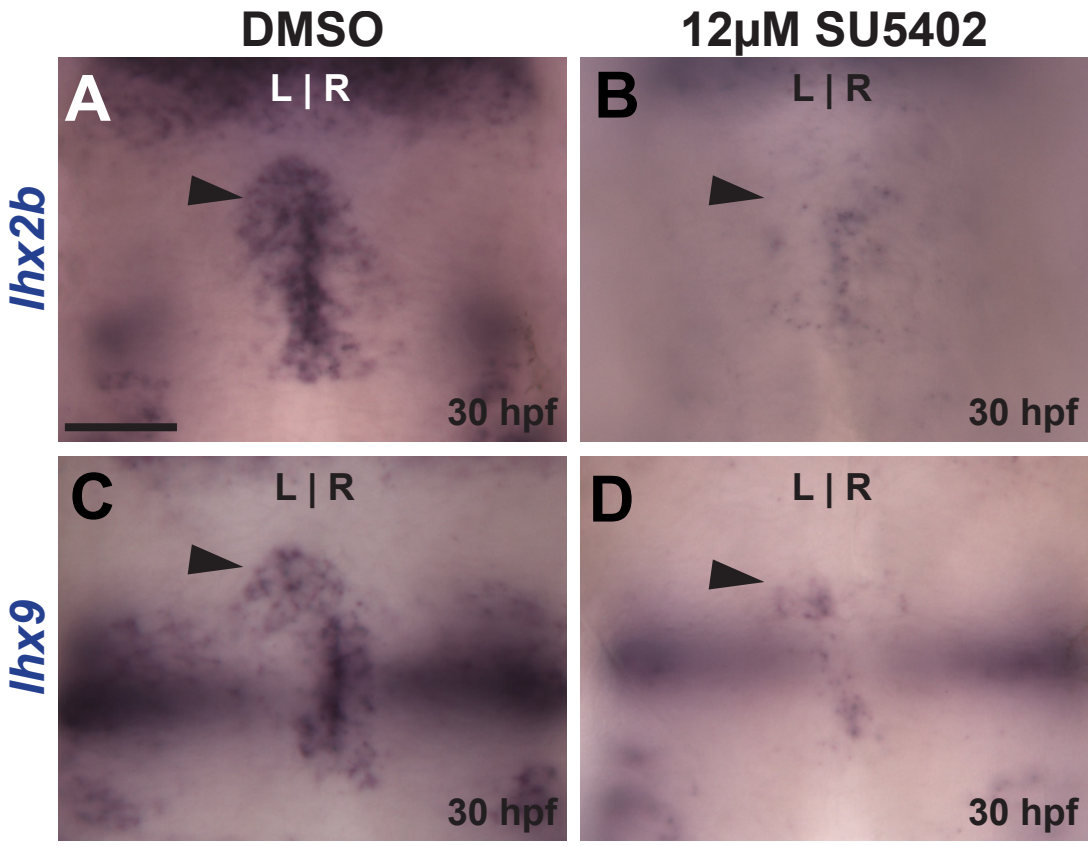

Figure 30. *lhx2b* and *lhx9* expression is responsive to Fgf signaling. All images are dorsal views at 30 hpf. Embryos were treated with DMSO and 12μM SU5402 from 24-30 hpf. (A) *lhx2b* expression is robust in the anterior pineal complex anlage (black arrow). (B) *lhx2b* is drastically reduced in SU5402 treated embryos. C) *lhx9* expression is robust in the anterior pineal complex anlage (black arrow). D) *lhx9* is drastically reduced in SU5402 treated embryos. Scale bar in A= 25 micrometers.

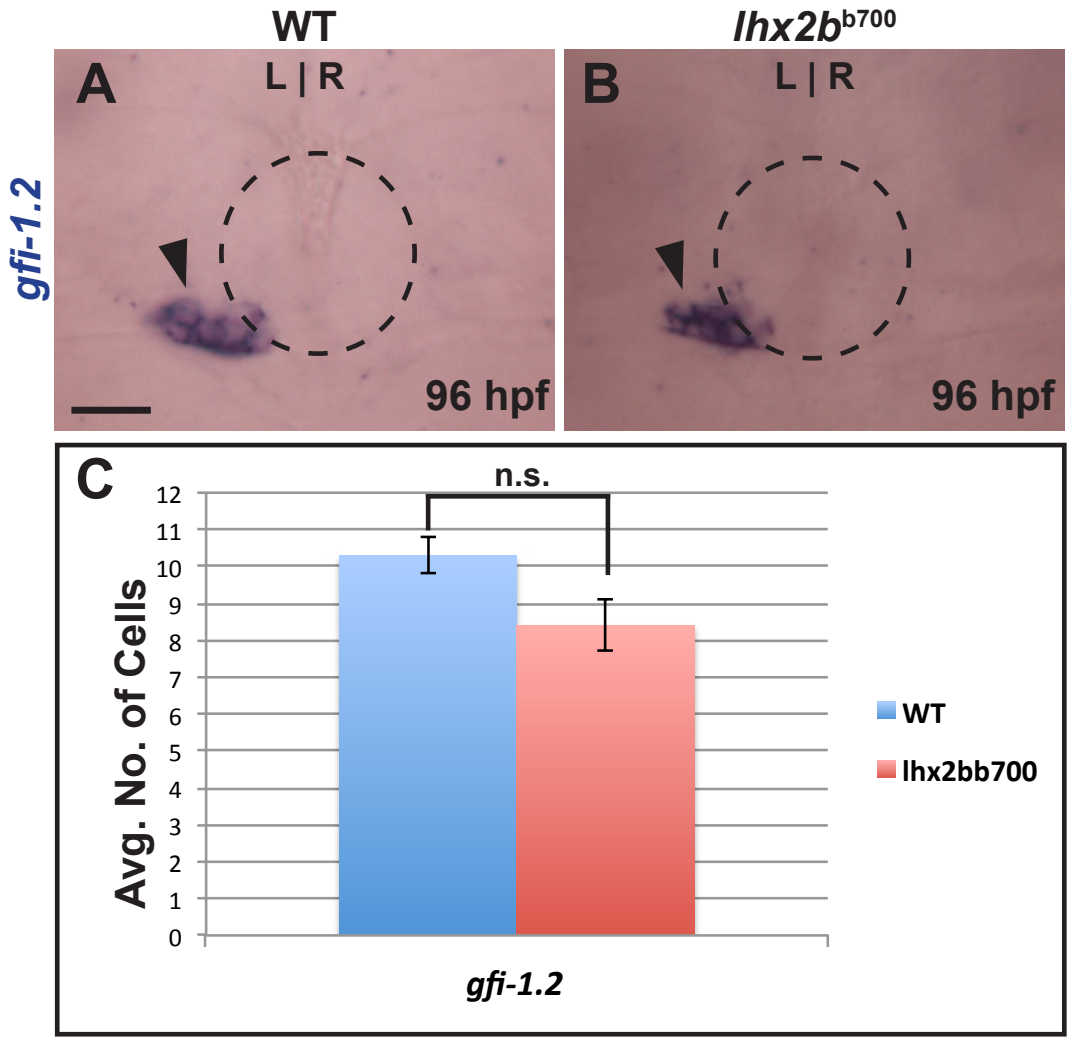

Figure 31. Lhx2b mutants might have fewer parapineal cells. A,B) Dorsal views of 96 hpf WT and *lhx2b*^{b700} mutants labeled with *gfi-1.2* to indicate the parapineal cells (black arrows). (C) Graph quantifying the number of parapineal cells in WT and *lhx2b*^{b700} mutants. Error bars indicate S.E.M. Scale bar in A= 25 micrometers.

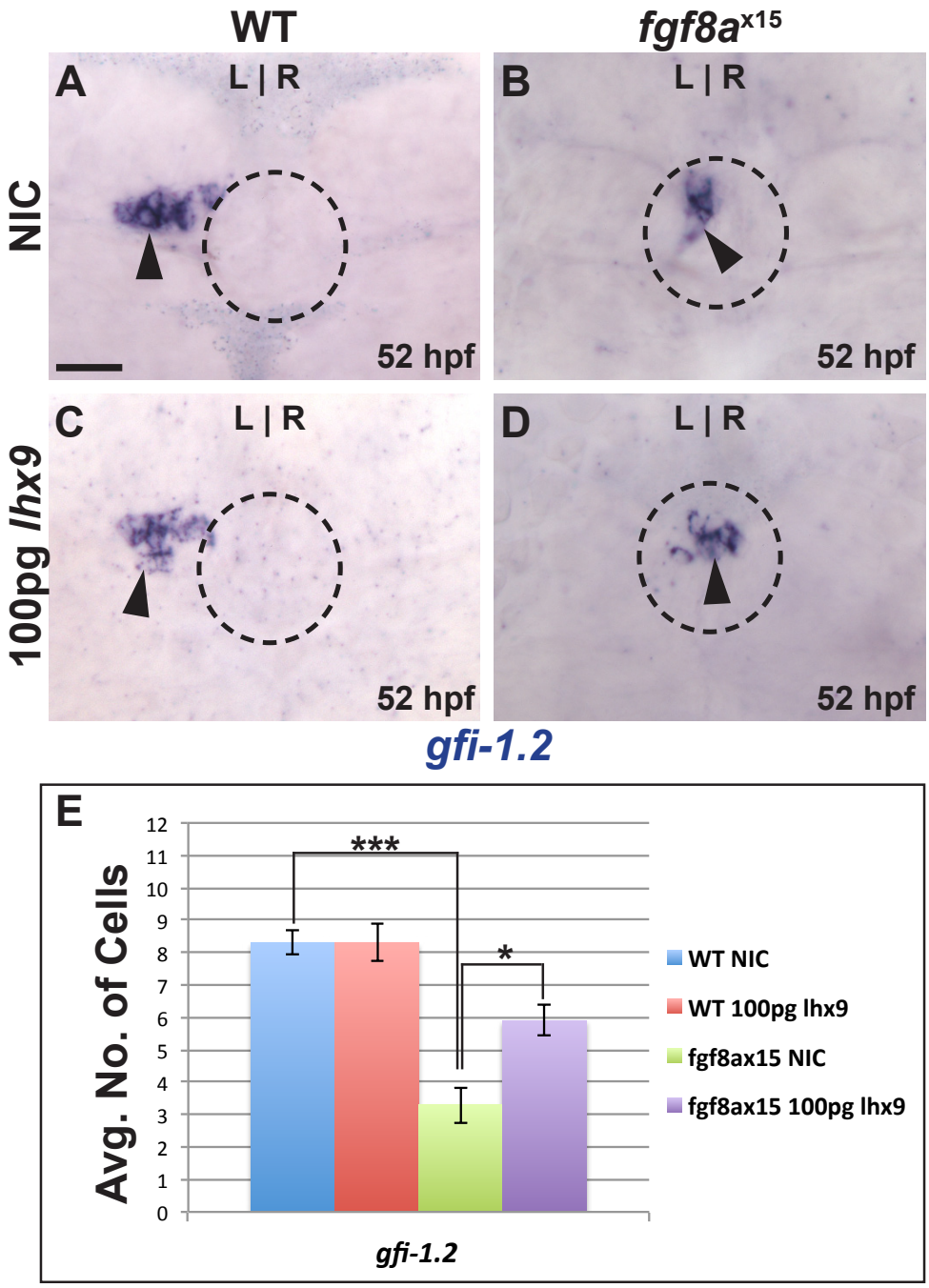

Figure 32. *lhx9* overexpression can partially rescue parapineal deficits in *fgf8a*^{x15} mutants. All images are dorsal views labeled with *gfi-1.2* to indicate parapineal cells. (A,C) Relative to non-injected (NIC) WT siblings, injection of 100pg of *lhx9* mRNA caused no change in the number of parapineal cells. (B,D) Compared to non-injected *fgf8ax15* mutants, injection of 100pg *lhx9* mRNA increases the number of parapineal cells. (E) Graph quantifying the number of parapineal cells. Error bars indicate S.E.M. (*p<0.05; ***p<0.0005 by T-test). Scale bar in A= 25 micrometers.

examined *gfi-1.2* expression in *lhx2b*^{b700} mutants, a putative null for *lhx2b* function (Seth A and Culverwell J, 2006). At 96 hpf, the number of parapineal cells in *lhx2b*^{b700} mutants is lower than WT siblings (8.4±0.7; n=5 and 10.3±05; n=4 respectively) although not significantly different (Fig.31A,B,C). We also wanted to know if providing either *lhx2b* or *lhx9* mRNA could rescue parapineal cell number in *fgf8a*^{x15} mutants. Injection of 100pg of *lhx9* mRNA in to *fgf8a*^{x15} heterozygous crosses resulted in a small, but significant increase in parapineal cell number in *lhx9* mRNA injected *fgf8a*^{x15} mutants (5.9±0.5; n=8) compared with non-injected *fgf8a*^{x15} mutants (3.3±0.6; n=11) (Fig.32D,B,E). In contrast, injection of 100pg *lhx9* mRNA into their wild-type siblings had no effect on parapineal cell number. Non-injected and *lhx9* mRNA injected WT had an equivalent number of parapineal cells (8.3±0.4; n=11 and 8.3±0.6; n=12 respectively) (Fig.32A,B,E). The above data, provide tantalizing evidence that Lhx2b and Lhx9 could be crucial effectors of Fgf mediated parapineal cell differentiation.

Discussion

We have found that two transcription factors, *lhx2b* and *lhx9*, are expressed robustly in the anterior pineal complex anlage and seem to be regulated by Fgf signaling. Unlike other epithalamic genes regulated by Fgf signaling, such as *erm* and *sprouty4* (Furthauer et al., 2002), *lhx2b* and *lhx9* seem to exhibit tissue specific expression in the pineal complex anlage. Loss of Fgf8a, results in the reduction of differentiated habenular neurons, as well as fewer parapineal cells

(Regan et al., 2009). We suspect that Lhx2b and Lhx9 might be specific mediators of cell fate in the anterior pineal complex.

Although many questions remain, these two transcription factors fulfill some of the requirements for factors involved in parapineal cell fate decisions. For one, a mutation in *lhx2b* does result in a reduced number of parapineal cells in the relative few *lhx2b*^{b700} mutants examined. Also, injection of *lhx9* mRNA can partially restore the number of differentiated parapineal cells in *fgf8a*^{x15} mutants while leaving WT parapineal number unchanged. In the future, we need to characterize the combined loss of Lhx2b and Lhx9 during parapineal differentiation. The loss of Lhx2b alone resulted in a modest though non-significant reduction in the number of parapineal cells. We suspect that Lhx9 could be partially compensating for the loss of Lhx2b in *lhx2b*^{b700} mutants as these two proteins function redundantly during ventral thalamus development (Peukert et al., 2011). Also, the ability of *lhx9* mRNA to rescue parapineal number suggests that Lhx9 has some role in parapineal differentiation. Perhaps the simultaneous loss of both genes will more fully recapitulate the phenotypes seen in *fgf8a*^{x15} mutants (increase in cone cells at the expense of parapineal cells). These experiments would provide us with a much more detailed understanding of parapineal differentiation and a framework for future research.

CHAPTER V

CONCLUSIONS AND FUTURE DIRECTIONS

The formation of the parapineal organ is one of the first, and perhaps most critical, steps in the generation of an asymmetric epithalamus in zebrafish. We have shown that differentiation of specified parapineal precursors into parapineal neurons requires Fgf signaling. Curiously, elevating Fgf activity in wild-type larvae does not increase the number of parapineal neurons suggesting Fgf8a is required permissively to ensure that parapineal differentiation occurs. Through an improved cell fate analysis procedure, we have established that precursor cells that would normally contribute to the parapineal adopt a pineal cone photoreceptor fate. This reassignment of cell fate is not driven by changes in Bmp signaling, which promotes the specification of pineal photoreceptors. Thus, it appears that a transcriptional network driven by the Fgf signaling pathway acts upon parapineal precursors to ensure their correct differentiation. Two LIM homeobox transcription factors, Lhx2b and Lhx9, could be important in ensuring this process as their expression in the pineal complex is responsive to Fgf signaling. Together, these transcription factors show strong localization to the anterior pineal complex compared to other Fgf responsive genes. Overexpression of *lhx9* mRNA partially rescues the number of parapineal cells in *fgf8a*^{x15} mutants. This suggests that Lhx2b and Lhx9 might directly regulate parapineal cell differentiation downstream of Fgf signaling and not simply

regulate the competency of specified parapineal precursors to respond to additional signals.

Fgf Signaling Has Multiple Roles During Parapineal Development

Previously, Fgf8a was shown to be required for the migration of parapineal cells (Regan et al., 2009). According to the model of Regan et al (2009), Fgf8a promotes migration of parapineal cells away from the midline and, in the absence of epithalamic Nodal signaling, can provide a directional cue for parapineal migration (Regan et al., 2009; Roussigne et al., 2011). However, the authors do not note any change in parapineal cell number in *fgf8a*^{ti282} mutants. Therefore, one possibility is that the levels of Fgf signaling required for parapineal migration and differentiation may not be the same. In Regan et al. (2009), the authors used *fgf8a*^{ti282}, a hypomorphic allele that disrupts splicing of approximately 70% of *fgf8a* transcripts (Draper et al., 2001). The amount of wild-type Fgf8a in *fgf8a*^{ti282} in combination with Fgf17 could be sufficient to promote parapineal differentiation but inadequate to ensure migration. We have found some support for this hypothesis. Treating embryos with a low concentration of SU5402 results in an inhibition of migration without significant changes to parapineal cell number. In addition, embryos with overactive epithalamic Wnt signaling show a significant delay in parapineal cell migration of about 24 hours without apparent issues with cell number suggesting that differentiation of parapineal cells doesn't depend on migration (Carl et al., 2007). The *fgf8a* mutant allele used in our studies, *fgf8a*^{x15}, is a likely null resulting from a premature stop codon, which truncates much of

the protein (Kwon and Riley, 2009). According to our data, complete loss of Fgf8a results in severe reductions in mature parapineal cells which might exhibit a larger repertoire of epithalamic phenotypes.

Fgf acts during early to mid-somitogenesis to correctly establish the midline of the forebrain through a gene regulatory loop of the *sine occulus homeobox* homologs *six3b* and *six7* (J. Neugebauer and J. Yost, personal communications). Neugebauer and Yost suggest that without careful "tuning" of the midline by Fgf signaling, epithalamic Nodal signaling cannot be properly established. Importantly, this early role of Fgf signaling in midline formation does not directly impact cell fate within parapineal precursors, as larvae deficient in both Six3b and Six7 still form a parapineal organ although its position is randomized (Inbal et al., 2007). Thus, Fgf signaling controls the establishment of left-sided Nodal signaling, is required for habenular neurogenesis (Regan et al., 2009), and governs differentiation and migration of parapineal neurons (Regan et al., 2009; Clanton et al., 2013). This clearly demonstrates the importance of Fgf signaling in many facets of epithalamic development.

Fgf8a is Required for Parapineal and Habenular Development

We have noted that *fgf8a*^{x15} mutants, much like *fgf8a*^{ti282} mutants, display deficits in differentiated habenular neurons as well as reduced neuropil volumes in both the left and right habenular nuclei (Regan et al., 2009) (J.A.C. and B. Dean, unpublished observation). It is emerging that Fgf8a is likely involved in the earliest stages of habenular patterning (B. Dean unpublished results). A leading

model describing parapineal formation suggests that early neurogenesis in the left habenula, in concert with a slight leftward bias in *fgf8a* expression, presages asymmetric migration of parapineal cells (Regan et al., 2009; Roussigne et al., 2009). Indeed, the development of the habenulae and the parapineal organ appear to be intimately linked. Habenular precursors have been mapped to a position just ventral to parapineal precursors in the anterior epithalamus (Concha et al., 2003). Additionally, the emergence of post-mitotic neurons in the left habenula seems closely coordinated with the emergence of the parapineal from the pineal complex anlage (Roussigne et al., 2009). Finally, Fgf8a signaling seems to be robust in the developing habenulae. As a result, we suggest that the habenulae, via Fgf8a, could have an important role in patterning parapineal cells. Some evidence for this idea has recently emerged in mice. Mice with targeted mutations in *fgf8*, like *fgf8a* mutant zebrafish, have fewer cells in the habenular nuclei (Martinez-Ferre and Martinez, 2009; Regan et al., 2009). However, the deficits of epithalamic cell types seen in *fgf8* mutant mice extend to the pineal organ (Martinez-Ferre and Martinez, 2009). We observe no change in total cell number in the pineal complex. This suggests that Fgf8 has a broad role in patterning the entire epithalamus in mice, but may play a subtler role in the zebrafish to pattern habenular and parapineal cells.

So far, we cannot resolve with certitude whether the parapineal defects in *fgf8a* mutants are the result of direct Fgf activity within the cells of the pineal complex or a byproduct of habenular agenesis. To fully address this, we will need more sophisticated ways to attenuate Fgf signaling in a tissue specific manner thereby

isolating the loss of Fgf signaling to a particular region of the epithalamus.

Fgf Signaling Governs a Binary Fate Decision in Pineal Complex Precursors

During embryogenesis, secreted ligands, such as Fgfs, often emanate from organizing centers in the brain that pattern surrounding tissues (Sansom and Livesey, 2009). The isthmic organizer and the anterior forebrain (rostral organizing center) use multiple Fgf ligands to control cell number and fate in the midbrain/hindbrain and the telencephalon respectively in a concentration dependent manner (Sato et al., 2004; Iwata and Hevner, 2009; Suzuki-Hirano and Shimogori, 2009). Epithalamic Fgf signaling (Fgf8a and Fgf17) could play a similar morphogenic role in specifying pineal complex cell types. As mentioned above, Fgf8 knockout mice exhibit severe deficits in all epithalamic cell types, including the pineal organ (Martinez-Ferre and Martinez, 2009), precluding the analysis of how different cell fates are specified within the pineal complex. In the zebrafish, the pineal complex is largely intact, allowing us to examine the role of Fgf signaling in the generation of pineal complex subtypes. However, our data suggest that Fgf signaling does not act as a morphogen in the pineal complex, i.e. intensity and duration of Fgf signaling does not specify different pineal complex cell types. In *fgf8a*^{x15}mutants, the total cell number in the pineal complex number is the same as WT. Rather, when Fgf signaling is reduced, specified parapineal precursors undergo a cell fate switch to express Arrestin 3a, a marker for cone photoreceptors. Other pineal complex cell types are unaffected by the loss of

Fgf8a. This is a surprising result, as examples of Fgf signaling participating in binary cell fate decisions in the developing nervous system are not commonly reported with one example being in the neural tube of ascidian larvae (Minokawa et al., 2001).

Despite broad expression of the Fgf receptor *fgfr4* and the Fgf target gene *erm* throughout the anterior pineal complex, parapineal precursors appear to be the only cells that change fate when Fgf signaling is abrogated. This indicates that the response of a subset of anterior pineal complex progenitors (likely parapineal precursors) to Fgf signaling is regulated by some other factor(s). One unanswered question in our studies is how, in the absence of Fgf signaling, most of the specified parapineal precursors instead give rise to pineal cones. It is emerging that the epithalamus is a rich signaling environment with Wnt, Bmp, Notch, as well as Fgf signaling, all being active during development. Wnt signaling only seems to govern the size of the future epithalamus during forebrain patterning, as well as the directionality of parapineal cell migration, but does not seem to regulate specific cell fates (Masai et al., 1997; Carl et al., 2007). Bmp signaling and Notch signaling combine to regulate cell fate in the pineal complex, but do not seem to have a direct effect on parapineal fate (C.Doll and J.Clanton unpublished observations). Indeed, the expression of *bmp2a*, the only Bmp ligand specific to the pineal complex, is very transient (data not shown). Additionally, pSmad, an indicator of Bmp activity, is not present in the likely parapineal precursors. Thus, the formation of parapineal neurons does not involve the interaction between the Fgf and Bmp signaling pathway. Rather

parapineal differentiation might require the expression of transcription factors downstream of Fgf signaling.

It has been theorized that the formation of a particular neuronal subtype depends on a "combinatorial code" of genes (Hobert et al., 2010). Thus, the kind and relative levels of a suite of individual transcription factors define the terminal identity of a neuron. At this time, we are aware of only two transcription factors, Tbx2b and Flh, are required to form the pineal complex (pineal organ and parapineal organ). Previously, we found that a small number of cells at the anterior dorsal midline of the pineal complex anlage strongly express *tbx2b* but only transiently express *flh*, which is required for pineal neurogenesis, and proposed that parapineal precursors were specified by the combination of *tbx2b* expression and *flh* exclusion (Snelson et al., 2008a). We have speculated that having high *tbx2b* expression and low *flh* expression could bias pineal complex progenitors to become parapineal cells versus pineal cells (Snelson et al., 2008a; Clanton et al., 2013) (Fig.2). This limitation of parapineal competency to *tbx2b*$^{+}$, *flh*$^{-}$ cells agrees with our data that overexpression of Fgf8a is unable to induce supernumerary parapineal cells. However, *flh* expression appears to be entirely dispensable for parapineal formation as *flh* mutants specify a normal number of parapineal cells. Also, since we do not have a Tbx2b antibody, it is impossible to quantify the level of Tbx2b expression in different regions of pineal complex. Additionally, a small number of differentiated parapineal cells form in tbx2b mutants indicates that Tbx2b might not be indispensable for parapineal formation. Likewise, preliminary Tbx2b overexpression experiments indicated that Tbx2b

might not be instructing parapineal fate (S. Khuansuwan unpublished results). Thus, the specification of parapineal cells is more complex than available models suggest.

In addition, our current models for the specification of parapineal precursors cannot explain how specified parapineal precursors adopt a pineal cone cell fate in the absence of Fgf signaling. Curiously, Tbx2b does not appear to have any direct role in the specification of pineal cone cells, although it is required to produce extra cone cells in the absence of Fgf signaling. Preliminary data suggests that Nuclear receptor subfamily 2 group E, member 3 (NR2E3), a transcription factor expressed in the pineal complex, might inhibit parapineal fate and promote the formation of pineal rod photoreceptors (S. Khuansuwan unpublished results). It is unclear if changes in Nr2e3 expression could contribute to the cell fate switch seen in *fgf8a*^{x15} mutants. Fgf8a;Nr2e3 double mutants could help resolve this question. Additionally, the enrichment of *lhx2b* and *lhx9* in the anterior pineal complex, in concert with sustained expression of *tbx2b*, could be key events that help to resolve parapineal/cone fate. It has been theorized that the formation of a particular neuronal subtype depends on a "combinatorial code" of genes (Hobert et al., 2010). Thus, the kind and relative levels of a suite of individual transcription factors define the terminal identity of a neuron. Future experiments analyzing the function of these genes should help uncover which other signals define parapineal cell fate. The acquisition of parapineal cell fate is the key step in changing a non-migratory neuronal cell type (pineal cell) into a cell that is capable of directed migration. How parapineal cells make this fate

decision could reveal novel mechanisms to explain how cells attain migratory capabilities. This might prove important beyond the formation of brain asymmetries and into more fundamental areas of cell biology.

Fgf Signaling and Parapineal Cells: An Evolutionary Perspective

Although the pineal organ can be found in almost all vertebrate groups, the parapineal organ or a related structure called the parietal organ is only present in lampreys, teleosts, and lizards (Concha and Wilson, 2001; Ekstrom and Meissl, 2003). In larval zebrafish, the parapineal is a small cluster of cells that lies ventral to pineal organ and abuts the left habenulae. This arrangement echoes the organization of the pineal complexes of other teleosts as well as lampreys (Ekstrom et al., 1983; Melendez-Ferro et al., 2002). The parapineal organs of lamprey and teleosts are composed of similar cell types. Ultrastructural and immunohistochemical analysis reveals that the parapineal organ is composed mainly of neurons, but teleosts (eel and trout) contain a varied and limited number of poorly developed and scattered photoreceptors, while in adult lampreys, opsin-containing photoreceptors in the parapineal organ are more numerous and cluster in the ventral portion of the organ (van Veen et al., 1980; van Veen, 1982; Vigh-Teichmann et al., 1983). Several key differences in parapineal formation between lamprey and teleosts have emerged. For one, in zebrafish, parapineal and pineal cells arise from a common anlage. Unlike zebrafish, the lamprey parapineal and pineal anlagen appear to emerge from separate primordia during the early stages of pineal complex development

(Ekstrom et al., 1983)In zebrafish, prior to the onset of migration, parapineal precursor cells are indistinguishable from the surrounding pineal cells (Snelson et al., 2008b). Therefore, a mechanism is needed to set aside a subset of pineal complex anlage cells to become the parapineal organ, prior to the onset of pineal cell differentiation. This mechanism could also serve to isolate putative parapineal precursors from pineal derived factors that could alter their fate. This divergence in parapineal and pineal cell fates appears to be driven by the sequential action of Tbx2b and Fgf8a. It is unclear if a similar mechanism may exist in lamprey. .

In addition to initially developing as separate anlagen, the differentiation of the lamprey parapineal organ lags behind that of the pineal organ (Melendez-Ferro et al., 2002). During the larval stages, differentiated cell types, including photoreceptors and neurons, appear in the lamprey pineal organ (Melendez-Ferro et al., 2002). However, at this time, the lamprey parapineal organ remains a cohesive, but undifferentiated group of cells anterior to the pineal organ (Melendez-Ferro et al., 2002). Alterations in Fgf signaling could underlie the distinctions between parapineal formation of the teleost and lamprey. Lamprey *fgf8/17*, a putative ortholog to teleost *fgf8a*, is expressed in the forebrain during larval stages, including the putative epithalamus (Guerin et al., 2009). However, the expression of *fgf8/17* in the lamprey brain is activated much later in forebrain development when compared to teleosts (zebrafish and stickleback) (Reifers et al., 1998; Jovelin et al., 2007; Guerin et al., 2009). Delaying the onset of epithalamic *fgf8/17* expression may allow the parapineal anlage to “wait” for the

proper time to differentiate. It has been speculated that the temporal advancement of forebrain development in teleosts, as indicated by *fgf8a* and *fgf17* expression, allows for expansion of the telencephalon relative to that of the lamprey. This accelerated development in teleosts may afford less time for pineal complex development and would force parapineal cells to differentiate over a similar time span to pineal cells and other regions of the forebrain. The delay of Fgf expression in the lamprey would allow the parapineal precursors to develop more slowly, perhaps remaining in a state that is sensitive to photoreceptor-inducing signals in the pineal complex anlage and resulting in a greater number of photoreceptors in the lamprey parapineal organ.

Like the parapineal organ, the parietal organ is lies near the pineal organ and forms axonal connections to the left habenular nucleus (Concha and Wilson, 2001). However, while the parapineal organ is a relatively simple cluster of two basic cell types (neurons and rudimentary photoreceptors), the parietal organ is a more complex, retina-like structure complete with rod cells, cone cells, and neurons (Ekstrom and Meissl, 2003). We have demonstrated that a mutation in one secreted factor, Fgf8a, can cause normally specified parapineal cells to adopt a fate as ectopic cone photoreceptors, which are never seen in the wild type parapineal organ of zebrafish. Fgf expression data from lizards are currently lacking. Nevertheless, it seems reasonable to speculate that modulation of the spatial and temporal expression of molecules such as Fgf ligand, led to elaboration of the simple parapineal into the parietal organ during evolution.

REFERENCES

Agetsuma, M., Aizawa, H., Aoki, T., Nakayama, R., Takahoko, M., Goto, M., Sassa, T., Amo, R., Shiraki, T., Kawakami, K. et al. (2010) 'The habenula is crucial for experience-dependent modification of fear responses in zebrafish', *Nature neuroscience* 13(11): 1354-6.

Amo, R., Aizawa, H., Takahoko, M., Kobayashi, M., Takahashi, R., Aoki, T. and Okamoto, H. (2010) 'Identification of the zebrafish ventral habenula as a homolog of the mammalian lateral habenula', *The Journal of neuroscience : the official journal of the Society for Neuroscience* 30(4): 1566-74.

Ando, H., Kobayashi, M., Tsubokawa, T., Uyemura, K., Furuta, T. and Okamoto, H. (2005) 'Lhx2 mediates the activity of Six3 in zebrafish forebrain growth', *Developmental biology* 287(2): 456-68.

Atkinson-Leadbeater, K., Bertolesi, G. E., Johnston, J. A., Hehr, C. L. and McFarlane, S. (2009) 'FGF receptor dependent regulation of Lhx9 expression in the developing nervous system', *Developmental dynamics : an official publication of the American Association of Anatomists* 238(2): 367-75.

Barth, K. A., Kishimoto, Y., Rohr, K. B., Seydler, C., Schulte-Merker, S. and Wilson, S. W. (1999) 'Bmp activity establishes a gradient of positional information throughout the entire neural plate', *Development* 126(22): 4977-87.

Barth, K. A., Miklosi, A., Watkins, J., Bianco, I. H., Wilson, S. W. and Andrew, R. J. (2005) 'fsi zebrafish show concordant reversal of laterality of viscera, neuroanatomy, and a subset of behavioral responses', *Current biology : CB* 15(9): 844-50.

Berghard, A., Hagglund, A. C., Bohm, S. and Carlsson, L. (2012) 'Lhx2-dependent specification of olfactory sensory neurons is required for successful integration of olfactory, vomeronasal, and GnRH neurons', *FASEB journal : official publication of the Federation of American Societies for Experimental Biology* 26(8): 3464-72.

Borg, B., Ekstrom, P. and Van Veen, T. (1983) 'The Parapinela Organ of Teleosts', *Accta Zoolog.* 64: 211-218.

Bottcher, R. T. and Niehrs, C. (2005) 'Fibroblast growth factor signaling during early vertebrate development', *Endocrine reviews* 26(1): 63-77.

Branney, P. A., Faas, L., Steane, S. E., Pownall, M. E. and Isaacs, H. V. (2009) 'Characterisation of the fibroblast growth factor dependent transcriptome in early development', *PloS one* 4(3): e4951.

Bruel-Jungerman, E., Davis, S. and Laroche, S. (2007) 'Brain plasticity mechanisms and memory: a party of four', *The Neuroscientist : a review journal bringing neurobiology, neurology and psychiatry* 13(5): 492-505.

Butler, A. B. and Hodos, W. (1996) *Comparative Vertebrate Neuroanatomy: Evololution and Adaptation*, New York: Wiley-Liss.

Carl, M., Bianco, I. H., Bajoghli, B., Aghaallaei, N., Czerny, T. and Wilson, S. W. (2007) 'Wnt/Axin1/beta-catenin signaling regulates asymmetric nodal

activation, elaboration, and concordance of CNS asymmetries', *Neuron* 55(3): 393-405.
Cau, E. and Blader, P. (2009) 'Notch activity in the nervous system: to switch or not switch?', *Neural Dev* 4: 36.
Cau, E., Quillien, A. and Blader, P. (2008) 'Notch resolves mixed neural identities in the zebrafish epiphysis', *Development* 135(14): 2391-401.
Cau, E. and Wilson, S. W. (2003) 'Ash1a and Neurogenin1 function downstream of Floating head to regulate epiphysial neurogenesis', *Development* 130(11): 2455-66.
Clanton, J. A., Hope, K. D. and Gamse, J. T. (2013) 'Fgf signaling governs cell fate in the zebrafish pineal complex', *Development* 140(2): 323-32.
Clanton, J. A., Shestopalov, I., Chen, J. K. and Gamse, J. T. (2011) 'Lineage labeling of zebrafish cells with laser uncagable fluorescein dextran', *Journal of visualized experiments : JoVE*(50).
Clay, H. and Ramakrishnan, L. (2005) 'Multiplex fluorescent in situ hybridization in zebrafish embryos using tyramide signal amplification', *Zebrafish* 2(2): 105-11.
Concha, M. L., Bianco, I. H. and Wilson, S. W. (2012) 'Encoding asymmetry within neural circuits', *Nature reviews. Neuroscience* 13(12): 832-43.
Concha, M. L., Burdine, R. D., Russell, C., Schier, A. F. and Wilson, S. W. (2000) 'A nodal signaling pathway regulates the laterality of neuroanatomical asymmetries in the zebrafish forebrain', *Neuron* 28(2): 399-409.
Concha, M. L., Russell, C., Regan, J. C., Tawk, M., Sidi, S., Gilmour, D. T., Kapsimali, M., Sumoy, L., Goldstone, K., Amaya, E. et al. (2003) 'Local tissue interactions across the dorsal midline of the forebrain establish CNS laterality', *Neuron* 39(3): 423-38.
Concha, M. L. and Wilson, S. W. (2001) 'Asymmetry in the epithalamus of vertebrates', *Journal of anatomy* 199(Pt 1-2): 63-84.
Crossley, P. H. and Martin, G. R. (1995) 'The mouse Fgf8 gene encodes a family of polypeptides and is expressed in regions that direct outgrowth and patterning in the developing embryo', *Development* 121(2): 439-51.
Crossley, P. H., Martinez, S. and Martin, G. R. (1996) 'Midbrain development induced by FGF8 in the chick embryo', *Nature* 380(6569): 66-8.
Dharmaretnam, M. and Rogers, L. J. (2005) 'Hemispheric specialization and dual processing in strongly versus weakly lateralized chicks', *Behavioural brain research* 162(1): 62-70.
Draper, B. W., Morcos, P. A. and Kimmel, C. B. (2001) 'Inhibition of zebrafish fgf8 pre-mRNA splicing with morpholino oligos: a quantifiable method for gene knockdown', *Genesis* 30(3): 154-6.
Dufourcq, P., Rastegar, S., Strahle, U. and Blader, P. (2004) 'Parapineal specific expression of gfi1 in the zebrafish epithalamus', *Gene Expr Patterns* 4(1): 53-7.
Echevarria, D., Vieira, C., Gimeno, L. and Martinez, S. (2003) 'Neuroepithelial secondary organizers and cell fate specification in the developing brain', *Brain research. Brain research reviews* 43(2): 179-91.

Ekstrom, P., Borg, B. and van Veen, T. (1983) 'Ontogenetic development of the pineal organ, parapineal organ, and retina of the three-spined stickleback, Gasterosteus aculeatus L. (Teleostei). Development of photoreceptors', *Cell and tissue research* 233(3): 593-609.

Ekstrom, P. and Meissl, H. (2003) 'Evolution of photosensory pineal organs in new light: the fate of neuroendocrine photoreceptors', *Philosophical transactions of the Royal Society of London. Series B, Biological sciences* 358(1438): 1679-700.

Facchin, L., Burgess, H. A., Siddiqi, M., Granato, M. and Halpern, M. E. (2009) 'Determining the function of zebrafish epithalamic asymmetry', *Philosophical transactions of the Royal Society of London. Series B, Biological sciences* 364(1519): 1021-32.

Falcon, J., Migaud, H., Munoz-Cueto, J. A. and Carrillo, M. (2010) 'Current knowledge on the melatonin system in teleost fish', *General and comparative endocrinology* 165(3): 469-82.

Firnberg, N. and Neubuser, A. (2002) 'FGF signaling regulates expression of Tbx2, Erm, Pea3, and Pax3 in the early nasal region', *Developmental biology* 247(2): 237-50.

Furthauer, M., Lin, W., Ang, S. L., Thisse, B. and Thisse, C. (2002) 'Sef is a feedback-induced antagonist of Ras/MAPK-mediated FGF signalling', *Nature cell biology* 4(2): 170-4.

Furthauer, M., Van Celst, J., Thisse, C. and Thisse, B. (2004) 'Fgf signalling controls the dorsoventral patterning of the zebrafish embryo', *Development* 131(12): 2853-64.

Gamse, J. T., Kuan, Y. S., Macurak, M., Brosamle, C., Thisse, B., Thisse, C. and Halpern, M. E. (2005) 'Directional asymmetry of the zebrafish epithalamus guides dorsoventral innervation of the midbrain target', *Development* 132(21): 4869-81.

Gamse, J. T., Shen, Y. C., Thisse, C., Thisse, B., Raymond, P. A., Halpern, M. E. and Liang, J. O. (2002) 'Otx5 regulates genes that show circadian expression in the zebrafish pineal complex', *Nat Genet* 30(1): 117-21.

Gamse, J. T., Thisse, C., Thisse, B. and Halpern, M. E. (2003) 'The parapineal mediates left-right asymmetry in the zebrafish diencephalon', *Development* 130(6): 1059-68.

Geschwind, N. and Levitsky, W. (1968) 'Human brain: left-right asymmetries in temporal speech region', *Science* 161(3837): 186-7.

Gilmour, D. T., Maischein, H. M. and Nusslein-Volhard, C. (2002) 'Migration and function of a glial subtype in the vertebrate peripheral nervous system', *Neuron* 34(4): 577-88.

Goto, K., Kurashima, R., Gokan, H., Inoue, N., Ito, I. and Watanabe, S. (2010) 'Left-right asymmetry defect in the hippocampal circuitry impairs spatial learning and working memory in iv mice', *PloS one* 5(11): e15468.

Guerin, A., d'Aubenton-Carafa, Y., Marrakchi, E., Da Silva, C., Wincker, P., Mazan, S. and Retaux, S. (2009) 'Neurodevelopment genes in lampreys reveal trends for forebrain evolution in craniates', *PloS one* 4(4): e5374.

Guillemot, F. and Zimmer, C. (2011) 'From cradle to grave: the multiple roles of fibroblast growth factors in neural development', *Neuron* 71(4): 574-88.
Hammerschmidt, M., Pelegri, F., Mullins, M. C., Kane, D. A., van Eeden, F. J., Granato, M., Brand, M., Furutani-Seiki, M., Haffter, P., Heisenberg, C. P. et al. (1996) 'dino and mercedes, two genes regulating dorsal development in the zebrafish embryo', *Development* 123: 95-102.
Hans, S., Christison, J., Liu, D. and Westerfield, M. (2007) 'Fgf-dependent otic induction requires competence provided by Foxi1 and Dlx3b', *BMC developmental biology* 7: 5.
Hasan, A., Kremer, L., Gruber, O., Schneider-Axmann, T., Guse, B., Reith, W., Falkai, P. and Wobrock, T. (2011) 'Planum temporale asymmetry to the right hemisphere in first-episode schizophrenia', *Psychiatry research* 193(1): 56-9.
Heilman, K. M. and Van Den Abell, T. (1980) 'Right hemisphere dominance for attention: the mechanism underlying hemispheric asymmetries of inattention (neglect)', *Neurology* 30(3): 327-30.
Hobert, O., Carrera, I. and Stefanakis, N. (2010) 'The molecular and gene regulatory signature of a neuron', *Trends in neurosciences* 33(10): 435-45.
Ile, K. E., Kassen, S., Cao, C., Vihtehlic, T., Shah, S. D., Mousley, C. J., Alb, J. G., Jr., Huijbregts, R. P., Stearns, G. W., Brockerhoff, S. E. et al. (2010) 'Zebrafish class 1 phosphatidylinositol transfer proteins: PITPbeta and double cone cell outer segment integrity in retina', *Traffic* 11(9): 1151-67.
Inbal, A., Kim, S. H., Shin, J. and Solnica-Krezel, L. (2007) 'Six3 represses nodal activity to establish early brain asymmetry in zebrafish', *Neuron* 55(3): 407-15.
Itoh, N. (2007) 'The Fgf families in humans, mice, and zebrafish: their evolutional processes and roles in development, metabolism, and disease', *Biological & pharmaceutical bulletin* 30(10): 1819-25.
Iwata, T. and Hevner, R. F. (2009) 'Fibroblast growth factor signaling in development of the cerebral cortex', *Development, growth & differentiation* 51(3): 299-323.
Jovelin, R., He, X., Amores, A., Yan, Y. L., Shi, R., Qin, B., Roe, B., Cresko, W. A. and Postlethwait, J. H. (2007) 'Duplication and divergence of fgf8 functions in teleost development and evolution', *Journal of experimental zoology. Part B, Molecular and developmental evolution* 308(6): 730-43.
Kawakami, R., Shinohara, Y., Kato, Y., Sugiyama, H., Shigemoto, R. and Ito, I. (2003) 'Asymmetrical allocation of NMDA receptor epsilon2 subunits in hippocampal circuitry', *Science* 300(5621): 990-4.
Kohl, M. M., Shipton, O. A., Deacon, R. M., Rawlins, J. N., Deisseroth, K. and Paulsen, O. (2011) 'Hemisphere-specific optogenetic stimulation reveals left-right asymmetry of hippocampal plasticity', *Nature neuroscience* 14(11): 1413-5.
Kolterud, A., Alenius, M., Carlsson, L. and Bohm, S. (2004) 'The Lim homeobox gene Lhx2 is required for olfactory sensory neuron identity', *Development* 131(21): 5319-26.
Kopec, C. D., Real, E., Kessels, H. W. and Malinow, R. (2007) 'GluR1 links structural and functional plasticity at excitatory synapses', *The Journal of*

neuroscience : the official journal of the Society for Neuroscience 27(50): 13706-18.

Kozlowski, D. J., Murakami, T., Ho, R. K. and Weinberg, E. S. (1997) 'Regional cell movement and tissue patterning in the zebrafish embryo revealed by fate mapping with caged fluorescein', *Biochemistry and cell biology = Biochimie et biologie cellulaire* 75(5): 551-62.

Kwon, H. J. and Riley, B. B. (2009) 'Mesendodermal signals required for otic induction: Bmp-antagonists cooperate with Fgf and can facilitate formation of ectopic otic tissue', *Dev Dyn* 238(6): 1582-94.

Larison, K. D. and Bremiller, R. (1990) 'Early onset of phenotype and cell patterning in the embryonic zebrafish retina', *Development* 109(3): 567-76.

Lee, A., Mathuru, A. S., Teh, C., Kibat, C., Korzh, V., Penney, T. B. and Jesuthasan, S. (2010) 'The habenula prevents helpless behavior in larval zebrafish', *Current biology : CB* 20(24): 2211-6.

Levin, M. (2005) 'Left-right asymmetry in embryonic development: a comprehensive review', *Mechanisms of development* 122(1): 3-25.

Liang, J. O., Etheridge, A., Hantsoo, L., Rubinstein, A. L., Nowak, S. J., Izpisua Belmonte, J. C. and Halpern, M. E. (2000) 'Asymmetric nodal signaling in the zebrafish diencephalon positions the pineal organ', *Development* 127(23): 5101-12.

Lo, Y. C., Soong, W. T., Gau, S. S., Wu, Y. Y., Lai, M. C., Yeh, F. C., Chiang, W. Y., Kuo, L. W., Jaw, F. S. and Tseng, W. Y. (2011) 'The loss of asymmetry and reduced interhemispheric connectivity in adolescents with autism: a study using diffusion spectrum imaging tractography', *Psychiatry research* 192(1): 60-6.

Lu, P. N., Lund, C., Khuansuwan, S., Schumann, A., Harney-Tolo, M., Gamse, J. T. and Liang, J. O. (2013) 'Failure in closure of the anterior neural tube causes left isomerization of the zebrafish epithalamus', *Developmental biology* 374(2): 333-44.

Marcos-Mondejar, P., Peregrin, S., Li, J. Y., Carlsson, L., Tole, S. and Lopez-Bendito, G. (2012) 'The lhx2 transcription factor controls thalamocortical axonal guidance by specific regulation of robo1 and robo2 receptors', *The Journal of neuroscience : the official journal of the Society for Neuroscience* 32(13): 4372-85.

Martinez-Ferre, A. and Martinez, S. (2009) 'The development of the thalamic motor learning area is regulated by Fgf8 expression', *The Journal of neuroscience : the official journal of the Society for Neuroscience* 29(42): 13389-400.

Masai, I., Heisenberg, C. P., Barth, K. A., Macdonald, R., Adamek, S. and Wilson, S. W. (1997) 'floating head and masterblind regulate neuronal patterning in the roof of the forebrain', *Neuron* 18(1): 43-57.

Melendez-Ferro, M., Villar-Cheda, B., Abalo, X. M., Perez-Costas, E., Rodriguez-Munoz, R., Degrip, W. J., Yanez, J., Rodicio, M. C. and Anadon, R. (2002) 'Early development of the retina and pineal complex in the sea lamprey:

comparative immunocytochemical study', *The Journal of comparative neurology* 442(3): 250-65.
Miller, R. (1996) *Axonal conduction time and human cerebral laterality: A psychobiological theory*, Amsterdam: Harwood Academic Publisher.
Miller-Bertoglio, V. E., Fisher, S., Sanchez, A., Mullins, M. C. and Halpern, M. E. (1997) 'Differential regulation of chordin expression domains in mutant zebrafish', *Developmental biology* 192(2): 537-50.
Minokawa, T., Yagi, K., Makabe, K. W. and Nishida, H. (2001) 'Binary specification of nerve cord and notochord cell fates in ascidian embryos', *Development* 128(11): 2007-17.
Mohammadi, M., McMahon, G., Sun, L., Tang, C., Hirth, P., Yeh, B. K., Hubbard, S. R. and Schlessinger, J. (1997) 'Structures of the tyrosine kinase domain of fibroblast growth factor receptor in complex with inhibitors', *Science* 276(5314): 955-60.
Nakamura, H., Sato, T. and Suzuki-Hirano, A. (2008) 'Isthmus organizer for mesencephalon and metencephalon', *Development, growth & differentiation* 50 Suppl 1: S113-8.
Ota, S., Tonou-Fujimori, N., Nakayama, Y., Ito, Y., Kawamura, A. and Yamasu, K. (2010) 'FGF receptor gene expression and its regulation by FGF signaling during early zebrafish development', *Genesis* 48(12): 707-16.
Park, M., Penick, E. C., Edwards, J. G., Kauer, J. A. and Ehlers, M. D. (2004) 'Recycling endosomes supply AMPA receptors for LTP', *Science* 305(5692): 1972-5.
Park, M., Salgado, J. M., Ostroff, L., Helton, T. D., Robinson, C. G., Harris, K. M. and Ehlers, M. D. (2006) 'Plasticity-induced growth of dendritic spines by exocytic trafficking from recycling endosomes', *Neuron* 52(5): 817-30.
Pera, E. M., Ikeda, A., Eivers, E. and De Robertis, E. M. (2003) 'Integration of IGF, FGF, and anti-BMP signals via Smad1 phosphorylation in neural induction', *Genes & development* 17(24): 3023-8.
Peukert, D., Weber, S., Lumsden, A. and Scholpp, S. (2011) 'Lhx2 and Lhx9 determine neuronal differentiation and compartition in the caudal forebrain by regulating Wnt signaling', *PLoS biology* 9(12): e1001218.
Pyati, U. J., Webb, A. E. and Kimelman, D. (2005) 'Transgenic zebrafish reveal stage-specific roles for Bmp signaling in ventral and posterior mesoderm development', *Development* 132(10): 2333-43.
Quillien, A., Blanco-Sanchez, B., Halluin, C., Moore, J. C., Lawson, N. D., Blader, P. and Cau, E. (2011) 'BMP signaling orchestrates photoreceptor specification in the zebrafish pineal gland in collaboration with Notch', *Development* 138(11): 2293-302.
Ramel, M. C. and Hill, C. S. (2012) 'Spatial regulation of BMP activity', *FEBS letters* 586(14): 1929-41.
Rebagliati, M. R., Toyama, R., Fricke, C., Haffter, P. and Dawid, I. B. (1998) 'Zebrafish nodal-related genes are implicated in axial patterning and establishing left-right asymmetry', *Developmental biology* 199(2): 261-72.

Regan, J. C., Concha, M. L., Roussigne, M., Russell, C. and Wilson, S. W. (2009) 'An Fgf8-dependent bistable cell migratory event establishes CNS asymmetry', *Neuron* 61(1): 27-34.

Reifers, F., Adams, J., Mason, I. J., Schulte-Merker, S. and Brand, M. (2000) 'Overlapping and distinct functions provided by fgf17, a new zebrafish member of the Fgf8/17/18 subgroup of Fgfs', *Mechanisms of development* 99(1-2): 39-49.

Reifers, F., Bohli, H., Walsh, E. C., Crossley, P. H., Stainier, D. Y. and Brand, M. (1998) 'Fgf8 is mutated in zebrafish acerebellar (ace) mutants and is required for maintenance of midbrain-hindbrain boundary development and somitogenesis', *Development* 125(13): 2381-95.

Roehl, H. and Nusslein-Volhard, C. (2001) 'Zebrafish pea3 and erm are general targets of FGF8 signaling', *Current biology : CB* 11(7): 503-7.

Rogers, L. J. (2008) 'Development and function of lateralization in the avian brain', *Brain research bulletin* 76(3): 235-44.

Roussigne, M., Bianco, I. H., Wilson, S. W. and Blader, P. (2009) 'Nodal signalling imposes left-right asymmetry upon neurogenesis in the habenular nuclei', *Development* 136(9): 1549-1557.

Roussigne, M., Blader, P. and Wilson, S. W. (2011) 'The zebrafish epithalamus clears a path through the complexity of brain lateralization', *Developmental neurobiology*.

Sansom, S. N. and Livesey, F. J. (2009) 'Gradients in the brain: the control of the development of form and function in the cerebral cortex', *Cold Spring Harbor perspectives in biology* 1(2): a002519.

Sato, T., Joyner, A. L. and Nakamura, H. (2004) 'How does Fgf signaling from the isthmic organizer induce midbrain and cerebellum development?', *Development Growth & Differentiation* 46(6): 487-494.

Seth A and Culverwell J, W. M., Toro S, Rick JM, Neuhauss SC, Varga ZM, Karlstrom RO (2006) 'belladonna/(Ihx2) is required for neural patterning and midline axon guidance in the zebrafish forebrain', *Development* 133(4): 725-735.

Shinohara, Y., Hirase, H., Watanabe, M., Itakura, M., Takahashi, M. and Shigemoto, R. (2008) 'Left-right asymmetry of the hippocampal synapses with differential subunit allocation of glutamate receptors', *Proceedings of the National Academy of Sciences of the United States of America* 105(49): 19498-503.

Snelson, C. D., Burkart, J. T. and Gamse, J. T. (2008a) 'Formation of the asymmetric pineal complex in zebrafish requires two independently acting transcription factors', *Dev Dyn* 237(12): 3538-44.

Snelson, C. D., Burkart, J. T. and Gamse, J. T. (2008b) 'Formation of the asymmetric pineal complex in zebrafish requires two independently acting transcription factors', *Developmental dynamics : an official publication of the American Association of Anatomists* 237(12): 3538-44.

Snelson, C. D., Santhakumar, K., Halpern, M. E. and Gamse, J. T. (2008c) 'Tbx2b is required for the development of the parapineal organ', *Development* 135(9): 1693-702.

Sperry, R. W. (1961) 'Cerebral Organization and Behavior: The split brain behaves in many respects like two separate brains, providing new research possibilities', *Science* 133(3466): 1749-57.

Staudt, N. and Houart, C. (2007) 'The prethalamus is established during gastrulation and influences diencephalic regionalization', *PLoS biology* 5(4): e69.

Sun, T. and Walsh, C. A. (2006) 'Molecular approaches to brain asymmetry and handedness', *Nature reviews. Neuroscience* 7(8): 655-62.

Suzuki-Hirano, A. and Shimogori, T. (2009) 'The role of Fgf8 in telencephalic and diencephalic patterning', *Seminars in cell & developmental biology* 20(6): 719-25.

Thiebaut de Schotten, M., Dell'Acqua, F., Forkel, S. J., Simmons, A., Vergani, F., Murphy, D. G. and Catani, M. (2011) 'A lateralized brain network for visuospatial attention', *Nature neuroscience* 14(10): 1245-6.

Thisse, B. and Thisse, C. (2005) 'Functions and regulations of fibroblast growth factor signaling during embryonic development', *Developmental biology* 287(2): 390-402.

Thisse, C. and Thisse, B. (2008) 'High-resolution in situ hybridization to whole-mount zebrafish embryos', *Nature protocols* 3(1): 59-69.

van Veen, T. (1982) 'The parapineal and pineal organs of the elver (glass eel), Anguilla anguilla L', *Cell and tissue research* 222(2): 433-44.

van Veen, T., Ekstrom, P., Borg, B. and Moller, M. (1980) 'The pineal complex of the three-spined stickleback, Gasterosteus aculeatus L.: a light-, electron microscopic and fluorescence histochemical investigation', *Cell and tissue research* 209(1): 11-28.

Vigh-Teichmann, I., Korf, H. W., Nurnberger, F., Oksche, A., Vigh, B. and Olsson, R. (1983) 'Opsin-immunoreactive outer segments in the pineal and parapineal organs of the lamprey (Lampetra fluviatilis), the eel (Anguilla anguilla), and the rainbow trout (Salmo gairdneri)', *Cell and tissue research* 230(2): 289-307.

Walker, C. (1999) 'Haploid screens and gamma-ray mutagenesis', *Methods in cell biology* 60: 43-70.

Woo, K. and Fraser, S. E. (1995) 'Order and coherence in the fate map of the zebrafish nervous system', *Development* 121(8): 2595-609.

Wu, Y., Kawakami, R., Shinohara, Y., Fukaya, M., Sakimura, K., Mishina, M., Watanabe, M., Ito, I. and Shigemoto, R. (2005) 'Target-cell-specific left-right asymmetry of NMDA receptor content in schaffer collateral synapses in epsilon1/NR2A knock-out mice', *The Journal of neuroscience : the official journal of the Society for Neuroscience* 25(40): 9213-26.

Zakin, L. and De Robertis, E. M. (2010) 'Extracellular regulation of BMP signaling', *Current biology : CB* 20(3): R89-92.